Characterisation of Autophagy Modulation by Thiopurines in Inflammatory Bowel Disease

Connan Dayton Masson

A thesis submitted in partial fulfilment of the requirements of Edinburgh Napier University, for the award of Master by Research

July 2020

Abstract

Background

Inflammatory bowel disease (IBD), which includes Crohn's disease (CD) and ulcerative colitis, are chronic diseases of the gastrointestinal tract. Genetic studies have identified strong association between genes involved in autophagy, ER-stress/unfolded protein response (UPR) and IBD. Stimulating autophagy may be beneficial for the treatment of IBD, and thiopurines, a class of drugs in clinical use for IBD, have been shown to induce autophagy. The aim of this study was to investigate the mechanism of action of thiopurines azathioprine (AZA), 6-MP and 6-TG in the context of autophagy, with focus on the interplay between autophagy and ER-stress/UPR signalling pathways.

Methods

Autophagy was evaluated by confocal fluorescence microscopy and live-cell imaging of autophagy marker LC3. Cell viability was assessed by Alamar Blue assay, and induction of apoptosis assessed by Annexin V/PI staining. Activation of ER stress and UPR signalling was investigated by reverse transcription polymerase chain reaction (RT-PCR), quantitative RT-PCR (RT-qPCR) and immunoblotting. Modulation of mechanistic target of rapamycin (mTORC1) was assessed by immunoblotting.

Results

AZA, 6-MP and 6-TG are strong inducers of autophagy, with AZA inducing autophagy more rapidly than 6-MP or 6-TG. AZA and 6-TG increased early apoptosis, while 6-TG reduced cell viability and inhibited cell growth. Thiopurines did not induce ER stress, however, 6-TG activated the UPR pathway. AZA induced autophagy via mechanisms involving modulation of mTORC1 signalling.

Conclusions

Thiopurines are strong inducers of autophagy. There are differences in AZA, 6-MP and 6-TG mechanism of action, therefore, a better understanding may lead to personalised application, and improve the therapeutic efficacy of thiopurines in IBD.

Contents

Abstract **1**
List of Tables **7**
Acknowledgments **8**
Abbreviations **9**
Chapter 1. Introduction **14**
1.1. Inflammatory bowel disease 14
1.2. Intestinal microbiome 16
1.3. Environmental factors 17
1.4. Genetic factors associated with IBD 18
1.4.1. NOD2 18
1.4.2. Innate immunity and the role of macrophages in IBD 21
1.4.3. Autophagy genes associated with CD 23
1.4.4. Autophagy 24
1.4.5. The autophagy pathway 25
1.4.6. Autophagy Signalling 27
1.4.7. Intersection of NOD2 and autophagy in IBD 28
1.4.8. Intestinal barrier integrity 29
1.4.9. Epithelial Barrier Integrity in IBD 29
1.4.10. Composition of the intestinal epithelial barrier 30
1.5. ER Stress 34
1.6. The Unfolded Protein Response 34
1.6.1. IRE1 signalling 35
1.6.2. PERK pathway 36
1.6.3. ATF6 pathway 36
1.7. ER Stress and UPR signalling in IBD 39
1.8. Clinical Relevance of Thiopurines 41
1.8.1. Potential Mechanism of Action of Thiopurines 43
1.9. Research aims 45
Chapter 2. Materials and Methods **46**
2.1. Cell Culture 46
2.2. Transfection and plasmids 46

2.3. Cell treatments 47
2.4. Western immunoblotting 47
2.5. Fixed cell imaging 49
2.6. Live cell imaging 50
2.7. Autophagy Assays 50
2.8. Real time quantitative PCR (RT-qPCR) 51
2.9. Reverse transcription PCR (RT-PCR) 52
2.10. Flow Cytometry 53
2.11. Annexin/PI Staining 53
2.12. Alamar Blue Assay 55
2.13. Statistical Analysis 55
Chapter 3. Induction of autophagy by thiopurines in HEK293 cells 56
3.1. Introduction 56
3.2. Results 56
3.2.1. Live cell imaging of thiopurine induced autophagy 57
3.2.2. Fixed-cell imaging of thiopurine induced autophagy 60
3.2.3. Fixed-cell imaging of sustained thiopurine induced autophagy 62
3.2.4. Effect of thiopurines on metabolic activity and cell morphology 64
3.3. Summary 66
Chapter 4. Characterisation of autophagy induction by thiopurines in macrophages 68
4.1. Introduction 68
4.2. Results 69
4.2.1. Differentiation of THP-1 derived macrophages 69
4.2.2. Characterisation of THP-1 derived macrophages 71
4.2.3. Time-Course of autophagy induction by thiopurines in THP-1 derived macrophages 74
4.2.4. Autophagy activity of THP-1 derived macrophages treated with a range of thiopurine concentrations 77
4.2.5. Sustained autophagy induction in response thiopurine treatment. 82
4.2.6. Activation of autophagy by thiopurines 85
4.2.7. The effects of thiopurines on apoptosis 88
4.3. Summary 91

Chapter 5. Characterisation of the ER-stress and unfolded protein response to thiopurines in macrophages 92
5.1. Introduction 92
5.2. Results 96
5.2.1. Evaluation of the ER stress response to thiopurines in macrophages 96
5.2.2. Characterisation of UPR gene expression in response to thiopurine treatment 98
5.2.3. Assessment of Eif2α phosphorylation in response to thiopurine treatment 101
5.2.4. EDEM1 protein expression in response to thiopurine treatment 102
5.2.5. Modulation of mTORC1 activity in response to thiopurines 105
5.3. Summary 108
Chapter 6. Discussion 109
6.1. Overview 109
6.2. HEK293 cells: A reporter cell line for autophagy modulation 109
6.3. Induction of autophagy by thiopurines in HEK293 cells 110
6.4. Effect of thiopurines on the metabolic activity of HEK293 cells 112
6.5. THP-1 cells: An *in vitro* cell model of macrophage function 113
6.6. Induction of autophagy by thiopurines in THP-1 derived macrophages 114
6.7. Effect of thiopurines on autophagy activity in THP-1 derived macrophages 117
6.8. Interplay between autophagy and apoptosis 119
6.9. Effects of thiopurines on the ER-Stress response in THP-1 derived macrophages 121
6.10. Induction of the UPR by thiopurines 124
6.11. Role of thiopurines and UPR in mitochondrial homeostasis 124
6.12. Regulation of mTORC1 signalling by thiopurines 126
6.13. Clinical Significance of Thiopurine-induced autophagy activity 128
6.13.1. Personalised therapies in IBD patients 128
6.13.2. Use of combination therapy in IBD 129
6.13.3. Clinical impact of TPMT activity in autophagy activity 129
6.14. Future Research 130
6.14.1. ATF6 signalling in response to thiopurines 130
6.14.2. mTORC1 signalling in response to thiopurines 130
6.14.3. Further assessment of autophagy signalling 131

6.14.4. Therapeutic effect of imidazole derivatives 131
6.14.5. Future use of *in vitro* and *ex vivo* models for IBD 132
6.14.6 Thiopurine induced mitochondrial dysfunction 133
6.15. Conclusion 133
7. References **135**

List of Figures

Figure 1 - Crohn's disease and ulcerative colitis disease characteristics. 15
Figure 2 - Factors associated with IBD pathogenesis. 15
Figure 3 - NOD2 signalling in response to bacterial invasion. 20
Figure 4 - Autophagosome formation. 27
Figure 5 - Intestinal Epithelial Barrier during IBD. 33
Figure 6 - UPR signalling during ER stress. 38
Figure 7 - The Function of Paneth cells and autophagy in Intestinal epithelium physiology. 40
Figure 8 - The Metabolism of Thiopurines. 42
Figure 9 - Analysis of autophagy flux. 51
Figure 10 - Induction of autophagy by thiopurines. 58
Figure 11 - Quantification of autophagy induction by thiopurines. 59
Figure 12 - Induction of autophagy by thiopurines at 4h time point. 59
Figure 13 - Induction of autophagy by thiopurines at 8h time point. 59
Figure 12 - Induction of autophagy by thiopurines at 8h time point using fixed-cell imaging 61
Figure 13 - Induction of autophagy by thiopurines at 24h time point. 63
Figure 14 - Effect of thiopurines on metabolic activity and cell growth 65
Figure 15 - PMA treatment induces THP-1 morphological changes and cellular adherence. 70
Figure 16 - Morphological changes during polarisation of THP-1 cells. 72
Figure 17 - Macrophage marker expression in polarised THP-1 cells. 73
Figure 18 – Time course of autophagy induction in thiopurine treated THP-1 derived macrophages. 75
Figure 19 - Quantification of LC3 puncta in thiopurine treated THP-1 derived macrophages during a time course 76
Figure 20 - Fixed cell imaging of immunostained LC3 in THP-1 derived macrophages treated with an AZA concentration curve. 78
Figure 21 - Fixed cell imaging of immunostained LC3 in THP-1 derived macrophages treated with a 6-MP concentration curve. 79
Figure 22 - Fixed cell imaging of immunostained LC3 in THP-1 derived macrophages treated with a 6-TG concentration curve. 80
Figure 23 - Quantification of LC3 puncta in THP-1 derived macrophages treated with a thiopurine concentration curve. 81

Figure 24 - Fixed cell imaging of Immunostained LC3 in THP-1 derived macrophages treated for 24h with thiopurines. 83
Figure 25 - Quantification of LC3 puncta in THP-1 derived macrophages treated for 24h with thiopurines. 84
Figure 26 - THP-1 macrophages transiently transfected with GFP-RFP-LC3 plasmid to assess thiopurine-induced autophagy activation. 86
Figure 27 - Quantification of thiopurine-induced autophagy induction in GFP-RFP-LC3 transfected THP-1 derived macrophages. 87
Figure 28 (i-vi) – Annexin V/PI staining utilising flow cytometry in thiopurine treated THP-1 macrophages. 89
Figure 29 - Quantification of Annexin V/PI staining in thiopurine treated THP-1 macrophages. 90
Figure 30 - The Unfolded Protein Response. 94
Figure 31 - End-point PCR analysis of XBP1 splicing in response to thiopurines. ... 97
Figure 32 (i-v) – Real-time PCR analysis of UPR associated genes in response to thiopurines. 99
Figure 33 (i-v) – Melt curves of UPR associated genes in response to thiopurines. 100
Figure 34 - Eif2α phosphorylation in response to thiopurine treatment. 102
Figure 35 - EDEM1 protein expression in response to thiopurine treatment. 104
Figure 36 - mTORC1 signalling pathway. 106
Figure 37 - Modulation of mTORC1 activity in response to thiopurine treatment. .. 107
Figure 38 – Autophagy activation in Macrophages. 119
Figure 39 - XBP1 variants observed during End-point PCR. 123

List of Tables

Table 1 - Differences between blood-derived and intestinal-derived macrophages . 23
Table 2 - Pharmacological Agents 47
Table 3 - Antibodies 49
Table 4 - Primer Sequence 53
Table 5 – Voltage parameters 54
Table 6 – Compensation 54

Acknowledgments

I would firstly like to thank Dr Craig Stevens for his continuous support and expertise throughout my studies. I would also like to thank Professor Peter Barlow and Dr Jenny Fraser for providing me with advice within the lab and during the writing of my thesis. Also, Dr Sally Brown for her support as an independent panel chair during my studies. Fellow researchers David Hughes, Alice Arnold and Isla Bruce also made this process enjoyable and were always there for advice and encouragement. I would finally like thank my friends and family who were always there to support me when needed.

Abbreviations

IBD - Inflammatory bowel disease

CD – Crohn's disease

UC – Ulcerative Colitis

ER – Endoplasmic reticulum

UPR – Unfolded protein response

AZA - Azathioprine

6-MP – 6-Mercaptopurine

6-TG – 6-Thioguanine

LC3 – Microtubule-associated protein 1A/1B- light chain 3

GFP – Green fluorescent protein

RFP – Red fluorescent protein

PI – Propidium Iodide

RT-PCR – Reverse transcription polymerase chain reaction

RT-qPCR - Reverse transcription quantitative polymerase chain reaction

mTORC1 - Mechanistic target of rapamycin 1

GI – Gastrointestinal

UK – United Kingdom

NHS – National Health Service

AIEC - Adherent invasive *Escherichia. Coli*

TNF-α – Tumour necrosis factor alpha

IL – Interleukin

SCFA - Short chain fatty acids

Treg – Regulatory T cells

NSAID - Non-steroidal anti-inflammatory drugs

NOD2 - Nucleotide-binding oligomerization domain-containing protein 2

SNP - Single nucleotide polymorphisms

LRR - Leucine rich repeat

MDP - Muramyl dipeptide

PRR - Pattern recognition receptor

NLR - Nod like receptors

TLR - Toll-like receptors

PAMP - Pathogen-associated molecular pattern

DAMP - Damage-associated molecular pattern

RIP2 - Receptor-interacting-serine/threonine-protein kinase 2

TRAF - TNF receptor associated factors

cIAP2 - Cellular inhibitor of apoptosis 2

MAPK - Mitogen-activated protein kinases

ERK - Extracellular signal-regulated kinase

NF-κB – Nuclear factor - κB

NEMO - NF-κB essential modulator

IKK - IκB kinase complex

LPS – Lipopolysaccharide

HD5 – Alpha-defensin 5

DC – Dendritic cell

TIM-4 – T-Cell membrane protein 4

CD4 – Cluster of differentiation 4

TGF-β – Transforming growth factor beta

PBMC - Peripheral blood mononuclear cell

CCL7 – C-C motif chemokine ligand 7

GM-CSF – Granulocyte-macrophage colony-stimulating factor

MDM - Monocyte-derived macrophages

TH17 – T-helper 17

ATG16L1 - Autophagy-related protein 16-1

IRGM - Immunity-related GTPase family protein M

XBP1 – X-box binding protein 1

ORMDL3 – ORMDL sphingolipid biosynthesis regulator 3

eif2α – Eukaryotic initiation factor 2

ATF4 – Activating transcription factor 4

ULK1 – Unc-51 like autophagy activating kinase

FIP200 – FAK family-interacting protein of 200kDa

VPS34 – Vacuolar protein sorting 34

PI3P – Phosphatidylinositol 3-phosphate

WIPI - WD-repeat protein interacting with phosphoinositides

DFCP1 – Double FYVE-containing protein 1

LIR – LC3 interacting region

AMPK - AMP-activated protein kinase

ATP – Adenosine triphosphate

Bcl2 – B-cell lymphoma 2

MAM – Mitochondria-associated membranes

MHC – Major Histocompatibility complex

LRRK2 – Leucine-rich repeat kinase 2

DSS – Dextran sodium sulphate

IEC – Intestinal epithelial cell

MMP – Matrix metalloproteinase

ERAD – ER-associated degradation

IRE1 - Inositol-requiring enzyme 1

PERK - Double-stranded RNA-activated protein kinase (PKR)-like kinase

ATF6 - Activation transcription factor 6

LD – Luminal domain

BiP – Binding immunoglobulin protein

RIDD - Regulated IRE1-dependent decay

CHOP - C/EBP homologous protein

S1P - Serine protease site-1 protease

S2P - Metalloprotease site 2-protease

EDEM1 - ER degradation-enhancing alpha-mannosidase-like protein 1

RCAN1 - Regulator of calcineurin 1

6-TGN – 6-thioguanine nucleotides

RAC1 – Ras-related C3 botulinum toxin substrate 1

HPRT - Hypoxanthine-guanine phosphoribosyl transferase

TPMT - Thiopurine methyltransferase

6-MMP - 6-methyl mercaptopurine

6-MMPR - 6-methyl mercaptopurine ribnucleotide

IMPDH - Inosine monophosphate dehydrogenase

XO - Xanthine oxidase

6-MeTIMP - 6-methylthioinosine monophosphate

GMPS - Guanosine monophosphate synthetase

TU - Thiouric acid

6-TIMP - Thioinosine monophosphate

6-TXMP - 6-thioxanthosine monophosphate

ROS – Reactive oxygen species

GSH – Glutathione

HEK293 - Human embryonic kidney 293 cells

DMEM - Dulbecco’s modified eagle’s media

RPMI - Roswell park memorial institute

PMA - Phorbol 12-myristate 13-acetate

DMSO - Dimethyl Sulfoxide

PBS - Phosphate buffered saline

EDTA – Ethylenediaminetetraacetic acid

NaCl – Sodium Chloride

SDS-PAGE – Sodium dodecyl sulfate-polyacrylamide gel electrophoresis

PFA – Paraformaldehyde

DAPI – 5’, 6-diamidino-2-phenylindole

ANOVA – Analysis of variance

PS – Phosphatidylserine

HDP - Host defence peptides

RNA – Ribonucleic acid

DNA – Deoxyribonucleic acid

NTC – No template control

DEPC – Diethyl pyrocarbonate

BFA - Brefeldin A

MMR – Mismatch repair

PI3K – Phosphoinositide 3-kinase

IFN – Interferon

NLRP3 - NOD-, LRR- and pyrin domain-containing protein 3

REDD1 - DNA damage and development 1

NRH - Nodular regenerative hyperplasia

Chapter 1. Introduction

1.1. Inflammatory bowel disease

Inflammatory bowel disease (IBD) is a chronic, relapsing inflammatory condition that can affect all of the gastrointestinal (GI) tract and consists of two main forms known as Crohn's disease (CD) and Ulcerative colitis (UC). As shown on **Figure 1**, UC commonly presents as mucosal inflammation that is limited to the colon whereas CD causes transmural inflammation that can affect the entire GI tract in a non-continuous manner, which can lead to complications such as fistulas, strictures and abscesses (Zhang and Li, 2014). Symptoms of IBD include weight loss, abdominal pain, diarrhoea and GI bleeding (Cummins and Crean, 2016). Currently, 300,000 individuals suffer from IBD in the UK (Crohn's & Colitis UK, 2018). With there being no cure for the disease, patients face years of medication, invasive colonoscopy surveillance and a high likelihood of surgery to mitigate symptoms and maintain remission (Shaw *et al*., 2019). The average annual cost for IBD treatment in the UK is approximately £3000-6000 per patient (Ghosh and Premchand, 2015). An NHS audit undertaken in 2010 estimated an annual direct cost of more than £1 billion for the treatment and surgery associated with IBD (Ghosh and Premchand, 2015). IBD cases have risen dramatically by 85.1% since 1990, with the disease originally considered an issue particularly within westernised societies due to lifestyle, however it is now considered global disease issue (Alatab *et al*., 2020; Bernstein and Shanahan, 2008). The peak age of IBD occurrence is typically between the age of 15 to 35 years old, with up to 10% of patients being under the age of 20, with IBD particularly effecting younger populations based within urbanised areas (M'Koma, 2013; Novak and Mollen, 2015). CD and UC are diagnosed through biopsy, endoscopy and other imaging methods, taking into consideration signs and symptoms present within the patient. Difficulties can arise when distinguishing CD and UC, in some cases patients will be diagnosed with intermediate colitis until defining features of CD and UC become present (Alatab *et al*., 2020). The aetiology is unknown, however it is thought to be an intricate relationship between environmental factors, genetic factors, and the intestinal microbiome that results in breakdown of epithelial barrier integrity and an inappropriate inflammatory response **(Figure 2)** (Zhang and Li, 2014).

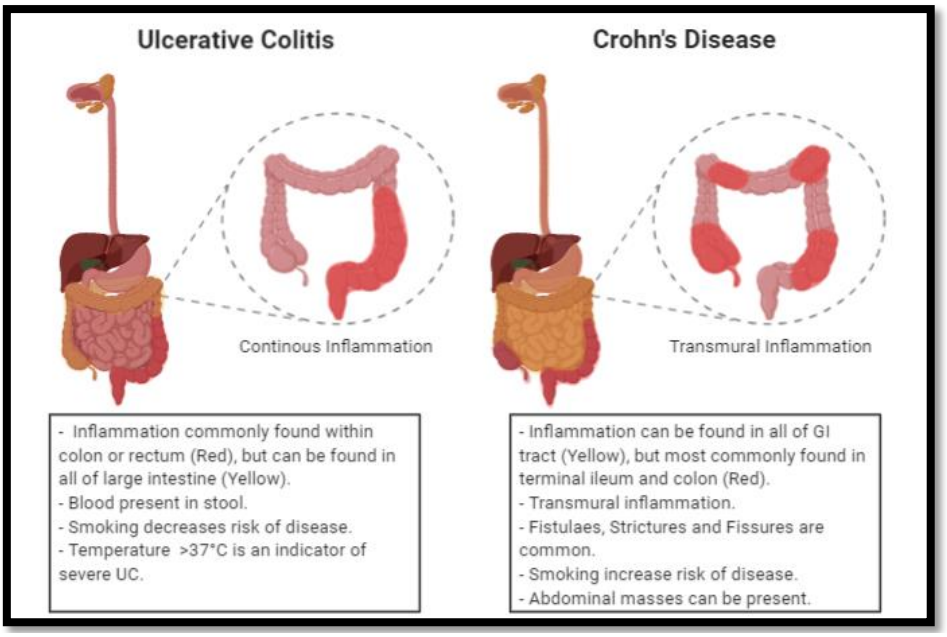

Figure 1 - Crohn's disease and ulcerative colitis disease characteristics.

Author's illustration shows the main characteristics of CD and UC. Image created using Biorender software.

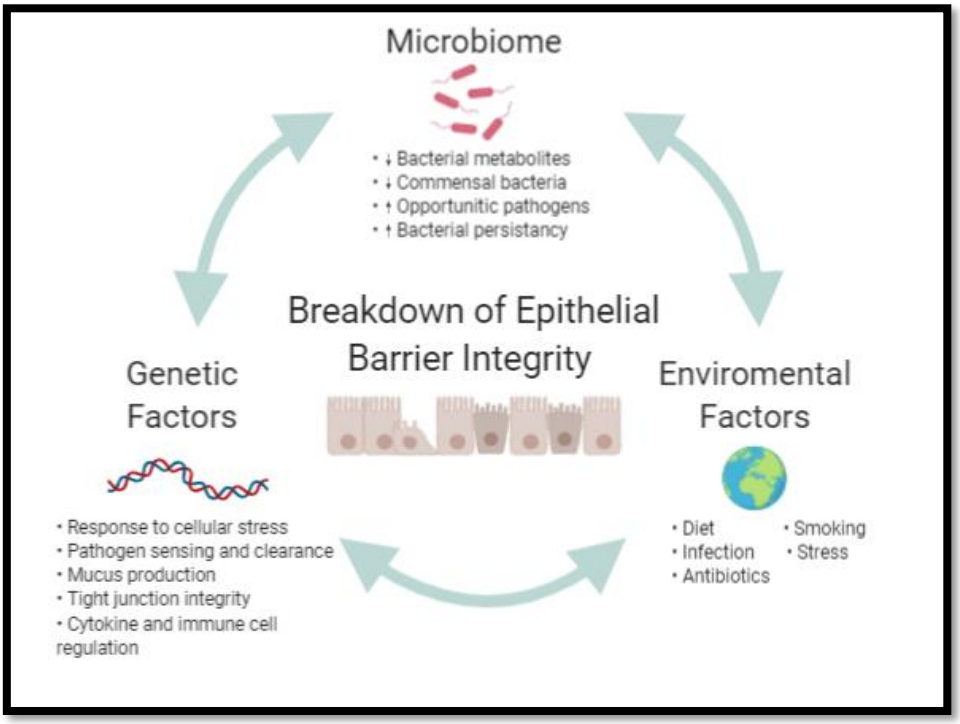

Figure 2 - Factors associated with IBD pathogenesis.

Three main factors are associated with IBD pathogenesis; environmental factors; genetic factors and the intestinal microbiome. All three factors are linked to breakdown of epithelial barrier integrity, which is a key event in IBD. Image created using Biorender software.

1.2. Intestinal microbiome

The intestinal microbiota is composed of up to 10^{14} enteric microbes and 500 different bacterial species (Thursby and Juge, 2017). These microbes are essential in intestinal homeostasis by providing nutrients, regulating metabolism and aiding in the development of the immune system within the host (Thursby and Juge, 2017). Abnormal microbial ecology is a common characteristic found in IBD patients, known as dysbiosis. A reduction in abundance and diversity of bacteria in the gut is found in IBD, with a decreased abundance of phyla within *Firmicutes* and *Bacterioides*, and an increase in phylum such as *Gammaproteobacteria*. An increase in bacteria such as *Enterobacteriaceae*, *Fusobacteriaceae* and a decrease in *Bacreroidales* was strongly correlated with disease severity (Zuo and Ng, 2018). The reduction of bacterial diversity in the microbiota can allow opportunistic pathogens to thrive and initiate inflammation (Zuo and Ng, 2018). The opportunistic pathogen, adherent invasive *Escherichia coli* (AIEC), a member of the *Enterobacteriaceae phyla,* has been isolated in both UC and CD patients (Darfeuille-Michaud *et al*., 2004). AIEC can colonise on the intestinal epithelial barrier and invade the epithelial barrier through Peyer's patches, where the earliest lesions of CD are observed (Rolhion and Darfeuille-Michaud, 2007). Once they are intracellular, AIEC can persist and stimulate macrophages to produce excessive amounts of tumour necrosis factor-alpha (TNF-α), exacerbating inflammation (Bringer *et al*., 2012)

Firmicutes and *Bacteroidetes* are predominant members of a healthy microbiota. A member of the Firmicute family, *Faecalibacterium praunitizii* is well characterised for its anti-inflammatory properties, and restoration of *F.prausnititzii* is associated with maintaining remission in UC patients (Rolhion and Darfeuille-Michaud, 2007). In addition to immune regulation by anti-inflammatory cytokines such as IL-10, *Firmicutes* also produce short chain fatty acids (SCFAs), which regulate metabolism in colonic epithelial cells and regulate immunity by assisting the proliferation of Treg cells (Smith *et al*., 2013; Venegas *et al*., 2019). SCFA's also regulate the expression of host defence peptides, such as the cathelicidin LL-37, which help to prevent the expansion of pathogenic bacteria in the intestine due to their profound antimicrobial properties (Schauber *et al*., 2003).

1.3. Environmental factors

Environmental factors play a critical role on the onset of IBD, with epidemiology studies relating IBD pathogenesis with industrialisation and a westernised lifestyle (Ananthakrishnan *et al*., 2018). Risk factors associated with IBD include diet, antibiotic use, hygiene, infection and pollution; all with considerable amounts of evidence to suggest their potential for altering the microbiome (Ananthakrishnan *et al*., 2018). A popularised theory to explain the implications of environmental factors in IBD is the hygiene hypothesis. This hypothesis suggests that changes in the gut microbiota through factors such as antibiotics, dietary changes, and increases in sanitation, all found within westernised countries, leads to a loss of microbial diversity and consequently a loss of immunological tolerance (Abegunde *et al*., 2016).

The use of antibiotics has been found to be effective in IBD patients, which is thought to be due to ability to reduce the burden of pathogenic bacteria in the microbiota (Abegunde *et al*., 2016). On the contrary, regular antibiotic use has been correlated with the on-set of IBD, potentially due the non-specific effects of antibiotics leading to the reduction of commensal bacteria and dysbiosis (Aniwan *et al*., 2018). Non-steroidal anti-inflammatory drugs (NSAID) are also associated with CD activity, but not UC (Long *et al*., 2017). As well as NSAID's, smoking appears to have contradicting effects in CD and UC, illustrating the complexity of both disease subtypes. Smoking is one of the most well studied factors in IBD and has been found to exacerbate inflammation in CD and be protective in UC patients (Ramos and Papadakis, 2019). Theories to explain this protective mechanism include the potential of nicotine to induce mucin synthesis, which is impaired in UC patients (Bastida and Beltrán, 2011).

A high-fibre diet has been found to decrease CD risk by up to 40% (Ananthakrishnan *et al*., 2013). Whereas diets containing highly processed meats and high saturated fatty acids increase the risk of IBD (Ramos and Papadakis, 2019). Fibre is fermented in the large bowel by anaerobic bacteria that results in the production of the SCFA, butyrate, which influences microbiota composition, immune regulation and aids in intestinal barrier integrity by preventing the translocation of opportunistic pathogens such as AIEC across Peyer's patches (De Filippo *et al*., 2010; Roberts *et al*., 2010; Vinolo *et al*., 2011). Ultraviolet light exposure based on geographical location has also been correlated with the incidences of IBD, with individuals exposed to less ultraviolet

light based in northern latitudes exhibiting an increased risk of IBD (Holmes *et al*., 2015). The vitamin D receptor has major implications in IBD as it has been associated with immune regulation, nucleotide-binding oligomerization domain-containing protein 2 (NOD2) and autophagy signalling, all factors which have been directly linked to IBD pathogenesis (Verway, 2010). Vitamin D_3 (1, 25(OH) D3) administration was associated within a decrease in TNF-α gene expression and colitis in mice models, illustrating the impact that Vitamin D_3 deficiency could have on IBD patients (Abegunde *et al*., 2016). Therefore, the environmental factors discussed could lead to the dysregulation of the immune response and microbial dysbiosis, which can subsequently lead to breakdown of the intestinal barrier in a genetically susceptible host.

1.4. Genetic factors associated with IBD

Genetics plays a major role in the pathogenesis of IBD, with the latest genetic association study identifying 240 different susceptibility loci for IBD (De Lange *et al*., 2017). Epidemiological studies illustrate that ~15% of CD patients have an affected family member and the concordance rate for monozygotic twins suffering from CD is 50%, in contrast to dizygotic twins, which is less than 10% (Loddo and Romano, 2015). Although CD and UC exhibit distinct clinical characteristics, they share approximately 30% IBD-associated genetic loci (Khor *et al*., 2011). However, genetic factors appear to have more significant implications in CD than UC, with a 26-fold increased risk for developing CD if a previous sibling suffers from the disease compared to UC which is a 9-fold increase (Uhlig *et al*., 2014). Of the multiple IBD susceptibility loci discovered, NOD2 and genes involved in autophagy signalling have the most significant association with IBD pathogenesis.

1.4.1. NOD2

In CD, NOD2 remains the strongest genetic determinant, with three NOD2 single nucleotide polymorphisms (SNPs) accounting for approximately 80% of CD associated variants; the variants include *1007fs*, *R702W* and *G908R* located within the leucine rich repeat (LRR) domain, important for recognition of the bacterial cell wall component muramyl dipeptide (MDP) **(Figure 3)** (Parkhouse and Monie, 2015; Sidiq *et al*., 2016). Allele frequency studies have found that the insertion mutation, *1007fs*,

which results in truncation of the LRR domain, was found in up to 8-16% of CD patients, compared to 2-4% in healthy control groups (Heliö *et al*., 2003). In addition, meta-analysis studies show that *NOD2* homozygotes exhibit a 17.1-fold increase in CD development and 2.4-fold increase in *NOD2* heterozygotes (Economou *et al*., 2004).

NOD2 is a member of the pattern recognition receptor (PRR) family of proteins. PRRs, such as Nod like receptors (NLRs) and Toll-like receptors (TLRs), are critical in the innate immune response as they recognise pathogen antigens (pathogen-associated molecular patterns (PAMPs)) or molecules released from damaged cells (Damage-associated molecular patterns (DAMPs)) (Amarante-Mendes *et al*., 2018). NOD2 is highly expressed in Paneth cells located at the crypts of the small intestine and in myeloid lineages, including dendritic cells (DC) and macrophages (Eckmann and Karin, 2005). As shown on **Figure 3**, recognition of MDP by NOD2 promotes the oligomerisation and recruitment of RIP2, which allows the recruitment of TRAF2, TRAF6 and cIAP2. TRAF-6 recruitment leads to the activation of mitogen-activated protein kinases (MAPK) including p38 and ERK (Kobayashi *et al*., 2005). In addition, recruitment allows the ubiquitination of the NF-κB essential modulator (NEMO) and can activate NF-kB, through the activation of IκB kinase complex (IKK) and phosphorylation of IκBα (Negroni *et al*., 2018). Both the activation NF-kB and MAPK leads to production of a range of cytokines and host-defence peptides, including TNF-α, IL-1β, IL-10, IL-8 and *a*-defensins (Sidiq *et al*., 2016). NOD2 variants have been found to have impaired NF-kB production in the presence of bacterial lipopolysaccharide (LPS) and a reduction alpha-defensins 5 (HD5) and HD6 synthesis in Paneth cells of CD patients (Tan *et al*., 2015). This illustrates the importance of functional NOD2 signalling in bacterial sensing and immune regulation, two factors which have been directly implicated in IBD pathogenesis.

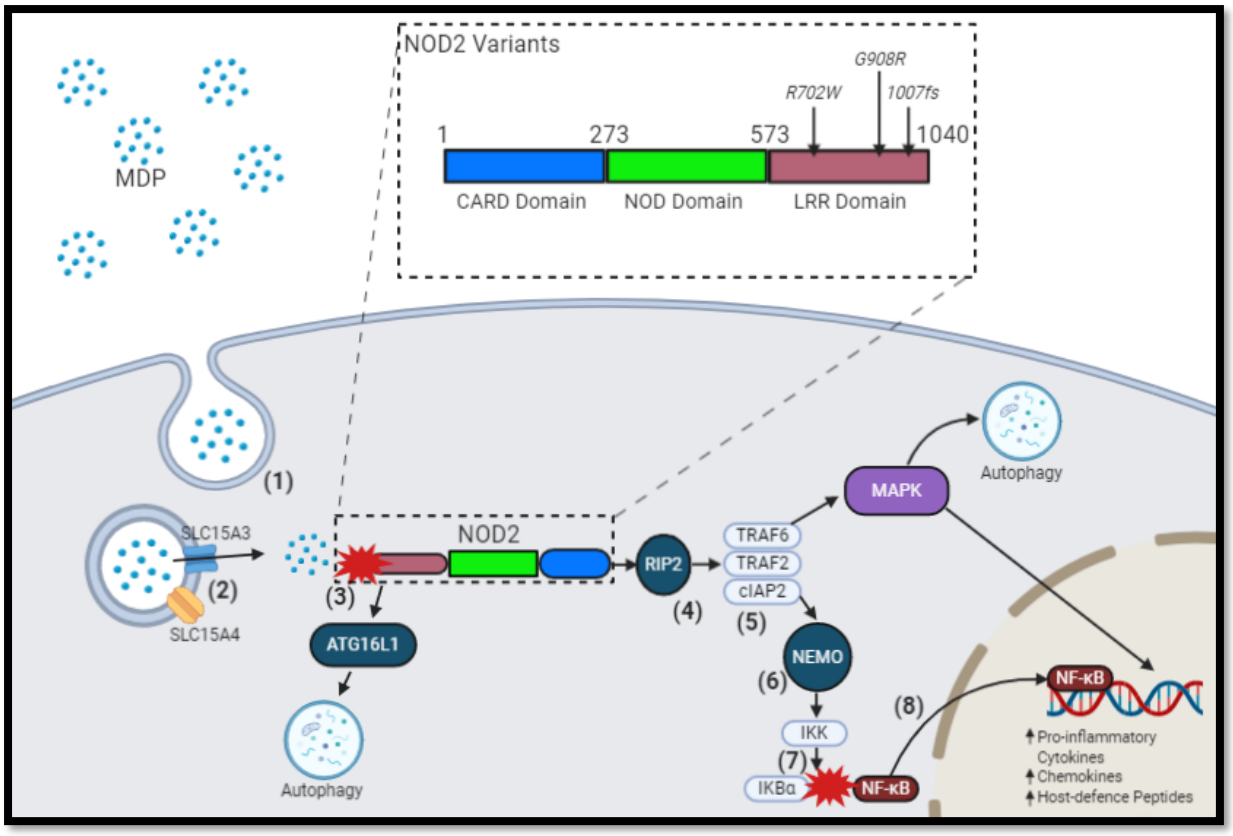

Figure 3 - NOD2 signalling in response to bacterial invasion.

Authors illustration of NOD2 signalling and CD-associated NOD2 variants. **(1)** Internalisation of bacterial derived-MDP fragments through multiple routes including phagocytosis, endocytosis and membrane bound channels. **(2)** SLC15A43 and SLC15A4 release MDP fragments from endosomes into cytoplasm of cell. **(3)** LRR domain recognises MDP and initiates NOD2 signalling, allowing movement of ATG16L1 to site of bacterial entry to subsequently activate autophagy. **(4)** Recognition of MDP allows oligomerisation and activation of RIP2. **(5)** TRAF6, TRAF2 and cIAP2 are recruited to the NOD2-RIP2 complex. MAPK's such as p38 and ERK are activated in a TRAF-6 dependent manner, which subsequently activate autophagy and pro-inflammatory cytokine signalling. **(6)** NEMO and TAK1 form a complex which subsequently activates IKK signalling. **(7)** phosphorylation of Iκα by IKK begins releases IκBα from NF-κB. **(8)** NF-κB translocates to the nucleus and upregulates pro-inflammatory cytokine, chemokine and host-defence peptide production. Image created using Biorender software.

1.4.2. Innate immunity and the role of macrophages in IBD

The innate immune system is an evolutionary conserved response in mammals, which functions as the first line of defence against pathogens attempting to invade barrier surfaces, including the skin, respiratory and GI (Corridoni *et al*., 2018; Gasteiger *et al*., 2017). Compared to adaptive immunity, innate immunity can be triggered more rapidly, lacking immunological memory, through the activation of PRR's. Once activated, innate immune cells utilise cell-mediated mechanisms such as phagocytosis, cytotoxicity or secretary molecules such as host defence peptides, cytokines and complement factors to neutralise pathogens (Gasteiger *et al*., 2017). Innate immune cells, such as macrophages and DC's, reside within the lamina propria of the intestinal epithelium and are responsible for the rapid discrimination of self and non-self-antigens that are sampled from the gut lumen via M-cells located in the gut-associated lymphoid tissue (Ahluwalia *et al*., 2018). Macrophages and DC's are also a key component in the crosstalk between the innate and adaptive immune system as they are well established antigen-presenting cells, which regulate lymphocyte proliferation through the presentation of antigens in major histocompatibility class (MHC) II proteins (Gaudino and Kumar, 2019).

As shown on **Table 1**, intestinal resident macrophages differ from other tissue resident macrophages. It is thought that most tissue macrophages derive from an embryonic and haematopoietic precursor that have little replenishment by blood-derived monocytes (Yona *et al*., 2013). In contrast, intestinal macrophages are replenished by blood-derived monocytes throughout childhood (Na *et al*., 2019). It is still under debate exactly which sub-populations of macrophages reside in intestinal tissue, however, it is believed to contain a heterogenous population of macrophages that are functionally distinct (De Schepper *et al*., 2018). For example, in a mouse model, it was discovered two separate populations of macrophages exist that are transcriptionally different. These included $TIM4^{-}$ $CD4^{-}$ macrophages that were blood-derived monocyte dependent, and long-lived, tissue resident, $TIM4^{+}$ $CD4^{+}$ macrophages that were blood derived-monocyte independent (Shaw *et al*., 2018). It has also been shown that the gut contains the largest pool of tissue resident macrophages in the body (Nakanishi *et al*., 2015). Intestinal-resident macrophages display a more immune regulatory, anergic phenotype due to their proximity to the gut microbiome (Rubio and Schmidt, 2018). Intestinal resident macrophages have a downregulation of receptors for LPS (CD14),

IL-2, IL-3, and complement factors C3 and C4 compared to blood monocytes from the same donor (Smythies *et al*., 2005). They have a downregulation in the production of proinflammatory cytokines associated with TLR ligands, such as TNFα, IL-1 and IL-6, and instead have increased bactericidal activity through increased phagocytic capabilities (Smythies *et al*., 2005). They also maintain homeostasis in the gut through the production of anti-inflammatory ligands such as IL-10 and prostaglandin E2 (Platt *et al*., 2010). The downregulation of pro-inflammatory cytokines in intestinal-resident macrophages was found to be regulated by TGF-β, a cytokine produced in intestinal epithelial cells, which highlights the crosstalk between the two cell types (Smythies *et al*., 2005). Crosstalk between the intestinal epithelium and the immune system has also been highlighted by work from Courth *et al*., (2015), which illustrated ligands from the peripheral blood mononuclear cell (PBMC) secretome, such as Wnt ligands, aided in the formation HD5 and HD6 in Paneth cells, which could not be induced by independent factors such as cytokines and infections.

Studies have illustrated an imbalance in homeostatic macrophage populations during colitis, with proinflammatory-blood derived monocytes (CD14+) being recruited within the lamina propria and a lack of expansion of regulatory tissue resident macrophages (Bain *et al*., 2013). Human biopsies from active IBD patients have also been shown to have an elevation in chemokine expression that promotes monocyte recruitment, including *CCL7* and *CCL8* (Bain *et al*., 2013). In addition, CD-associated monocytes exhibit a reduced production in Wnt ligands, suggesting an impairment in immune cell function that in turn can lead to Paneth cell dysfunction, due to the lack of Wnt-associated receptor activation (Courth *et al*., 2015). A decrease in granulocyte-macrophage colony-stimulating factor (GM-CSF) signalling activity, a ligand that promotes the differentiation of monocyte into regulatory macrophages, has been found to increase the risk of CD (Lotfi *et al*., 2019). An increase in GM-CSF specific autoantibodies and a decrease in the expression of CD116, a receptor specific to the GM-CSF ligand, on blood-derived monocytes has been observed in the serum of CD patients (Däbritz, 2015). Monocyte-derived macrophages (MDM) from CD patients are also more susceptible to infection with AIEC and persistent replication compared to MDM's from healthy controls and UC patients (Vazeille *et al*., 2015). AIEC persistency is commonly found in CD patients, which can cause chronic inflammation due to their

ability to invade epithelial cells and induce a TH17-associated proinflammatory response (Small *et al*., 2013)

Table 1 - Differences between blood-derived and intestinal-derived macrophages

Blood-Derived Macrophages	Intestinal-Resident Macrophages
TIM4- CD4-	TIM4+ CD4+
High expression of innate response receptors (CD14, CD89, CD11b)	Reduced expression costimulatory molecules (CD40, CD80 and CD86) Increased expression of chemokine receptor CX3CR1
Phagocytic activity leading to immune cell activation	Increased phagocytic activity without subsequent immune activation
Hyper-responsive to pathogen stimuli	Hypo-responsive to pathogen stimuli
High expression of TREM-1 leading to increased pro-inflammatory mediators (TNF-a, IL-1β, IL-6)	Absence of TREM-1
High Pro-inflammatory cytokine production in response to PRR activation (TNF-α, IL-1β, IL-6 and nitric oxide)	Production of anti-inflammatory cytokines IL-10 and TGF-β

1.4.3. Autophagy genes associated with CD

CD-associated SNPs have been identified within autophagy-related genes, including *autophagy-related protein 16-1* (*ATG16L1)* and *immunity-related GTPase family protein M* (IRGM) (Massey & Parkes, 2008). Autophagy regulates multiple aspects of intestinal homeostasis ranging from bacterial clearance, antigen presentation, goblet cell function and host defence peptide production within Paneth cells, all of which can be impaired in IBD (El-Khider and McDonald, 2016). Impairment in the function of *ATG16L1* allows the growth and persistency of opportunistic pathogens, AIEC and *Mycobacterium avium paratuberculosis* in macrophages, pathogens that have been speculated to trigger IBD-associated inflammation (Lapaquette *et al*., 2012; McNees *et al*., 2015). The *ATG16L1 T300A* variant associated with autophagy dysfunction is

found in up to 30% of CD patients (Hampe *et al*., 2007). In addition, the *ATG16L1 T300A* variant increases the susceptibility for disease risk by 3-fold in paediatric patients (Salem *et al*., 2015)

SNPs associated with *ATG16L1* have been found to impact the unfolded protein response (UPR) to endoplasmic reticulum (ER) stress. SNPs within the UPR-associated genes, *XBP1* and *ORMDL3,* have been identified as risk factors for IBD (Kaser *et al*., 2008). Interestingly, an increase in autophagy is observed in *XBP1* -/- mice, which correlated with increased presence of ER stress markers including phosphorylation of eif2α and ATF4 (Adolph *et al*., 2013). The increased presence of proteins associated with ER stress was also found in the intestinal mucosa of IBD patients and healthy controls harbouring the *ATG16L1 T300A* variant, indicating the importance of functional autophagy within UPR/ER stress signalling (El-Khider and McDonald, 2016). These studies provide evidence that CD-associated polymorphisms regulate autophagy activity, and that autophagy is a key mechanism utilised by other pathways implicated in CD pathogenesis such as the ER-stress/UPR.

1.4.4. Autophagy

Macro-autophagy (referred henceforth as ‘autophagy’) is an evolutionarily conserved homeostatic lysosomal degradation pathway that involves the degradation and recycling of cellular constituents that range from misfolded proteins to damaged organelles through the use of a unique double membrane-bound vesicle, known as an autophagosome (Fritz *et al*., 2011). Physiologically, its function regulates cell remodelling and prevents premature cell aging through the degradation of damaged proteins and organelles. Autophagy functions at a basal level to maintain homeostasis within protein and organelle turnover. However, it can also be induced as a survival response through the presence of stress stimuli such as hypoxia, starvation and infection (King, *et al.*, 2011). The stimulation of autophagy as a survival response was first characterised in yeast by Ohsumi and colleagues who observed the gradual increase of spherical bodies, which were termed autophagic bodies, when grown in a nutrient deprived media (Takeshige *et al*., 1992) . Autophagy is activated in response to multiple physiological stresses including hypoxia, nutrient deficiency, cellular toxins and pathogen invasion (Badadani, 2012). Autophagy regulates a diverse range of

cellular processes, including cell fate, growth, oxidative stress, organelle turnover and cell differentiation (Badadani, 2012). Due to the wide range of physiological roles that autophagy is involved in, it has been linked to the pathophysiology of a growing number of diseases in addition to IBD, including cancer, neurodegenerative diseases, infectious diseases and metabolic diseases such as type 2 diabetes (Jiang and Mizushima, 2014)

1.4.5. The autophagy pathway

Autophagy performs its homeostatic function by encapsulating target constituents (cargo) in a vesicle termed an autophagosome, which is then able to fuse with a lysosome to form an autophagolysosome where cargo are degraded by lysosomal proteases (Wong *et al*., 2011). As illustrated in **Figure 4**, autophagosome formation can be split into four distinct steps. These are the initiation and encapsulation of cargo within a double membrane called a phagophore, the maturation of the phagophore to form an autophagosome, the fusion of a lysosome to form an autophagolysosome and finally the degradation of the cargo within the autophagolysosome (Moulis and Vindis, 2017).

The process of autophagy is regulated by the intricate interaction between autophagy related (Atg) proteins. The role of various Atg proteins have been extensively reviewed (Klionsky, 2005; Yorimitsu and Klionsky, 2005), however, this study will primarily focus on the importance of ATG16L1 and Atg8 (also known as LC3 in its mammalian ortholog) during autophagy. Two distinct ubiquitin-like conjugation systems are crucial for the extension and sealing of the autophagosomal membrane, these two conjugation systems are the Atg12 conjugation system and the LC3 conjugation system (El-Khider and McDonald, 2016). The Atg12 conjugation system involves the recruitment of the ATG12-ATG5-ATG16L1 complex, which begins with the conjugation of Atg12 to Atg5 that is catalysed by both Atg7 and Atg10 (Ohsumi and Mizushima, 2004). During this event, the LC3 conjugation system is activated beginning with the processing of proLC3 by the cysteine protease, ATG4, to expose its carboxyl terminal glycine that creates the cytosolic form of LC3, LC3-I (Tanida *et al*., 2004). In nutrient rich conditions, LC3-I is widely distributed across the cytoplasm and nucleus (Ladoire *et al*., 2012). However, when autophagy is stimulated such as

during starvation, LC3 becomes redistributed where nuclear LC3 congregates within the cytoplasm through the deacetylation of LC3 by Sirt1 (Lee and Lee, 2016). Once LC3 is accumulated in the cytosol, ATG7 and ATG3 are activated, which allows the formation of an ATG3-LC3 intermediate (Ohsumi and Mizushima, 2004). This intermediate interacts with ATG12 within the ATG12-ATG5-ATG16L1 complex through ATG3 and allows the recruitment of the ATG3-LC3 to the infant autophagosome membrane, which causes LC3 to become conjugated to phosphatidylethanolamine (PE) (Fujita *et al*., 2008). The conjugation of LC3 to PE defines the transformation of LC3-I to LC3-II and allows the anchoring of the substrate to the autophagosomal membrane. LC3 is thought to be involved in the expansion and closure of the autophagosomal membrane (Lapaquette *et al*., 2015). LC3-II is also critical for selective autophagy as specific autophagy cargo receptors such as p62, NBR1 and NDP52 contain LC3-interacting regions (LIR) that are able to bind to LC3 and allow the cargo to undergo degradation (Hansen and Johansen, 2011). Most of the ATG proteins are only found on the isolation membranes but not on the autophagosomes themselves, only LC3 has been found to be fused to the autophagosome throughout the autophagy process. LC3 is removed from the autophagosomal membrane at the end of the process during the fusion of the lysosome, where it either is cleaved from the outer membrane by Atg4 for re-use or is degraded on the inner membrane through lysosomal enzymes. This therefore allows LC3 to be widely used marker for the formation of autophagosomes (Mizushima *et al.*, 2010).

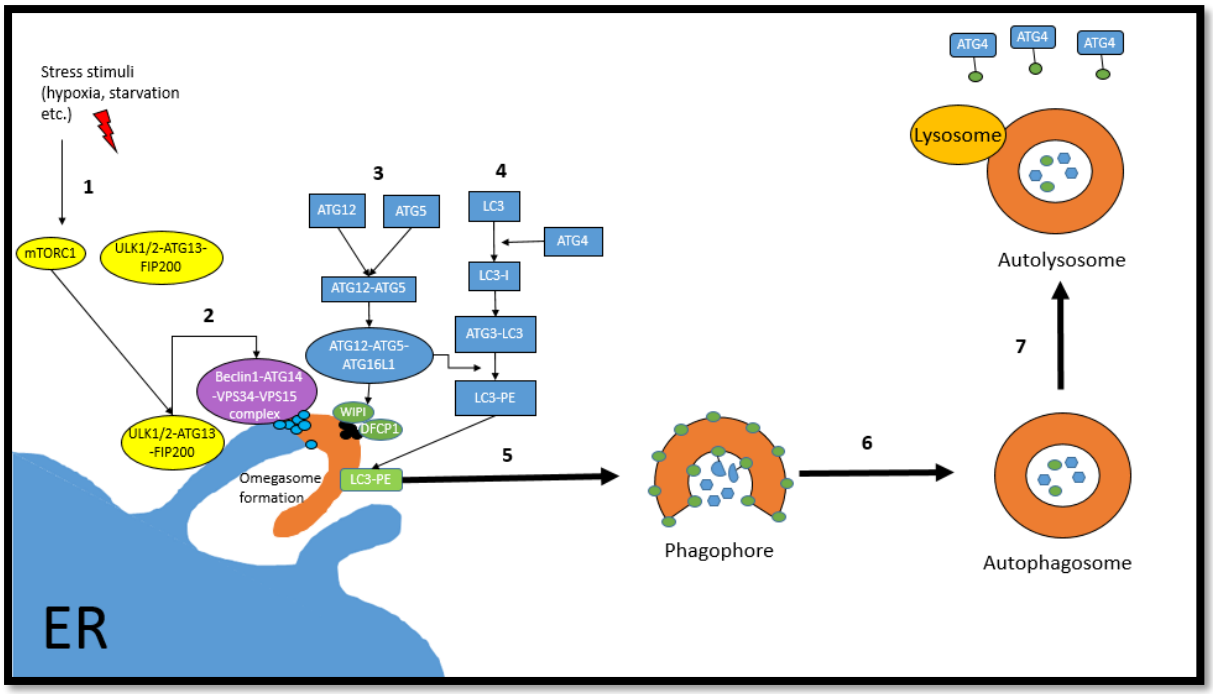

Figure 4 - Autophagosome formation.

Author's illustration of the molecular mechanisms within autophagosome formation **1.** Dissociation of mTORC1 from ULK1/2-ATG13-FIP200 complex due to the presence of stress stimuli **2.** ULK complex activates Beclin1-ATG14-VPS34-VPS15 complex on the ER surface. VPS34 (teal) marks the area of phagophore formation (omegasome) **3.** VPS34 synthesises PI3P that accumulates (Black) and is recognised by WIPI and DFCP1 that allows the recruitment of ATG12-ATG5-ATG16L1 complex **4.** Cytosolic LC3-I is converted to LC3-PE through the interaction with ATG12 within the ATG12-ATG3-ATG16L1 complex. LC3-PE conjugation allows it to be anchored to the autophagosomal membrane **5.** Omegasome becomes detached from the ER to form a phagophore in which LC3-II (green) covers both the outer and inner membrane. LC3 is involved in the expansion and closure of the membrane. LC3 is also involved in the anchoring of specific cargo within the membrane through the interaction with LIR on constituents. **6.** Full closure of the phagophore results in the formation of the autophagosome, a vesicle that encapsulates constituents preparing them for degradation **7.** The lysosome binds to the autophagosome releasing lysozymes that degrade the constituents. LC3 on the outer membrane is removed through the interaction with ATG4 to be recycled and LC3 within the inner membrane is degraded along with the constituents.

1.4.6. Autophagy Signalling

The regulation of autophagy in response to stress stimuli primarily involves signalling through mammalian target of rapamycin complex 1 (mTORC1) and AMP-activated protein kinase (AMPK) (El-Khider and McDonald, 2016). The initiation of autophagy utilises two specific protein kinases, which are the ULK1/2-ATG13-FIP200 complex and the Beclin1-Vps34-Vps15-ATG14 complex that are regulated through interactions with mTORC1 and Bcl2, respectively. In nutrient rich conditions, the mTORC1

complex is bound to the ULK1/2-ATG13-FIP200 complex and inhibits ULK1/2 kinase activity through the phosphorylation of ULK1/2 and ATG13 (Lapaquette *et al*., 2015). AMPK under physiological conditions is inhibited due to the high concentrations of ATP within the cell (El-Khider and McDonald, 2016). However, once the cell is exposed to a stress stimuli, the mTORC1 complex becomes inactive through AMPK (in the presence of increased intracellular AMP production) and allows the dissociation of the ULK complex (Pezze *et al*., 2016). This allows the ULK complex to recruit and activate the Beclin1-ATG14-Vps34-Vps15 complex to the membrane that is marked by ATG9, subsequently allowing the recruitment of ATG proteins such as ATG16L1 and LC3 and the induction of phagophore formation (Lamb *et al*., 2013; Lapaquette *et al.*, 2015). Specifically, Vps34, a class III phosphatidylinositol 3-kinase, marks the area in which phagophore develops from the ER through the formation of a structure called an omegasome, a pre-phagophore structure which is rich in PI3P (Axe *et al*., 2008). The accumulation of PI3P by the formation of the omegasome is recognised through effector molecules such as DFCP1 and WIPI that allows the important recruitment of the ATG12-ATG5-ATG16L1 complex, which is crucial for the elongation process (Devereaux *et al*., 2013; Lapaquette *et al*., 2015). The ER is well regarded as a major organelle for autophagosome biogenesis (Karanasios *et al*., 2013). However other, sources have been implicated in autophagosome biogenesis including the mitochondria, plasma membrane and the Golgi apparatus (Hailey *et al*., 2010; Geng *et al*.,2010; Ravikumar *et al*., 2011). For example, the mitochondria and ER have been found to communicate through mitochondria-associated membranes (MAMs), and disruption of MAMs leads to an impairment of autophagosome formation during starvation (Hamasaki *et al*., 2013). This is thought to be due to MAMs assisting the production of ATG4 and STX17, major proteins in autophagosome closure and some have speculated that MAMs are the site of origin for autophagosome formation (Hamasaki *et al*., 2013; Tsuboyama *et al*., 2016)

1.4.7. Intersection of NOD2 and autophagy in IBD

NOD2 has been shown to functionally intersect with ATG16L1, with NOD2 recruiting ATG16L1 to the plasma membrane during bacterial infection (Travassos *et al*., 2010). Interestingly, in the presence of the *1007fs* mutation found in NOD2, ATG16L1 does not localise to the plasma membrane during bacterial invasion (Travassos *et al*., 2010). Triggering of other functional PRR's, which have been known to induce

autophagy, could not compensate for the impairment in the NOD2-ATG16L1 signalling axis, leading to increased bacterial burden in the cell (Cooney *et al*., 2010) CD-associated DC's that harbour NOD2 variants were found to have a significant increase in bacterial persistency when infected with AIEC, which could be reversed when treated with the autophagy inducer, rapamycin (Cooney *et al*., 2010). Silencing of autophagy-related genes also resulted in a decrease in MHC II surface expression and antigen presentation within DC's (Cooney *et al*., 2010). NOD2 has also been associated with Paneth cell phenotype; patients containing one or more *NOD2* susceptibility alleles exhibit an increase in Paneth cell abnormalities compared to individuals with wild type *NOD2*. The frequency of Paneth cell abnormalities is further increased in individuals containing both the *NOD2* and *ATG16L1 T300A* variant (Vandussen *et al*., 2014). Therefore, impaired bacterial handling and immune priming caused by defective autophagy, through genetic factors, may be a key inducer of CD-associated inflammation.

1.4.8. Intestinal barrier integrity

SNP's have also been identified in genes associated with intestinal epithelial barrier integrity, such as *CDH1*, and genes associated with mucus production such as *AGR2* and *MUC2* (Antoni *et al*., 2014; McCole, 2014). *MUC2* is a critical gene associated with mucin production by intestinal goblet cells, which coats the outer epithelial surface and reduces the rate of invasion and colonisation of bacteria on the mucosa surface (Kim and Cheon, 2017; Van der Sluis *et al*., 2006). Interestingly, missense mutations within *MUC2* resulted in mice developing spontaneous distal intestinal inflammation, which was similar to the phenotype observed within UC (Heazlewood *et al*., 2008). AGR2 regulates the disulphide bond formation in proteins present in the ER (Park *et al*., 2009). AGR2 has also been found to be decreased in CD and UC patients (Zheng *et al*., 2006). Due to the high expression of AGR2 in Paneth cells and goblet cells, *AGR2* -/- mice exhibit abnormalities such as decrease in mucus production, a reduction in goblet cells, dysfunctional Paneth cells and spontaneous colitis (Zhao *et al*., 2010)

1.4.9. Epithelial Barrier Integrity in IBD

Intestinal epithelium integrity regulates the interaction of the microbiota and immune cells within the lamina propria, allowing restricted passage of small amounts of

bacteria for antigen sampling and immune surveillance (Slack *et al*., 2009). As shown in **Figure 5**, increased intestinal epithelial permeability allows an influx of pathogens, toxins and food antigens to initiate an inflammatory response, which is thought to be one of the underlying mechanisms for IBD pathogenesis (Kim and Cheon, 2017) A breakdown of epithelial barrier integrity, through double negative mutations within N-cadherin (involved in calcium-dependent cell to cell adhesion) has been found to develop IBD-like ileitis in mice highlighting the importance of epithelial barrier integrity in IBD (Hermiston and Gordon, 1995). In addition, total regeneration of the intestinal epithelial barrier, which has been termed mucosal healing, increases the likelihood of long-term remission and a reduced need for surgical treatment in IBD patients. (Okamoto and Watanabe, 2016).

Interestingly, mutations in genes directly linked to epithelial barrier integrity, such as MUC2, result in spontaneous colitis in murine models. In contrast, mutations in genes that are not directly associated with intestinal epithelium result in an increased susceptibility to dextran sodium sulphate (DSS) induced colitis (Hooper *et al*., 2019). For example, the *L1007fs* mutation in NOD2 and LRRK2 deficiency, which regulates immune signalling, were found to increase susceptibility to DSS-induced colitis (Liu *et al*., 2011; Maeda *et al*., 2005). IBD-associated colitis is only initiated with these factors in the presence of chemical inducers of colitis, such as DSS, which substitutes environmental triggers of IBD including intestinal bacteria, viruses, dietary antigens and reactive oxygen species (ROS) (Heazlewood *et al*., 2008). The importance of epithelial barrier integrity is supported by studies that show deletion of *ATG16L1* in intestinal epithelial cells (IEC) develop spontaneous ileitis (Tschurtschenthaler *et al*., 2017). However, deletion of *ATG16L1* in hematopoietic cells enhances susceptibility to DSS-induced intestinal barrier disruption in mice (Saitoh *et al*., 2008; Tschurtschenthaler *et al*., 2017). These findings suggest that the breakdown of the intestinal epithelium is the key initiator of IBD-associated colitis, and mutations not directly associated with the intestinal epithelium increase susceptibility and require an environmental trigger to initiate epithelium barrier breakdown.

1.4.10. Composition of the intestinal epithelial barrier

Specialised intestinal epithelial cells such as Paneth Cells and goblet cells, have been linked to IBD pathogenesis (Kim and Cheon, 2017). A reduction in goblet cells and

mucus production is a common pathological finding in IBD patients (Van der Sluis *et al*., 2006). MUC2 has also been found to be deficient in UC patients and correlated with disease severity (Larsson *et al*., 2011). In addition to mucus secretion, goblet cells depletion may impact in mucosal immunity as they are the primary producers of IL-7 in the colonic mucosa (Oshima *et al*., 2004; Watanabe *et al*., 1998). IL-7 is a pleotropic cytokine that regulates the proliferation of mature and immature T cell lineages. IL-7 has been found to selectively regulate effector T-cell migration to the gut through the regulation a $\alpha_4\beta_7$ integrin expression (Belarif *et al*., 2019). IL-7 has also been found to be deficient in the serum of untreated CD patients compared to treated patients (Andreu-Ballester *et al*., 2013). Therefore, there is supporting evidence to suggest that intestinal epithelial cells aid in regulation of mucosal immunity.

Paneth cells are another epithelial cell lineage that have been closely associated with IBD pathogenesis. As shown on **Figure 5**, Paneth cells are located in the crypts of the lumen and maintain intestinal homeostasis through the secretion of host defence peptides such as α-defensins and RegIIIγ (Wilson *et al*., 1999). Research on Paneth cell function is limited by the fact that there are no available cell lines derived from Paneth cell lineages (Courth *et al*., 2015). Furthermore, cell lines, such as colon cancer cell lines, often contain mutations in the Wnt pathway, a pathway heavily linked with defensin production and secretion (Courth *et al*., 2015). The importance of Paneth cell function in intestinal homeostasis is supported by findings that deletion of *Mmp7*, a metalloprotease involved in the processing of α-defensins, results in increased susceptibility to *salmonella typhimurium* infection in the intestinal mucosa (Wilson *et al*., 1999). Paneth cell dysfunction has also been found to regulate microbiota composition, with a reduction in anti-inflammatory associated bacterium including *Faecalibacterium* and an increase in pro-inflammatory bacterium *Erysipelotrichacae* found within paediatric CD patients (Vandussen *et al*., 2014). A common characteristic found in ileal CD patients is a reduction in the secretion of HD5 and HD6, indicating an impairment in Paneth cell function (Courth *et al*., 2015). Interestingly, researchers such as Adolph *et al*., (2013) have provided evidence to suggest that the inflammation observed in CD originates from Paneth cells, with dysfunction in Paneth cells leading to transmural inflammation in the form of skip lesions seen in CD. In addition, Paneth cells abnormalities have been directly correlated with granuloma formation, a common characteristic of CD-associated inflammation (Vandussen *et al*., 2014). Researchers

have also proposed Paneth cell abnormalities as a possible molecular biomarker for disease severity, by grouping patients with the presence of CD susceptibility loci, which has been associated with immune activation, a reduction in Paneth cell secretion and disease reoccurrence (Vandussen *et al*., 2014).

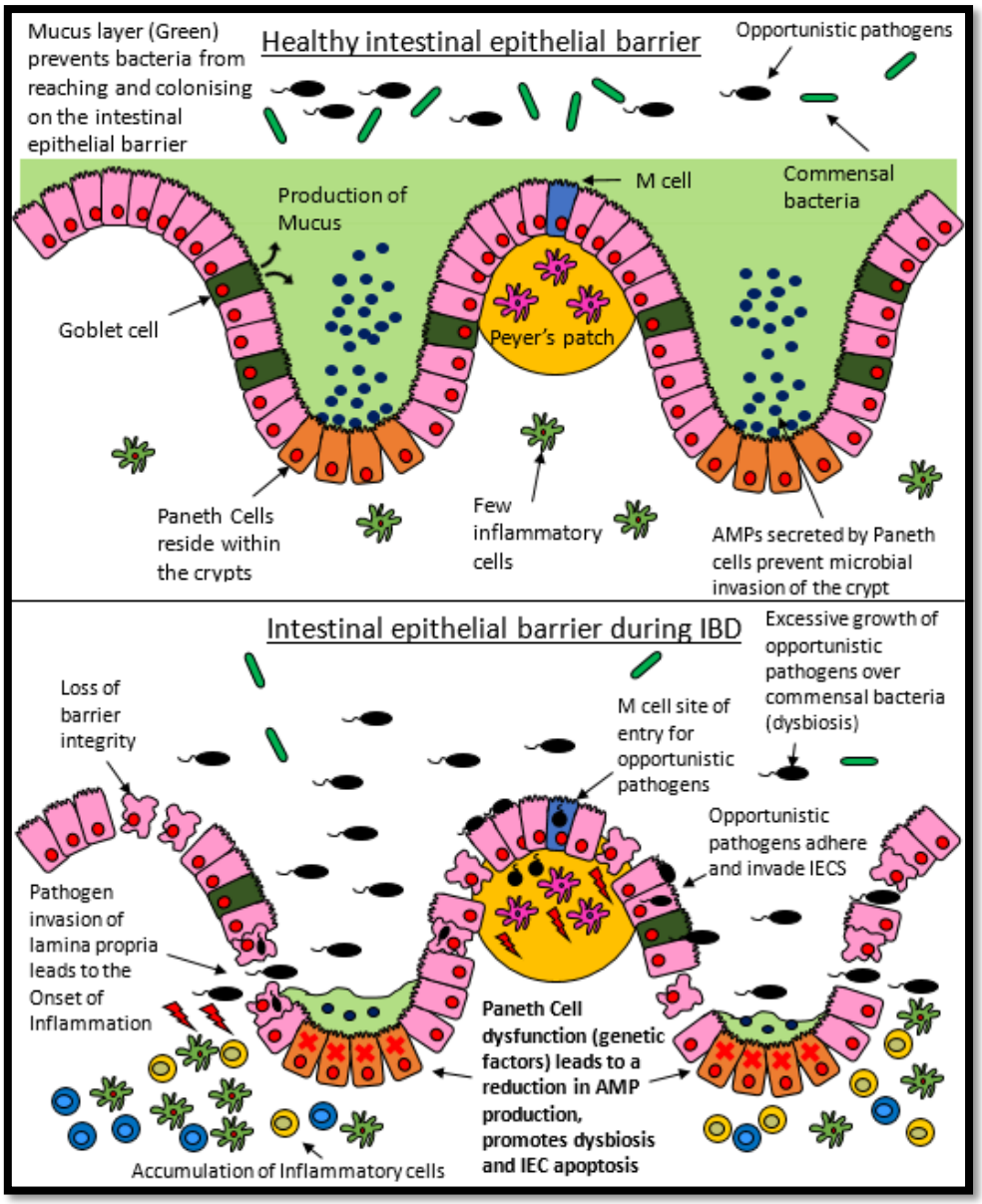

Figure 5 - Intestinal Epithelial Barrier during IBD.

Author's representation of the association of the intestinal epithelial barrier during the pathogenesis of IBD. The diagram above represents the healthy mucosal layer in which the intestinal epithelial barrier is intact and successfully separating the microbiome and the effector cells within the lamina propria. It achieves this through the production of mucus by goblet cells and the production of host defence peptides by Paneth cells within the crypts of Lieberkühn. The bottom diagram illustrates the intestinal epithelial barrier during IBD where barrier integrity is lost through multiple factors. One crucial factor, as shown in bold, is the dysfunction in Paneth cells that leads to a loss of HDP (AMP) production, breakdown of the protective barrier and promotes dysbiosis, which can result in the onset of inflammation.

1.5. ER Stress

The ER is a complex organelle mainly responsible for the synthesis, folding and movement of proteins, phospholipids and steroids across the cell (Schröder and Kaufman, 2005). The ER also contains the largest storage of calcium ions in the cell and regulates calcium concentrations through sarcoplasmic/endoplasmic reticulum calcium-ATPases and inositolo 1,4,5-triphosphate receptors that pump calcium between the cytoplasm and ER (Corazzari *et al*., 2017; Schröder and Kaufman, 2005). Calcium plays a critical role in cell metabolism, muscle contraction and apoptosis. In addition, many post-translational modifications, such as glycosylation, are calcium-dependent (Schröder and Kaufman, 2005). Many external insults can disturb the homeostatic balance between the accumulation and breakdown of proteins in the ER, these include hypoxia, nutrient starvation, infection and xenobiotics (Walczak *et al*., 2019). These factors can increase workload in the ER and lead to an accumulation of misfolded and unfolded proteins within the cell, known as ER stress. Sustained ER stress in the cell will lead to the activation of cell-death associated pathways and the initiation of apoptosis for the removal of compromised cells (Sano and Reed, 2013).

1.6. The Unfolded Protein Response

Eukaryotes have developed an adaptive mechanism to resolve ER-stress and maintain homeostasis and cell survival, this mechanism is known as the UPR (Chakrabarti *et al*., 2011). The UPR resolves ER stress by halting global protein synthesis, directing misfolded proteins to the ER-associated degradation (ERAD) pathway and increasing the folding capacity within the ER through membrane expansion and the synthesis of chaperone proteins (Cao and Kaufman, 2012). ERAD is separated into two subtypes, known as type 1 ERAD and type 2 ERAD. Type 1 ERAD involves the retro translocation of misfolded proteins through the ER membrane to the cytosol where they undergo ubiquitination and degradation through 26S proteasomes (Hampton, 2002). Type 2 ERAD is autophagy dependent, which targets insoluble forms of misfolded proteins which cannot be degraded by type 1 ERAD (Rashid *et al*., 2015). Autophagy was initially proposed to be induced only when misfolded proteins become too excessive for ERAD to degrade (Rashid *et al*., 2015). However, Houck *et al*., (2015) has found that both types of ERAD are activated simultaneously, where type 2 ERAD eliminates soluble ERAD-resistant misfolded

proteins, including aggregated proteins unable to enter the proteolytic chamber within the proteasome. As shown in **Figure 6**, the UPR consists of three main signalling pathways, inositol-requiring enzyme 1 (IRE1) pathway, double-stranded RNA-activated protein kinase (PKR)-like kinase (PERK) pathway and the activation transcription factor 6 (ATF6) pathway (Chakrabarti *et al*., 2011). IRE1, PERK and ATF6 are ER-resident transmembrane receptors which sense misfolded proteins through their luminal domain (LD) present on each receptor (Carrara *et al*., 2013). BiP (GRP78) is one of the most abundant chaperone proteins within the ER and assists in protein folding by preventing aggregation of polypeptide chains during the adolescent stages of protein folding (Adams *et al*., 2019). The function of BiP during the regulation of UPR signalling has been debated in depth elsewhere (Adams *et al*., 2019). However, it is widely accepted that BiP plays a sequestering role within IRE1, PERK and ATF6, which binds to the LD of each receptor preventing dimerization and the activation downstream signalling events in normal ER homeostasis (Adams *et al*., 2019).

1.6.1. IRE1 signalling

During ER stress, BiP becomes dissociated from each of the membrane embedded UPR sensors, regulating the activation of downstream UPR signalling (Gardner *et al*., 2013). IRE1 is the most conserved UPR sensor and is found in mammals, yeast and metazoans (Chen and Brandizzi, 2013). As a consequence of BiP dissociation, oligomerisation of IRE1 occurs, which allows the activation of the endoribonuclease effector domain that is present on IRE1 (Sidrauski and Walter, 1997). An increase in endonuclease activity leads to the splicing of 26 nucleotides from X-box binding protein 1 (XBP1) to a form a potent transcription factor, spliced XBP1 (XBP1s) (Adams *et al*., 2019). XBP1s contains a C-terminal transactivation domain and can translocate to the nucleus to upregulate the transcription of UPR-associated genes including those involved in ER biogenesis, ERAD, and protein folding (Wu *et al*., 2015). An increase in endonuclease activity also induces a process known as regulated IRE1-dependent decay (RIDD), where there is an increase in the degradation of ER membrane-localised mRNA, leading to a reduction in protein synthesis (Hollien and Weissmann, 2006). Cell fate will also be determined through the IRE1 pathway, which will initiate apoptosis through the selective degradation of UPR-associated genes by RIDD that will increase ER stress within the cell, driving apoptotic signalling (Chen and Brandizzi,

2013). RIDD will also increase apoptotic signalling through the degradation of anti-apoptotic microRNAs such as anti-*Casp2,* allowing the upregulation of the pro-apoptotic marker, caspase-2 (Upton *et al*., 2013).

1.6.2. PERK pathway

Dissociation of BiP from PERK leads to the autophosphorylation and dimerization of the receptor (Chakrabarti *et al*., 2011). Activation of PERK leads to the downstream phosphorylation of the α subunit (S51) within eukaryotic translation initiation factor 2α (eif2α) (Gebauer and Hentze, 2004). Eif2α is a vital component in protein translation initiation, therefore phosphorylation prevents the separation of eIF2α from eIF2B, thus preventing global translation initiation (Gebauer and Hentze, 2004). In combination to protein translation inhibition, PERK leads to the increase in pro-survival genes such as cellular inhibitor of apoptosis (cIAP), maintaining cell survival (Hamanaka *et al*., 2009). Genes containing an internal ribosome entry site sequence in their 5' untranslated region will be protected from translation inhibition, the most well-established of these genes is *ATF4* (Schröder and Kaufman, 2005). ATF4 plays both a pro-survival and pro-apoptotic role in the UPR. ATF4 can induce a pro-survival response by regulating protein secretion and amino acid transport, however, ATF4 can also induce the expression of pro-apoptotic genes, including C/EBP homologous protein (CHOP) (Harding *et al*., 2000). Sustained activation of CHOP will lead to the induction of apoptosis by the repression of Bcl-2, which is negatively correlated with CHOP expression (Wei *et al*., 2008).

1.6.3. ATF6 pathway

ATF6 is similar to IRE1 and PERK, where activation is regulated through the dissociation of BiP, which is thought to be regulated by N-terminal Golgi localization sequences in ATF6 (Chakrabarti *et al*., 2011). However, ATF6 is unique to PERK and IRE1 as it not activated through the phosphorylation of its C-terminal kinase domain. Instead, ATF6 translocates to the Golgi apparatus, where undergoes a series of irreversible proteolytic processes, including the cleavage of its LD by serine protease site-1 protease (S1P) and metalloprotease site 2-protease (S2P) (Shen and Prywes, 2004). Cleavage allows the ATF6's transcriptional domain, at 50kDa, to translocate to the nucleus where it regulates genes that contains ATF-cAMP response elements (Wang *et al*., 2000). This allows the upregulation of UPR-associated genes including

BiP, protein disulphide isomerase, and ERAD-associated ER degradation-enhancing alpha-mannosidase-like protein 1 (EDEM1) (Chakrabarti *et al*., 2011). UPR pathways also appear to be interlinked, as EDEM1 is also induced through the IRE1 pathway and ATF6 induces the expression of XBP1 (Yoshida *et al*., 2001). XBP1 signalling appears to be a negative regulator of ATF6 signalling, as findings from Yoshida *et al*., (2009) identified that an increase in XBP1u leads to a reduction in ATF6 signalling. XBP1u binds to ATF6α, leading to proteasomal degradation of the protein (Yoshida *et al*., 2009). ATF6 also regulates cell fate by inducing the expression of regulator of calcineurin 1 (RCAN1). RCAN1 can inhibit calcineurin 1 expression, which prevents the sequestering of Bcl-2 and therefore prevents pro-apoptotic signalling (Chakrabarti *et al*., 2011). Therefore, it appears that all UPR signalling pathways have a direct involvement in cell survival and apoptotic signalling.

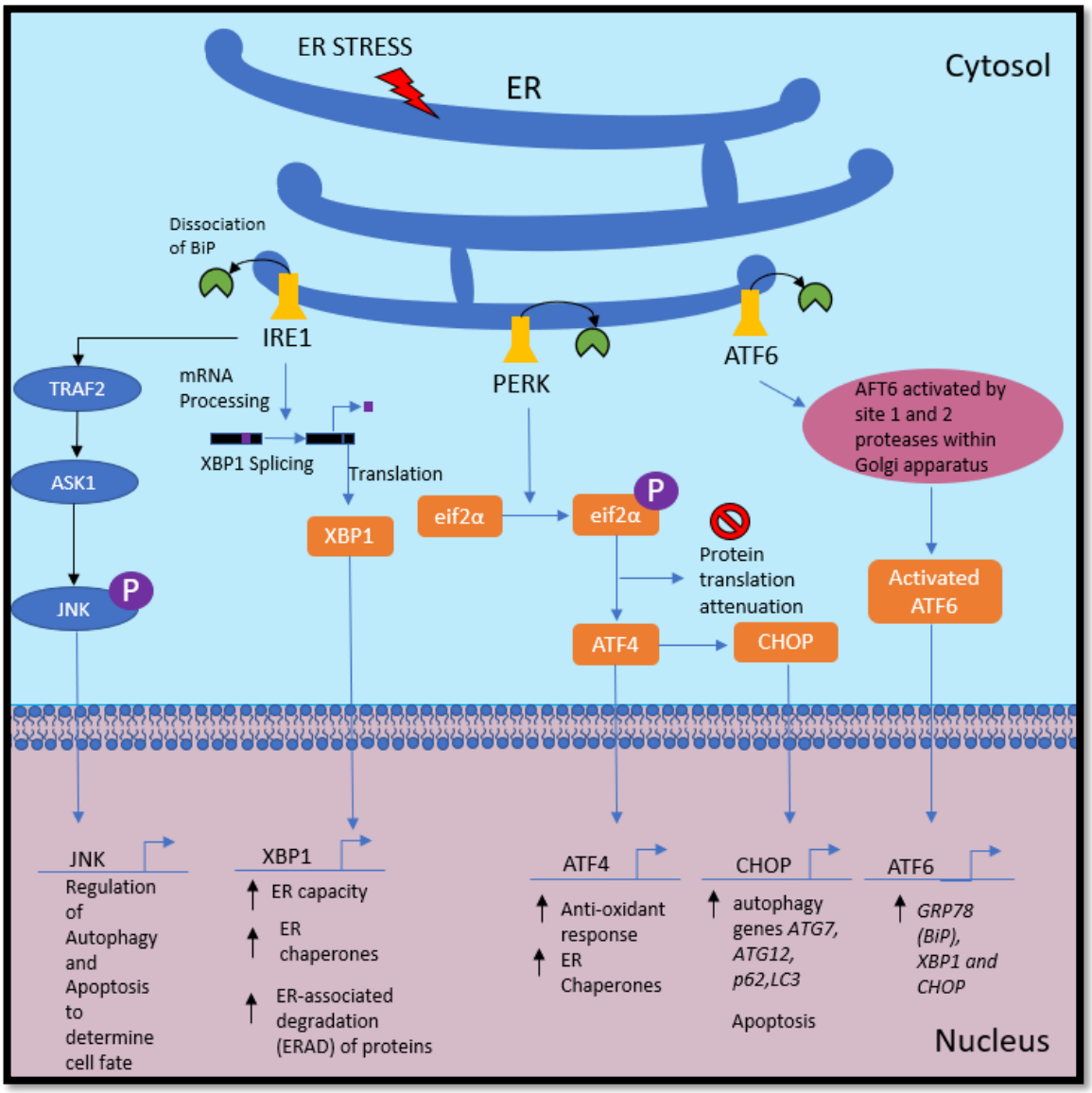

Figure 6 - UPR signalling during ER stress.

Author's representation of the three UPR arms which regulate proteostasis during ER stress. Activated IRE1 allows the splicing of XBP1, which increases protein folding and overall quality control of the proteins produced. XBP1 also increases the capacity of the ER through lipid biogenesis to cope with the increased stress. The PERK arm allows the phosphorylation of eif2α, which inhibits further protein production and allows the activation of ATF4. Increased ATF4 can determine cell fate through the manipulation of autophagy and apoptotic signalling. ATF4 also regulates the oxidative stress response during the presence of accumulating ROS. ATF6 is activated within the Golgi apparatus and subsequently allows the increased expression of UPR genes BiP, XBP1 and CHOP.

1.7. ER Stress and UPR signalling in IBD

As discussed previously, Paneth cell dysfunction has been linked to IBD, with susceptibility genes such as *NOD2* and *ATG16L1* being found to regulate α-defensin production and intracellular granule formation within Paneth cells respectively (Okamoto and Watanabe, 2016). Around 30% of newly synthesised proteins are misfolded during their formation within normal conditions (Liu *et al*., 2016). Therefore, highly secretory cells, such as Paneth cells, are more susceptible to elevated ER stress due to the increased likelihood of the accumulation of misfolded proteins within the ER, which can be induced through inflammatory mediators and microorganisms within the intestine (Kaser *et al*., 2008a).

The UPR is critical in maintaining cell homeostasis during ER stress and the ability for the UPR to activate autophagy to degrade misfolded proteins is crucial **(Figure 7)** (Ogata *et al*., 2006). Autophagy has been shown to be induced by the UPR through the induction of the PERK-eIF2α pathway. The PERK-eIF2α pathway transcribes ATF4 and CHOP, which can subsequently activate autophagy genes *p62, Atg16L1 and Map1lc3B* that all contain similar amino acid response elements (B'Chir *et al*., 2013). Adolph *et al*. (2013) concurred with the previous statement indicating variants within *XBP1* induced autophagy to compensate for the lack of UPR activation. When *Xbp1* null mice were treated with the mTORC1 inhibitor, rapamycin, there were a significant decrease in enteritis, NF-κB activation and apoptosis of cells. This effect was not observed within *ATG16L1/Xbp1* and *Atg7/Xbp1* null mice, indicating the importance of functional autophagy within inflammation (Adolph *et al*., 2013). It was also discovered silencing of *ATG7* and *XBP1* gave rise to discontinuous submucosal inflammation that was similar to what is seen in CD; indicating that insufficient autophagy activity is key to the inflammatory phenotype (Adolph *et al*., 2013). Without sufficient autophagy activity, sustained MAPK8 activation would occur leading to the dissociation of Bax from Bcl-2 and caspase-3 activation. This would lead to apoptosis of the cells and impair IEC barrier integrity (Wei *et al*., 2008).

The ER stress within Paneth cells caused by the *T300A* variant within *ATG16L1* has also been correlated with bacterial persistence (Deuring *et al*., 2014). This correlates with studies that have shown that NOD2, which regulates bacterial persistence, utilises autophagy to remove pathogens (Travassos *et al*., 2010). NOD2 has also been found

to induce IRE1α dependent splicing of *Xbp1,* a common UPR transcription factor that has been known to induce autophagy through *BECLIN-1* transcription (Margariti *et al*., 2013). This illustrates that NOD2, UPR and the autophagy pathway are interlinked and the inability for these pathways to induce autophagy is one of the key reasons for susceptibility to IBD.

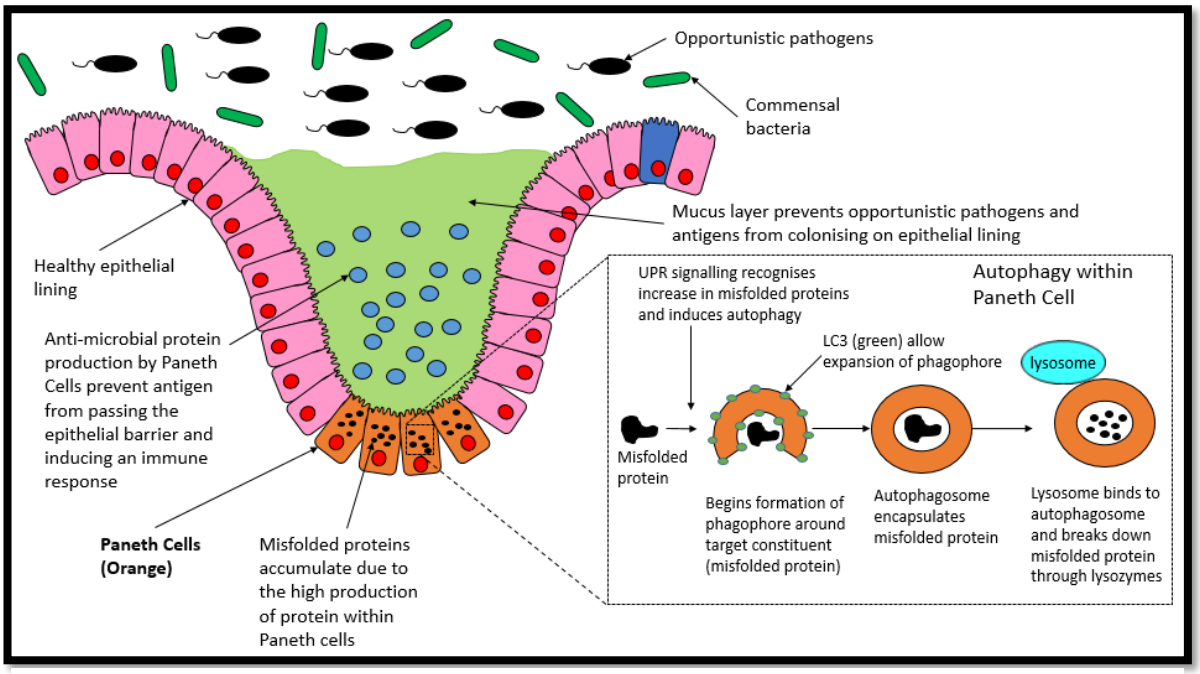

Figure 7 - The Function of Paneth cells and autophagy in Intestinal epithelium physiology.

Misfolded proteins accumulate within Paneth cells (orange) due to the high production of host defence peptides in the cell. Misfolded proteins that are generated during this process are removed through autophagy.

1.8. Clinical Relevance of Thiopurines

Thiopurines, which include azathioprine (AZA), 6-mercaptopurine (6-MP) and 6-thioguanine (6-TG), have been commonly used in IBD treatment as an immunosuppressant (Kapur and Hanauer, 2019). As shown on **(Figure 8)**, AZA is converted to 6-MP through a conjugation reaction using glutathione (GSH) (Eklund *et al*., 2006). The drug then undergoes a series of metabolic reactions to form two main metabolic groups that are the phosphorylated thioguanine nucleotides (6-TGNs), and methylated thioinosine phosphates (Atreya and Neurath, 2008). The nucleotides can then intercalate into genomic DNA that can lead to nucleotide mispairing and cell cycle arrest; ultimately causing immunosuppression and cytotoxicity (Stocco *et al*., 2015). Thiopurines are given to IBD patients to maintain remission, as meta-analysis data has shown that 73% of CD patients treated with AZA maintain remission over an 18-month period compared to 62% in a control group (Chande *et al*., 2015)

Discussion has been raised to the effectiveness of thiopurines as a monotherapy, as the onset of its therapeutic action ranges from 12-17 weeks from the beginning of treatment (Goel *et al*., 2015). For example, infliximab and AZA treatment together was found to be more effective in inducing and maintaining remission in patients compared to infliximab or AZA alone (Colombel *et al*., 2010). In addition, an increase of 24.1% in steroid free remission was observed in patients treated with combination therapy compared to monotherapy alone (D'Haens, 2008). The anti-metabolite effect of thiopurine treatment is only effective in relatively high doses, such as with oncological treatment, therefore the mechanism of action is not fully elucidated (Seinen *et al*., 2016). This is reinstated by the fact only 10-45% of IBD patients respond effectively to the treatment (Chaabane and Appell, 2016). In addition, 30% of IBD patients are forced to discontinue treatment due to adverse effects associated with thiopurines, including hepatoxicity and myelotoxicity (Haglund *et al*., 2013). Thiopurines could be exerting their effects in part through the modulation of the autophagy pathway. It was identified during thiopurine-induced hepatotoxicity, autophagy was increased to protect hepatocytes from the deleterious effects of thiopurines (Guijarro *et al*., 2012). This was supported by Chaabane & Appell *et al*. (2016) who illustrated autophagy was a protective mechanism preventing apoptosis through the removal of damaged mitochondria, preventing the accumulation of ROS.

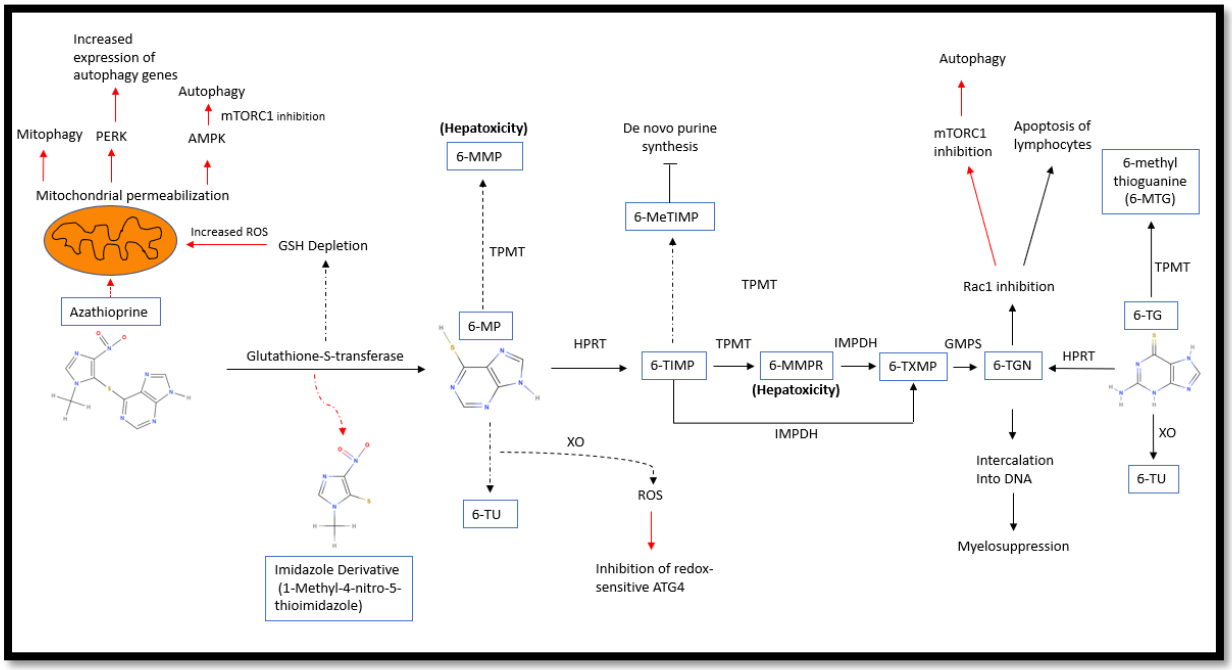

Figure 8 - The Metabolism of Thiopurines.

AZA is metabolised into 6-MP which is then subsequently metabolised further in 6-TGN. 6-TGN can either intercalate within DNA or inhibit RAC1 to cause immunosuppression. 6-TG bypasses the metabolic steps to be converted to 6-TGN by hypoxanthine-guanine phosphoribosyl transferase (HPRT). The arrows highlighted in red are hypothesised ways in which autophagy could be induced during thiopurine metabolism. Abbreviations: Thiopurine methyltransferase (TPMT), 6-methyl mercaptopurine (6-MMP), 6-methyl mercaptopurine ribnucleotide (6-MMPR), inosine monophosphate dehydrogenase (IMPDH), 6-thioguanine nucleotide (6-TGN), xanthine oxidase (XO), 6-methylthioinosine monophosphate (6-MeTIMP), guanosine monophosphate synthetase (GMPS), thiouric acid (TU), thioinosine monophosphate (6-TIMP), 6-thioxanthosine monophosphate (6-TXMP).

1.8.1. Potential Mechanism of Action of Thiopurines

As highlighted in red in **Figure 8**, many pathways could be involved in the stimulation of autophagy during thiopurine treatment. One of the key findings by Hooper *et al*., (2019) is that AZA-induced autophagy was attenuated in the presence of a PERK inhibitor, indicating PERK activation is critical in autophagy stimulation observed during thiopurine treatment. The mitochondria are severely affected during thiopurine treatment, with mitochondrial permeabilisation and increased ROS production being commonly observed (Chaabane and Appell, 2016). PERK has been previously found to be an oxidative stress sensor during extracellular matrix detachment and induces autophagy to relieve ROS accumulation (Avivar-Valderas *et al*., 2011). PERK has also been found to regulate communication between the mitochondria and ER through MAM's, by working as a tether and conveying pro-apoptotic signals during ROS-mediated ER stress (Verfaillie *et al*., 2012). In addition, PERK regulates mitochondrial morphology during ER-stress and protects the mitochondria by inducing the expression of parkin through ATF4, a known inducer of mitophagy (degradation of the mitochondria by autophagy) (Bouman *et al*., 2011; Lebeau *et al*., 2018). Therefore, there is the possibility that PERK plays a cytoprotective role within the mitochondria during thiopurine treatment; and this subsequent activation relieves ER stress within the cell.

One of the key unpublished findings by Hooper *et al*., (2019) was that the metabolite 6-MP was not as strong an inducer of autophagy as AZA, suggesting that the metabolism of AZA may be a key factor involved in autophagy stimulation. Two critical steps have been found to take place during the conversion of AZA to 6-MP. The first is the displacement of the imidazole ring which is present on the structure of AZA. This is due to the conversion of AZA to 6-MP by biogenic thiols, such as GSH, which allows the detachment of methyl-4-nitro-5-imidazole (Warner *et al*., 2016). The therapeutic action of imidazole derivatives during AZA metabolism has been briefly explored by Crawford *et al*., (1996), which hypothesised that imidazole heteroarylation of thiol groups enriched on lymphocyte membranes could be responsible for its immunosuppressive effects. Particular imidazole conjugates have also illustrated PI3K inhibitory activity (Mohan *et al*., 2016). If the imidazole derivatives that are released during AZA metabolism also exhibited the same inhibitory effect towards PI3K, this could explain how AZA could be inducing autophagy activity.

The second critical step during AZA metabolism is the consumption of intracellular GSH within the cell (Eklund *et al*., 2006). There are a variety of different mechanisms in which GSH consumption could potentially induce autophagy activity. Examples of this are the production of ROS during GSH depletion, potentially regulating ATG proteins such as thiol containing ATG4. Mitophagy has also been shown to be regulated by intracellular GSH within yeast cells (Deffieu *et al*., 2009). In addition, deletion of the glutathione-S-transferase subtype, GSTM1, resulted in a reduction in the response to AZA within IBD patients (Stocco *et al*., 2014a)

Hooper *et al*., (2019) also observed mTORC1 inhibition during AZA treatment. However, the inhibition of PERK did not affect mTORC1 activity, indicating that mTORC1 inhibition may be upstream or parallel to PERK during thiopurine treatment. The 6-TGN metabolite, 6-thioguanine-triphosphate, has been found to induce apoptosis within CD4+ cells through the inhibition of Rac1 (Tiede *et al*., 2003). Interestingly, Rac1 has been shown to mediate the localisation of mTORC1 to the cellular membrane within serum stimulated HeLa cells (Saci *et al*., 2011). Therefore, AZA could induce autophagy through the inhibition of mTORC1 by the suppression of Rac1. This concept is supported from a study that identified that the *ATG16L1* risk allele resulted in Rac1 hyperactivation and these individuals responded more effectively to thiopurine treatment (Wildenberg *et al*., 2017). mTORC1 and PERK signalling have been linked through an array of different mechanisms that differ depending on stress stimuli and proliferation rate of cells (Gandin *et al*., 2016). Therefore, it is critical to characterise the activity of these pathways during thiopurine treatment within cell lines that are relevant to IBD, such as IEC's and macrophages. mTORC1 has also been linked to other UPR signalling pathways, with mTORC1 inhibition leading to prolonged IRE1 clustering and increased splicing activity (Sanchez-Alvarez *et al*., 2017). It would therefore also be of interest to determine whether other UPR signalling pathways are activated, and if so, how they interact with mTORC1 during thiopurine treatment.

1.9. Research aims

Autophagy is dysfunctional in IBD patients, and pharmaceutical induction of autophagy may be therapeutically beneficial for the treatment of IBD (Mutalib *et al*., 2014). Previous studies have shown that AZA modulates autophagy activity independent of apoptosis through mechanisms involving the UPR kinase, PERK, and mTORC1. However, thiopurine metabolites, 6-MP and 6-TG, have not been investigated in this context.

The aims of this study are to:

- Characterise the effects of thiopurines on autophagy pathway activity.
- Investigate the effects of thiopurines on apoptosis.
- Characterise the effects of thiopurines on ER-stress/UPR signalling.
- Assess mTORC1 signalling in response to thiopurine treatment.

Chapter 2. Materials and Methods

2.1. Cell Culture

Human embryonic kidney 293 cells (HEK293) stably expressing GFP-LC3 (a gift from Dr Craig Stevens) were grown in Dulbecco's modified eagle's media (DMEM) (Gibco, Thermofisher Scientific, Paisley, UK) supplemented with 10% FBS (Gibco) and 1% penicillin/streptomycin (Gibco). Cells were incubated at 37°C in 5% CO_2 and were passaged every 2-3 days. THP-1 cells were grown in Roswell park memorial institute (RPMI) 1640 (Sigma-Aldrich, Irvine, UK) supplemented with 10% FBS, 1% L-glutamine (Gibco) and 1% penicillin/streptomycin. THP-1 cells were incubated at 37°C in 5% CO_2 and were passaged every 2-3 days. THP-1 monocytes were differentiated into macrophages by growth in RPMI supplemented with 20ng/ml of phorbol 12-myristate 13-acetate (PMA) (Tocris, Bristol, UK) for 48 hours, then rested for 24 hours in fresh RPMI prior to experiments.

2.2. Transfection and plasmids

Adherent THP-1 derived macrophages were detached from tissue culture plates using accutase 1 (PromoCell, Heidelberg, Germany) collected into 15ml falcon tubes (Falcon, Corning International, US) and centrifuged at 250xg for 10 minutes (Pendragon, Scientific Ltd). Supernatant was aspirated and cell pellets were resuspended in 100µl nucleofector solution (Lonza, Manchester, UK). 0.5µg of GFP-RFP-LC3 plasmid (A gift from Dr Craig Stevens, Edinbugh Napier University UK) was then added to the cell suspension, gently mixed and transferred to a nucleofector cuvette (Lonza). Cells were electroporated using the Y-001 programme according to the manufacturer's instructions with the Nucelofector 2b device (Lonza). Fresh RPMI (500µl) was added to the transfected cells and the cell suspension combined with a further 1ml of RPMI in a 6-well plate. Cells were incubated for 24hrs prior to analysis or further treatment.

2.3. Cell treatments

Cells were washed using 0.9% isotonic NaCl prior to treatment. Pharmacological agents were reconstituted and stored in Dimethyl Sulfoxide (DMSO, Sigma). Pharmacological agents were diluted to a working concentration in culture media and cells were treated for an appropriate incubation time. An equivalent amount of DMSO was used as a vehicle control. Incubation times and concentrations used for the optimisation of techniques was derived from previous findings by Hooper *et al*. (2019). All pharmacological agents used are detailed in **(Table 2)**.

Table 2 - Pharmacological Agents

Agent	Stock Concentration	Working Concentration	Incubation time (Hours)	Manufacturer
AZA	100mM/ml	20-120µM	0-24	Tocris
6-MP	90mM/ml	20-120µM	0-24	Tocris
6-TG	10mg/ml	20-120µM	0-24	Tocris
IL-13	100µg/ml	20ng/ml	24	Sigma
IL-14	100µg/ml	20ng/ml	24	Invivogen
LPS	5mg/ml	100ng/ml	24	Invivogen
IFN-γ	1mg/ml	20ng/ml	24	Peprotech
PMA	100µg/ml	5-20ng/ml	48	Tocris
Tunicamycin	5mg/ml	5µg/ml	8	Sigma
Brefeldin A	10mg/ml	1µg/ml	8	Cayman
Bafilomycin	1mg/ml	160nm	8	Santa Cruz Biotechnology

2.4. Western immunoblotting

Cells were washed with phosphate buffered saline (pH 7.4) (PBS) (Sigma), detached from tissue culture plates using 0.5% Trypsin-EDTA (Gibco), transferred into Eppendorf tubes, and centrifuged at 3000 RPM for 5 minutes. Supernatant was removed and cell pellets frozen at -80°C or lysed on ice for 30 minutes in buffer containing 1 x protease and phosphatase inhibitor cocktail (50mM Tris pH8, 150mM NaCl, 1mM EDTA and 1% NP-40). Lysates were then centrifuged at 12,000 RPM at 4°C for 5 minutes and supernatants stored at -20°C.

Protein concentration of lysate was measured using Bradford assay by adding 5µl of sample or BSA standard to 195µl of Bradford Reagent (Sigma-Aldrich) and measuring absorbance at 595nm using an MRX II absorbance reader (LT-5000 MS ELISA Reader).

25µg of protein lysate and 5µl of PageRuler Plus prestained protein ladder (Thermo Scientific) were resolved by sodium dodecyl sulfate-polyacrylamide gel electrophoresis (SDS-PAGE) at 180V for 50 minutes using a stacking gel (pH 6.8) and an 8-12% acrylamide resolving gel (pH 8.8). SDS-PAGE gels were manufactured using a Biorad casting frame. Resolving gel (30% Acrylamide, 1.5M Tris pH 8.85, 10% SDS, 10% Ammonium Peroxidosulphate, TEMED) was initially added to the casting frame with an additional layer of isopropanol to prevent the formation of air bubbles. Isopropanol was removed from the casting frame and an additional layer of stacking gel (30% Acrylamide, 1M Tris pH 6.68, 10% SDS, 10% Ammonium Peroxidosulphate, TEMED) was poured into the casting gel containing solidified resolving gel. A comb was placed into the stacking gel while the gel solidified. Electrophoresis was performed using a Mini-PROTEAN Tetra Vertical Electrophoresis cell (Bio-Rad, UK). Proteins were electrotransferred onto nitrocellulose membrane in Tris-Glycine buffer for 60 minutes at 100V, using a Mini-PROTEAN Cell. The efficiency of protein transfer was analysed by ponceau staining (Sigma). Membranes were blocked either with 10% non-fat skimmed milk (Marvel) or 5% BSA in PBS + 0.1% Tween (PBS/T) for 1 hour. Primary antibodies, diluted to 1:1000-1:2000 in PBS/T supplemented with either 10% Marvel or 5% BSA (VWR Chemical, Pennsylvania, US), were incubated with membrane at 4°C, overnight, and subsequently washed 3x with PBS/T for 5 minutes **(Table 3)**. Membranes were incubated with a secondary antibody diluted to either 1:2000-1:4000 in PBS/T supplemented with 10% Marvel or 5% BSA for 1 hour at RT, washed 3x in PBS/T for 5 minutes, and proteins visualised using an Odyssey imaging system (LI-COR Biosciences) **(Table 3)**.

Table 3 - Antibodies

Target Antigen	Antibody Type	Dilution	Diluent	Manufacturer
LC3	Rabbit Polyclonal	1:1000	1% FBS/PBS	MBL
Anti-Rabbit	HRP-conjugated Goat (680LT)	1:2000	5% BSA in PBS/T	Dako
CD163	Mouse Monoclonal	1:40	PBS	Biolegend
CD80	Mouse Monoclonal	1:40	PBS	Biolegend
CD68	Mouse Monoclonal	1:40	PBS	Biolegend
P-Eif2α	Rabbit Monoclonal	1:500	5% BSA in PBS/T	Cell Signalling
Total-Eif2α	Mouse Monoclonal	1:1000	10% Marvel in PBS/T	Invitrogen
Anti-Rabbit	HRP-conjugated Goat (800CW)	1:2000	5% BSA in PBS/T	Odyssey
EDEM1	Rabbit Polyclonal	1:1000	10% Marvel in PBS/T	Novus Bio
P-S6 Ribosomal Protein	Rabbit IgG	1:1000	5% BSA in PBS/T	Cell Signalling
Total-S6 Ribosomal Protein	Mouse IgG1	1:1000	10% Marvel in PBS/T	Cell Signalling
Beta-Actin	Rabbit Monoclonal	1:2000	10% Marvel in PBS/T	Cell Signalling
Anti-Mouse	HRP-conjugated Goat (800CW)	1:2000	10% Marvel in PBS/T	Odyssey
Anti-Mouse	HRP-conjugated Goat (680LT)	1:2000	10% Marvel in PBS/T	Dako

2.5. Fixed cell imaging

Cells were seeded in a 6-well plate (Costar, Corning international) containing a sterile 22mm coverslip (VWR international) and grown to 70-80% confluence. After appropriate treatment with pharmacological agents, cells were washed with PBS (Sigma) and fixed to the coverslip by incubating with PBS-4% Paraformaldehyde (PFA) (Sigma, Aldrich) for 15 minutes.

For cell lines stably expressing GFP-LC3, cells were washed in PBS, mounted directly onto slides, and nuclei stained using Vectashield mounting media with DAPI (Vector, Vector Laboratories). Coverslips were sealed around the edges to prevent dehydration using nail varnish and images captured using an LSM 880 confocal microscope with ZenBlue software (Carl Zeiss).

For staining with antibodies, cells were permeabilised by incubation with 0.1% Triton X (Fisher, Biosciences) for 10 minutes, washed with PBS and blocked for 30 minutes with 10% FBS at RT. Cells were again washed in PBS and incubated with primary antibody overnight at 4°C **(Table 3)**. Cells were subsequently washed in PBS and incubated with the secondary IgG antibody in the dark, at RT, for 1 hour. Coverslips were processed and images of cells captured using an LSM 880 confocal microscope as described above.

2.6. Live cell imaging

HEK293 cells stably expressing GFP-LC3 were grown in glass bottom plates (IBIDI, Gräfelfing, Germany) until the cells reached 70-80% confluence, then treated with pharmacological agents as appropriate and images captured on an LSM 880 confocal microscope (Zeiss) every 20 minutes for 24 hours. Cell growth conditions were maintained at 37°C and 5% CO2 for the duration of the experiment using a live cell imaging chamber (Pecon, Temperature and CO_2 controller 2000).

2.7. Autophagy Assays

Basal number of autophagosomes in untreated GFP-LC3 engineered HEK293 cells was determined to be between 1-4 LC3 puncta. Therefore, HEK293 cells exhibiting >5 LC3 puncta were regarded as having an induction of autophagy activity. Basal number of autophagosomes in untreated THP-1 derived macrophages was determined to be between 1-5 LC3 puncta. Therefore, THP-1 derived macrophages exhibiting >6 LC3 puncta were regarded as having an induction of autophagy activity. For fixed cell imaging utilising GFP-LC3 and immunostained LC3, LC3 puncta was quantified from 10 cells in 3 separate fields of view. For live cell imaging, LC3 puncta from 30 cells was quantified from one image every 2 hours. 30 cells were selected based upon previous autophagy-based investigations using immunofluorescence imaging, which counted between 20-50 cells (Biskou *et al*., 2019; Rai and Manjithaya, 2015; Runwal *et al*., 2019). Induction of autophagy was calculated as the percentage of cells over the set threshold for basal autophagy activity.

Basal threshold of GFP-RFP-LC3 puncta plus RFP-LC3 puncta in THP-1 macrophages was determined to be between 1-7 LC3 puncta. Therefore, any GFP-RFP-LC3 transfected THP-1 macrophage exhibiting >8 LC3 puncta was regarded as

exhibiting an induction of autophagy activity. As shown on **Figure 9**, an increase in RFP-LC3 foci is an indicator of an increase in autophagy activity. Therefore RFP-LC3 foci were quantified in GFP-RFP-LC3 THP-1 derived macrophages to determine an increase in autophagy activity. Ten cells transiently expressing GFP-RFP-LC3 were quantified from each treatment group. An increase in autophagy activity was calculated as the percentage of RFP-LC3 puncta in relation to the number of total puncta in each cell.

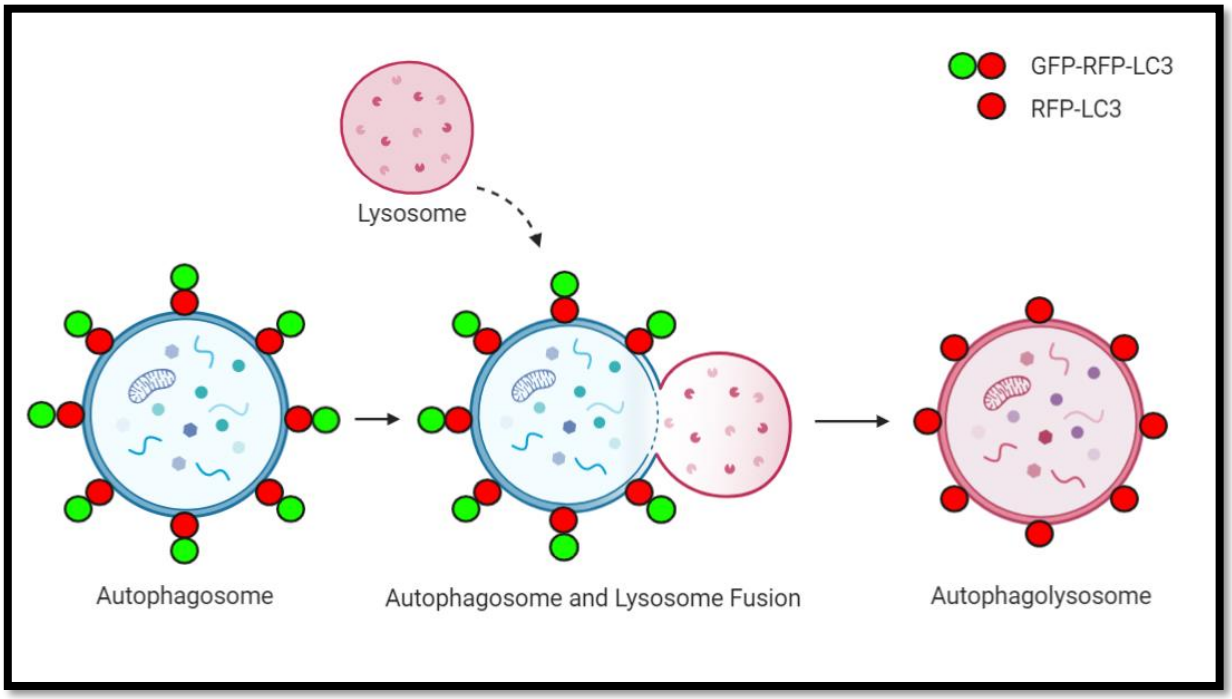

Figure 9 - Analysis of autophagy flux.

GFP-RFP-LC3 is bound to autophagosomes, which results in yellow fluorescence. During autophagolysosome formation, GFP fluorescence becomes quenched due to the low pH within the lysosome, whereas RFP remains stable, therefore autophagolysosomes fluoresce red. Image created using biorender software.

2.8. Real time quantitative PCR (RT-qPCR)

After appropriate treatment in 60mm^2 dishes, cells were scraped into PBS, and centrifuged at 3000 RPM for 5 minutes at 4ºC. Supernatant was removed and cell pellets were immediately frozen at -80ºC. Total RNA was extracted from pelleted cells using TRIsure (Bioline) according to manufacturing instructions and quantified using a NanoDrop 2000 spectrophotometer (Thermo Scientific). RNA integrity and quantity

were measured using an Agilent 2100 Bioanalyser according to manufacturer's instructions. 2μg of total RNA was reverse transcribed to cDNA using a High-Capacity RNA-to-cDNA kit (Applied Biosystems) following manufacturer's instructions with the inclusion of a no reverse transcriptase control for each treatment to control for genomic DNA contamination. For qPCR gene expression analysis, each reaction contained 25ng cDNA template, 150nM forward and reverse primer **(Table 4)**, PrecisionPlus qPCR Master Mix (Primer Design) and DEPC-treated water. A no-template control, which contain DEPC-treated water instead of cDNA, was used to monitor reagent contamination and potential primer-dimer formation. qPCR was performed and analysed using a StepOnePlus Real-time PCR system (Applied Biosystems).

A geNorm kit (Primerdesign) was used to select appropriate reference genes using qbase+ software. the $2^{-\Delta\Delta CT}$ method was used for relative quantification of gene expression.

2.9. Reverse transcription PCR (RT-PCR)

After appropriate treatment in 60mm^2 dishes cDNA was prepared as described above. Initially the presence of *actin* was evaluated to determine if RNA was successfully reverse transcribed and to determine the presence of genomic DNA contamination within control samples lacking reverse transcriptase. A mastermix was prepared containing Mango Mix (BioLine), 100pm/μl Actin forward and reverse primer (see **Table 4** for primer sequences), 50ng cDNA template and DEPC-treated water. For investigation of *XBP1*, the master mix composed of Mango Mix (BioLine), 100pm/μl XBP1 forward and reverse primer, 100ng cDNA and DEPC water. A no-template control, which contain DEPC-treated water instead of cDNA, was used to monitor reagent contamination. DNA amplification was performed within a 2720 thermocycler (Applied Biosystems) using the following conditions: 95°C for 5 minutes, cycle 35x at 95°C for 15 seconds, 56°C for 15 seconds,

72°C for 30 seconds and finally 72°C for 5 minutes. PCR products were resolved by electrophoresis on a 1% agarose gel and PCR products visualised using a G:Box System (Syngene, Cambridge, UK).

Table 4 - Primer Sequence

Target Gene	Forward Primer	Reverse Primer	Amplicon Size	Manufacturer
XBP1	GGAGTTAAGACAGCGCTTGGGGA	TGTTCTGGAGGGGTGACAACTGGG	164 & 138	Eurofins (UK)
Actin	GGGAAATCGTGCGTGACATT	CCACAGGACTCCATGCCC	202	Eurofins (UK)
EDEM1	CGGACGAGTACGAGAAGCG	CGTAGCCAAAGACGAACATGC	96	Eurofins (UK)
PERK	GGAAACGAGAGCCGGATTTATT	ACTATGTCCATTATGGCAGCTTC	111	Eurofins (UK)
ATF4	CTCCGGGACAGATTGGATGTT	GGCTGCTTATTAGTCTCCTGGAC	165	Eurofins (UK)
CHOP	AGCTGGAAGCCTGGTATGAGG	GTGCTTGTGACCTCTGCTGG	178	Eurofins (UK)
BiP	TATGGTGCTGCTGTCCAGGC	CTGAGACTTCTTGGTAGGCACC	162	Eurofins (UK)

2.10. Flow Cytometry

THP-1 derived macrophages (MO) were polarised to either M1 or M2 macrophages by incubation for 24 hours with IFN-γ (20ng/ml) and LPS (100ng/ml) or IL-4 (20ng/ml) and IL-13 (20ng/ml) respectively. Cell morphology was examined on a Primovert brightfield light microscope (Zeiss) and cells harvested by gentle scraping, washed with PBS, and incubated with M0 macrophage marker CD68, M2 macrophage marker CD163 and M1 macrophage marker CD80 **(Table 3)** in the dark for 15 minutes. Samples were then examined using flow cytometry (FACSCalibur, BD Medical Technology). Threshold for all treatment groups was set to 5000 events and stopping events to 10,000.

2.11. Annexin/PI Staining

Cells were stained using the TRITC Annexin V Apoptosis Detection Kit (BD Pharmingen). Briefly, cells were detached from the dish using accutase I for 30 minutes and transferred into a FACS tube. Cells were then washed twice in PBS, counted, and resuspended in Annexin V binding buffer at a concentration of $1x10^6$/ml. 100ul of cell suspension was transferred into a 5ml FACS tube and 5ul of Brilliant

Violet 421 Annexin V and 5ul of PI solution (BD Pharmingen) were added to the cell suspension. Cells were gently vortexed and left to incubate for 15 minutes at RT in the dark. 400ul of Annexin V binding buffer was added and analysed on a flow cytometer (FACSCelesta, BD Biosciences). Experimental staining controls were utilised to set gating parameter and voltage compensation. Voltages and compensation can be found in **Table 4 and Table 5,** respectively. Threshold for all treatment groups was set to 5000 events and stopping events to 10,000. Staining controls included untreated cells and cells treated with deionised H_20 for 30 minutes. Annexin V fluorescence was measured at an excitation wavelength of 405nm and an emission wavelength of 421nm. PI fluorescence was measured at an excitation wavelength of 488nm and an emission wavelength of 610nm. Cell viability was assessed through fluorescence of Annexin and PI on the cell surface. Annexin V^- PI^- cells were grouped as viable cells, Annexin V^+ PI^- cells as early apoptotic cells, and Annexin V^+ PI^+ as late apoptotic/necrotic cells.

Table 5 – Voltage parameters

Parameter	Voltage
FSC	330
SSC	244
BV421	229
PerCP-Cy5-5	538

Table 6 – Compensation

Fluorochrome	- % Fluorochrome	Spectral Overlap
PerCP-Cy5-5	BV421	76.24
BV421	PerCP-Cy5-5	64.73

2.12. Alamar Blue Assay

Pharmacological agents, prepared in growth media, were supplemented with 10% Alamar blue reagent (Invitrogen) prior to incubation with THP-1-derived macrophages in a 96-well plate for up to 24 hours. A no-cell control group was also incubated with 10% Alamar blue. An excitation wavelength of 544nm and emission wavelength of 590nm was measured in 2-hour cycles using an MRX II absorbance reader (LT-5000 MS ELISA Reader) and Manta software (Dynex Technologies, Worthing, UK). Absorbances were corrected to the no-cell control using MRX II software version 2.1. According to manufacturer's instructions, metabolic activity was calculated using the following calculation:

FI590: Fluorescent intensity at 544nm excitation (590nm emission)

$$\text{Percentage difference between treated And control cells} = \frac{(\text{FI590 of test agent treated cells} - \text{FI590 of media only})\ \text{x}100}{(\text{FI590 of untreated cells} - \text{FI590 of media only})}$$

2.13. Statistical Analysis

Due to time constraints, optimisation-based experiments were performed once, therefore statistical analysis was not evaluated. Statistical analysis was performed using GraphPad Prism version 7.0 (GraphPad Software, CA, USA) for experiments performed in triplicate. Quantitative results were expressed as ± Standard Error Mean (SEM). One-way ANOVA was performed with either Tukey's or Dunnett's multiple comparisons test, as appropriate.

Chapter 3. Induction of autophagy by thiopurines in HEK293 cells

3.1. Introduction

Thiopurines have previously been shown to modulate autophagy activity (Chabbane and Appell, 2016; Hooper *et al*, 2019). Chabbane and Appell, (2016) demonstrated that autophagy induction by thiopurines in colorectal cancer cells was a secondary cytoprotective effect that prevented apoptosis. In contrast, Hooper *et al.,* (2019) demonstrated that AZA induces autophagy independent of apoptosis via mechanisms involving modulation of mTORC1 signalling and stimulation of the UPR sensor PERK. Additionally, Oancea *et al*., (2016) showed that 6-TG enhanced autophagy in a TGN-dependent manner in gut epithelial cell lines, with 6-TG also reducing intracellular bacterial replication. Therefore, the initial aim was to assess modulation of autophagy in response to thiopurine treatment in HEK293 cells, a human embryonic kidney cell line that has been well characterised in terms of autophagy activity and have a very high efficiency for transfection (Musiwaro *et al*., 2013). HEK293 cells engineered to stably express the autophagy marker LC3 fused to green fluorescent protein (GFP-LC3) were available in the laboratory, therefore, initial characterisation of autophagy was carried out in HEK293 GFP-LC3 stable cells. HEK293 GFP-LC3 cells have the added advantage that live cell imaging of autophagy can be performed, as cell permeabilization is not required to visualise GFP-LC3.

Hypothesis: Thiopurines will induce autophagy in HEK293 GFP-LC3 cells, independent of apoptosis.

Aim 1) To characterise autophagy induction in response to thiopurine treatment.

Aim 2) To compare live-cell imaging and fixed-cell imaging for the measurement of autophagy induction in response to thiopurine treatment.

Aim 3) Assess thiopurine cytotoxicity and effects on induction of apoptosis.

3.2. Results

3.2.1. Live cell imaging of thiopurine induced autophagy

Live cell imaging was used to assess the modulation of autophagy over a 12h time course in thiopurine-treated HEK293 GFP-LC3 cells. As shown in **Figure 10,** all thiopurines tested induced an accumulation of autophagosomes. The largest increase in autophagosomes was observed at the 8h time point, with a 60% increase in cells exhibiting >5 LC3 puncta in response to AZA, a 57% increase in cells exhibiting >5 LC3 puncta in response to 6-MP, and a 37% increase in cells exhibiting >5 LC3 puncta in repose to 6-TG relative to control cells **(Figure 11)**. At the 12h time point an accumulation of autophagosomes was also observed in control cells, with 26% of cells exhibiting >5 LC3 Puncta. Therefore the 8h time point was selected for future experiments due to low levels of basal autophagy observed in control cells. AZA induced autophagosome accumulation more rapidly than 6-MP and 6-TG, with a 63% increase in cells exhibiting >5 LC3 puncta in response to AZA, a 6% increase in cells exhibiting >5 LC3 puncta in response to 6-MP, and a 13% increase in cells exhibiting >5 LC3 puncta in response to 6-TG relative to the control at the 4h time point **(Figure 11)**. Taken together these results suggest that all of the thiopurines tested induce autophagosome accumulation in HEK293 cells and that AZA induces autophagosome accumulation more rapidly than 6-MP and 6-TG.

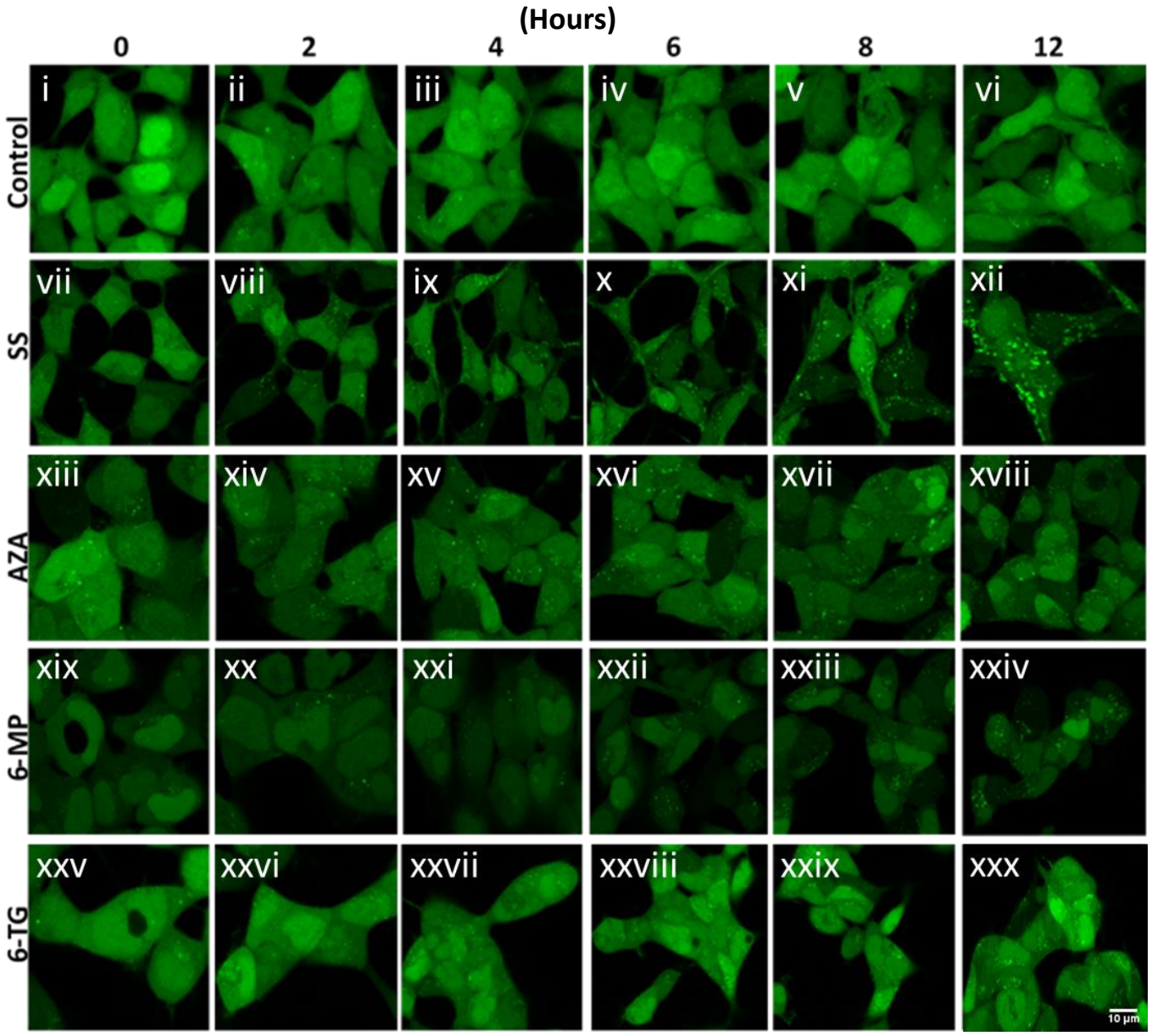

Figure 10 - Induction of autophagy by thiopurines.

HEK293 GFP-LC3 cells were either treated with DMSO (Control), serum starved (SS), or treated with 120µM of AZA, 120µM of 6-MP or 120µM of 6-TG and accumulation of autophagic puncta assessed by live cell imaging over 12h. Thirty cells were counted from 3 fields of view and percentage cells with >5 GFP-LC3 puncta quantified (+/- SEM) for all time points. Images were captured at 400x magnification using a Carl Zeiss LSM880 confocal microscope. n=1

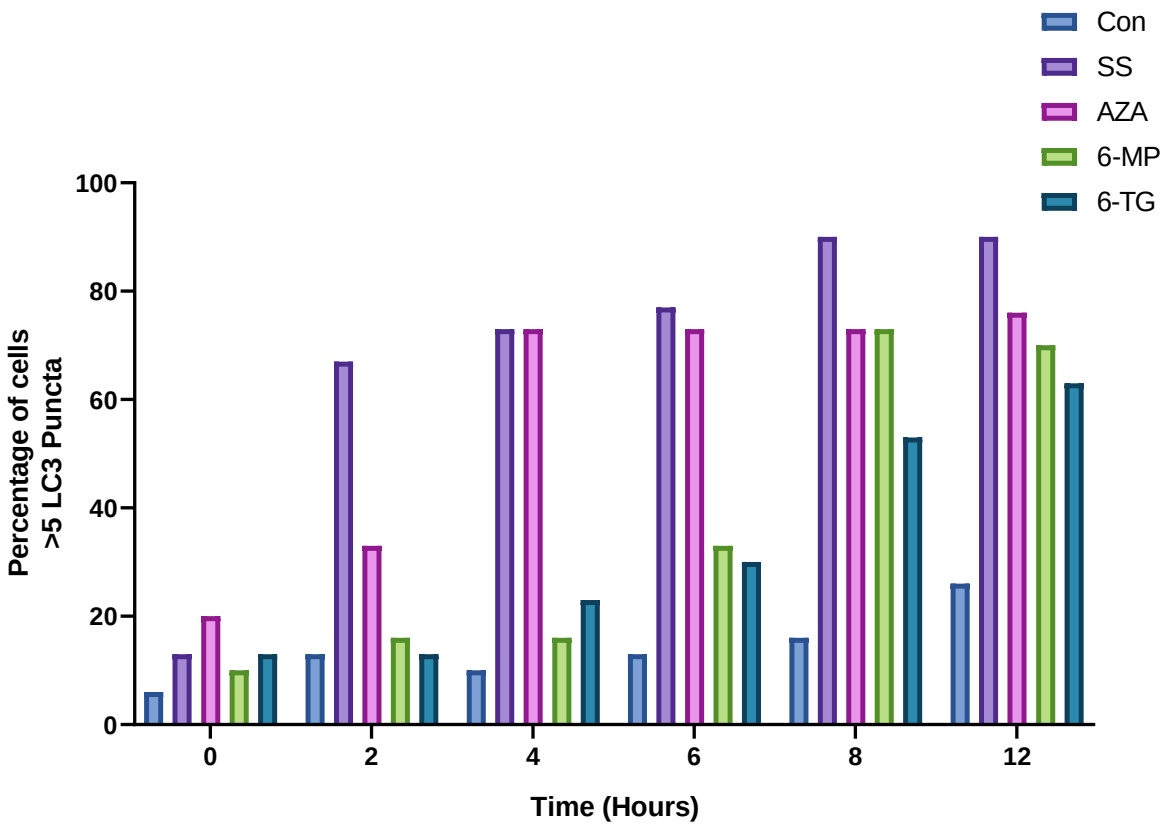

Figure 11 - Quantification of autophagy induction by thiopurines.

Bar graph quantifying the number of HEK293 GFP-LC3 cells exhibiting >5 LC3 puncta in response to thiopurine treatment at various time points. Thirty cells from 3 fields of view for each treatment group were quantified. n=1.

3.2.2. Fixed-cell imaging of thiopurine induced autophagy

Autophagosome accumulation in response to thiopurine treatment was assessed using fixed cell imaging to determine whether the response was comparable to that observed using live cell imaging. The 8h time point was selected as it was the timepoint when levels of basal autophagy were low and the largest accumulation of autophagosomes was observed in response to thiopurine treatment using live cell imaging. As shown in **Figure 12A** an increase in autophagosome accumulation was observed in response to thiopurine treatment, with a 30% increase in cells exhibiting >5 LC3 puncta in AZA treated cells relative to untreated control cells **(Figure 12B)**. Similarly, 6-TG treatment resulted in a 33% increase in cells exhibiting >5 LC3 puncta relative to the untreated control **(Figure 12B)**. In contrast, we did not observe an increase in LC3 puncta in response to 6-MP treatment in fixed cells, which is not in agreement with our findings using live-cell imaging. These results indicate that fixed cell imaging is not as sensitive as live cell imaging in the context of LC3 quantification, with autophagosome accumulation not observed in response to 6-MP treatment after 8h, while AZA produced only a 30% increase in cells exhibiting >5 LC3 autophagic puncta after 8h treatment compared to 60% observed with live-cell imaging. However, both experiments were performed once, which limits the ability to draw firm conclusions.

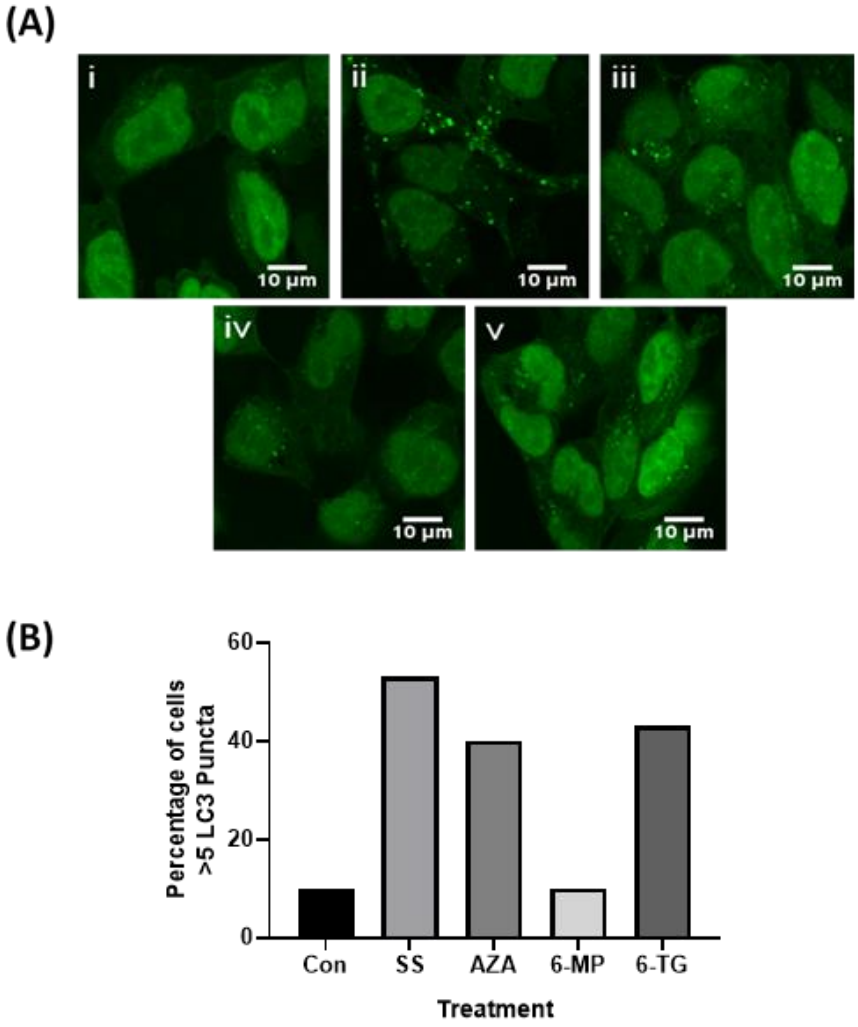

Figure 12 - Induction of autophagy by thiopurines at 8h time point using fixed-cell imaging.

(A) - HEK293 GFP-LC3 cells were treated with DMSO (Control) (i), serum starved (ii), or treated with 120µM AZA (iii), 120µM 6-MP (iv) or 120µM 6-TG (v) for 8h. Cells were fixed and mounted onto slides and thirty cells were counted from 3 fields of view and percentage cells with >5 GFP-LC3 puncta quantified (+/- SEM). Images captured at 630x magnification using a Carl Zeiss LSM880 confocal microscope. n=1.

(B) - Bar graph quantifying HEK293 cells exhibiting >5 LC3 puncta in response to 8h thiopurine treatment. Thirty cells from 3 fields of view for each treatment group were quantified. n=1.

3.2.3. Fixed-cell imaging of sustained thiopurine induced autophagy

Autophagosome accumulation was assessed at a later time-point using fixed cell imaging to determine if the autophagy activity observed at the 8h time-point was sustained. HEK293 GFP-LC3 cells were treated with thiopurines for 24h and LC3 puncta quantified. As shown in **Figure 13A**, an increase in autophagosome accumulation was observed in response to thiopurine treatment, with a 49% of cells exhibiting >5 LC3 puncta in AZA treated cells relative to untreated control cells **(Figure 13B)**. 6-MP and 6-TG treatment caused a 33% and 39% increase in cells exhibiting >5 LC3 puncta respectively compared to the untreated control cells **(Figure 13B)**. These fixed cell imaging results are comparable with results obtained from live cell imaging and demonstrate that autophagosome accumulation is sustained for at least 24h in response to thiopurine treatment.

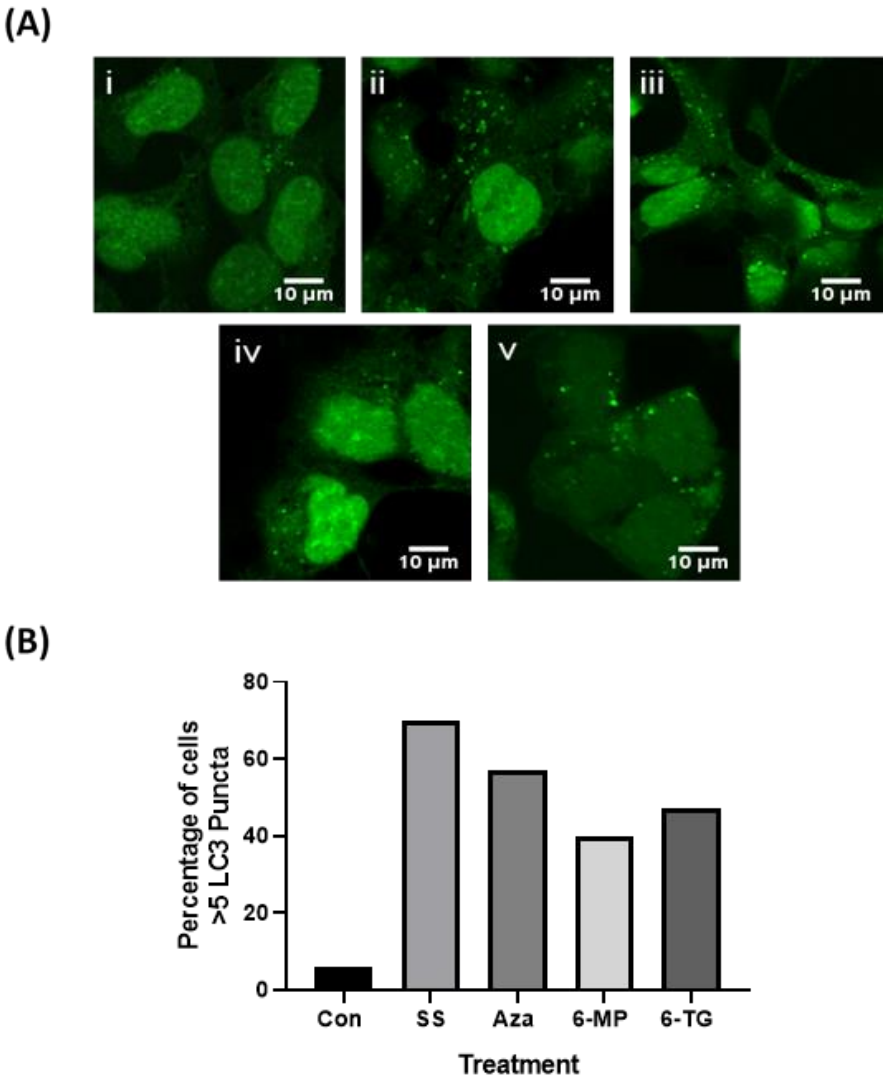

Figure 13 - Induction of autophagy by thiopurines at 24h time point.

(A) - HEK293 GFP-LC3 cells were either treated DMSO (Control) (i), serum starved (SS) (ii), or treated with 120µM AZA (iii), 120µM 6-MP (iv) or 120µM 6-TG (v) for 24h. Cells were fixed and mounted onto slides and thirty cells were counted from 3 fields of view and percentage cells with >5 GFP-LC3 puncta quantified. Images were captured at 630x magnification using a Carl Zeiss LSM880 confocal microscope. n=1.

(B) - Bar graph quantifying HEK293 cells exhibiting >5 LC3 puncta in response to 24h thiopurine treatment. Thirty cells from 3 fields of view for each treatment group were quantified. n=1.

3.2.4. Effect of thiopurines on metabolic activity and cell morphology

Using live cell imaging, changes in cell morphology were observed in 6-TG treated HEK293 GFP-LC3 cells. Morphological changes are often associated with physiological stress; therefore, the metabolic activity of cells was assessed using Alamar Blue assay to determine whether thiopurines were cytotoxic. HEK293 cells were treated with thiopurines at 120μM and brightfield images were captured at 0, 2, 4, 6, 8 and 24h time points. As shown in **Figure 14A**, AZA and 6-MP did not alter the metabolic activity of cells throughout the 24h incubation period. In contrast, 6-TG initially reduced the metabolic activity of cells to 65% at the 2h time point relative to control, which gradually recovered over time until 105% relative to the control was observed at the 24h time point. Light microscopy images shown in **Figure 14B** were consistent with these findings, with no observable differences in cell morphology observed in AZA, 6-MP and control treated cells. In contrast, 6-TG-treated cells exhibited a more compact morphology at the 2h time point **(Figure 14B panel XIV)**. A reduction in growth was also observed, with 6-TG-treated cells reaching a confluency of 50% compared to the control, with the control cells reaching almost 100% confluency after 24h **(Figure 14B, compare panels XXV and XIX)**. These results suggest that 6-TG treatment affected the growth and metabolic activity of cells.

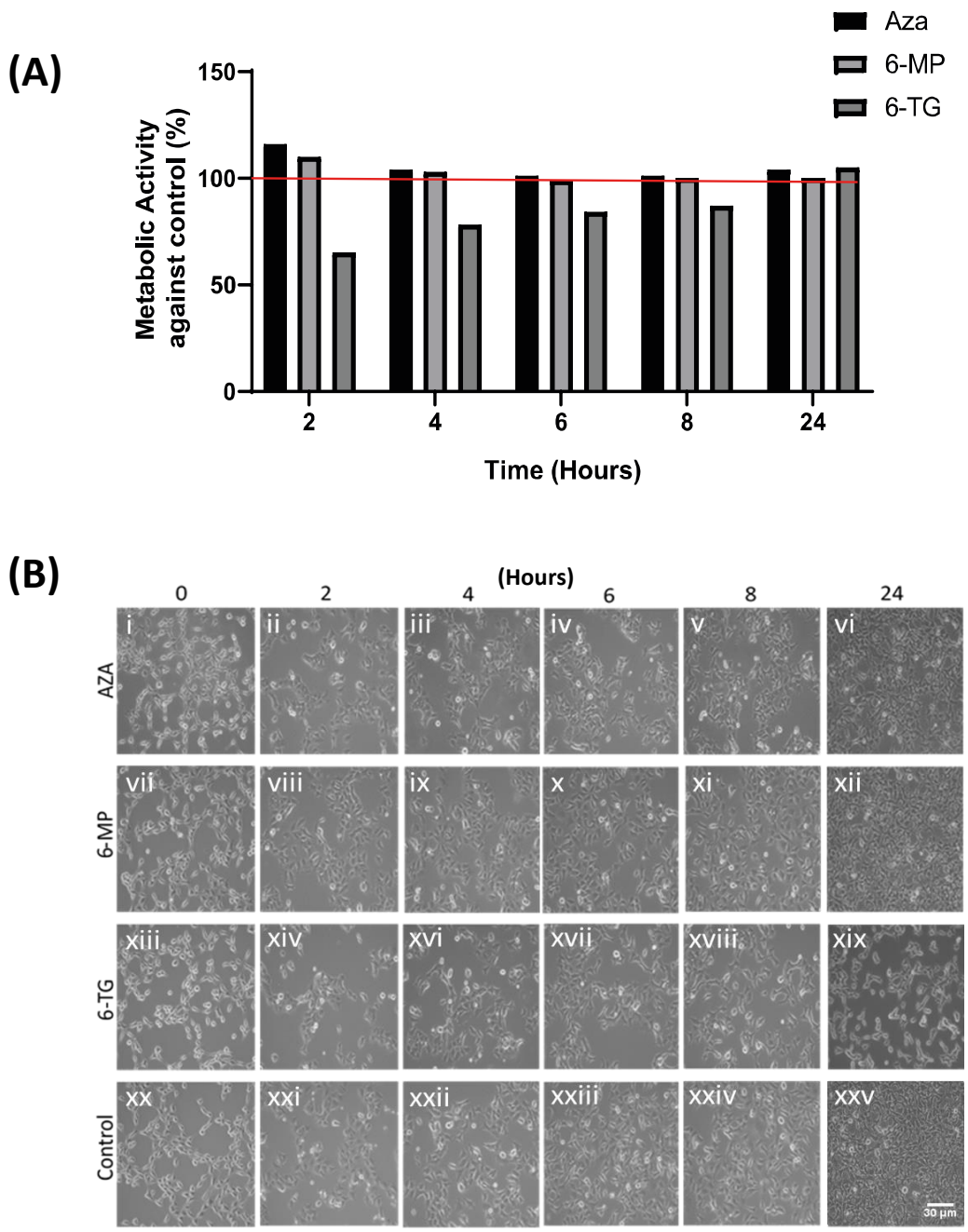

Figure 14 - Effect of thiopurines on metabolic activity and cell growth

(A) - HEK293 cells were either treated with DMSO (Control), 120µM AZA, 120µM 6-MP, or 120µM 6-TG for up to 24h and metabolic activity measured using Alamar Blue. n=1.

(B) – Effect of thiopurines on cell proliferation was assessed using light microscopy. HEK293 cells were either left untreated, or treated with 120µM AZA, 120µM 6-MP, or 120µM 6-TG. Images were captured at a 0, 2, 4, 6, 8, and 24h time points at 100x magnification. n=1.

3.3. Summary

Initially, a time course of thiopurine treatment was performed and induction of autophagy assessed using live cell imaging. AZA induced an accumulation of autophagosomes after 4h compared to 6-MP and 6-TG, which did not begin to induce autophagosome accumulation until the 6h time point. The largest increase in autophagosome accumulation was observed at 8h, therefore, the 8h time point was selected and used to compare live cell imaging results with fixed cell imaging. Although fixed cell imaging did not appear to be as sensitive method of measuring autophagosome accumulation when compared to live-cell imaging, a difference between the control, AZA and 6-TG treated cells was observed, with AZA and 6-TG clearly increasing autophagosome accumulation at the 8h time point. In contrast, 6-MP did not appear to increase autophagosome accumulation at 8h when fixed cell imaging was used. After a 24h incubation all thiopurine-treated cells exhibited an accumulation of autophagosomes using fixed-cell imaging, indicating that all thiopurines induce a sustained autophagy response.

Experiments performed within this chapter were performed once, to allow for optimisation of techniques prior to proceeding experiments with THP-1 macrophages. This prevented statistical analysis of data, which in turns limited the ability to reach definitive conclusions. In addition, the accumulation of autophagosomes observed using live cell and fixed cell imaging does not determine whether thiopurine treatment causes autophagy activation, as autophagosome accumulation can also result from inhibition of autophagy due to blockage of autophagosome-lysosome fusion. Therefore, additional experiments are required to determine whether thiopurines are activating autophagy.

Morphological changes were observed in 6-TG treated cells during live cell imaging, we therefore further investigated these morphological changes using light microscopy. The effects on cell morphology observed using live cell imaging were reproduced using light microscopy, with 6-TG treated cells exhibiting altered morphology and reduced growth compared to the control, AZA and 6-MP treated cells. These observations were further investigated using an Alamar blue assay, which showed

cells have reduced metabolic activity in response to 6-TG treatment at early time points when compared to the control, AZA and 6-MP.

Taken altogether, these results suggest that AZA and 6-TG can induce autophagosome accumulation at the 8h timepoint, which was not observed in 6-MP treatment. However, all thiopurines induced autophagosome accumulation at the 24h timepoint. In addition, 6-TG-treated cells shown a reduction in both growth and metabolic activity, which was not observed in AZA or 6-MP treatment. Additional experiments are required to determine whether autophagy is being activated in response to thiopurines.

Chapter 4. Characterisation of autophagy induction by thiopurines in macrophages

4.1. Introduction

Macrophage function is extremely important in CD pathogenesis (Mahida, 2000). Of note, it has recently been reported that AIEC were able to replicate within MDM from CD patients but not within MDM from UC patients or healthy subjects, suggesting that CD MDM are unable to control intracellular bacteria; which leads to a sustained inflammatory response (Vazeille *et al*., 2015). Several genetic variants have been identified as CD susceptibility factors which could directly affect the function of macrophages (Cho and Brant, 2011), with *in vitro* studies demonstrating the impact of CD-associated single nucleotide polymorphisms related to autophagy on AIEC survival (Lapaquette *et al*., 2012)

Monocytic THP-1 cells are the most commonly used cell line for *in vitro* studies investigating human macrophage function (Lund *et al*., 2016). They are very well characterised and can be differentiated into a variety of macrophage subsets (Starr *et al*., 2018), and therefore provide a good model in which to conduct the studies detailed herein.

Hypothesis: Thiopurines induce autophagy in THP-1 derived macrophages.

Aim 1: Differentiate THP-1 monocytes into macrophages.

Aim 2: Characterise autophagy induction by thiopurines in macrophages

Aim 3: Determine whether thiopurine induced autophagy occurs independent of apoptosis

4.2. Results

4.2.1. Differentiation of THP-1 derived macrophages

THP-1 monocytes can be differentiated to exhibit a macrophage like phenotype that closely resembles macrophages *in vivo*. Due to variation in published methodologies used to differentiate THP-1 cells, initial optimisation of PMA concentration was required. Concentrations of PMA over 100ng/ml have been shown to sensitise THP-1 cells to various stimuli (Lund *et al*., 2016), therefore, PMA concentrations ranging from 5ng/ml to 20ng/ml were assessed. The most commonly used read-out for differentiation of THP-1 cells to macrophages is adherence of cells accompanied by morphological changes. When undifferentiated, cells are in suspension and appear rounded, however they become adherent to the culture plate or flask, and exhibit morphological flattening when differentiation occurs (Lund *et al*., 2016). Therefore, the percentage of adherence was used to determine the effectiveness of each concentration of PMA for differentiation of THP-1 cells. As shown in **Figure 15A**, treatment with PMA at 20ng/ml induced the highest proportion of cell adherence, with cells exhibiting 98% adherence. **Figure 15B, panel ii** shows the morphological changes that can be observed with PMA differentiation at 20ng/ml, with cells exhibiting a flatter, more protruded phenotype compared to control **(Figure 15B, panel i)**. Both the adherence, and the morphological changes observed in PMA-treated samples indicated that differentiation of THP-1 cells has taken place.

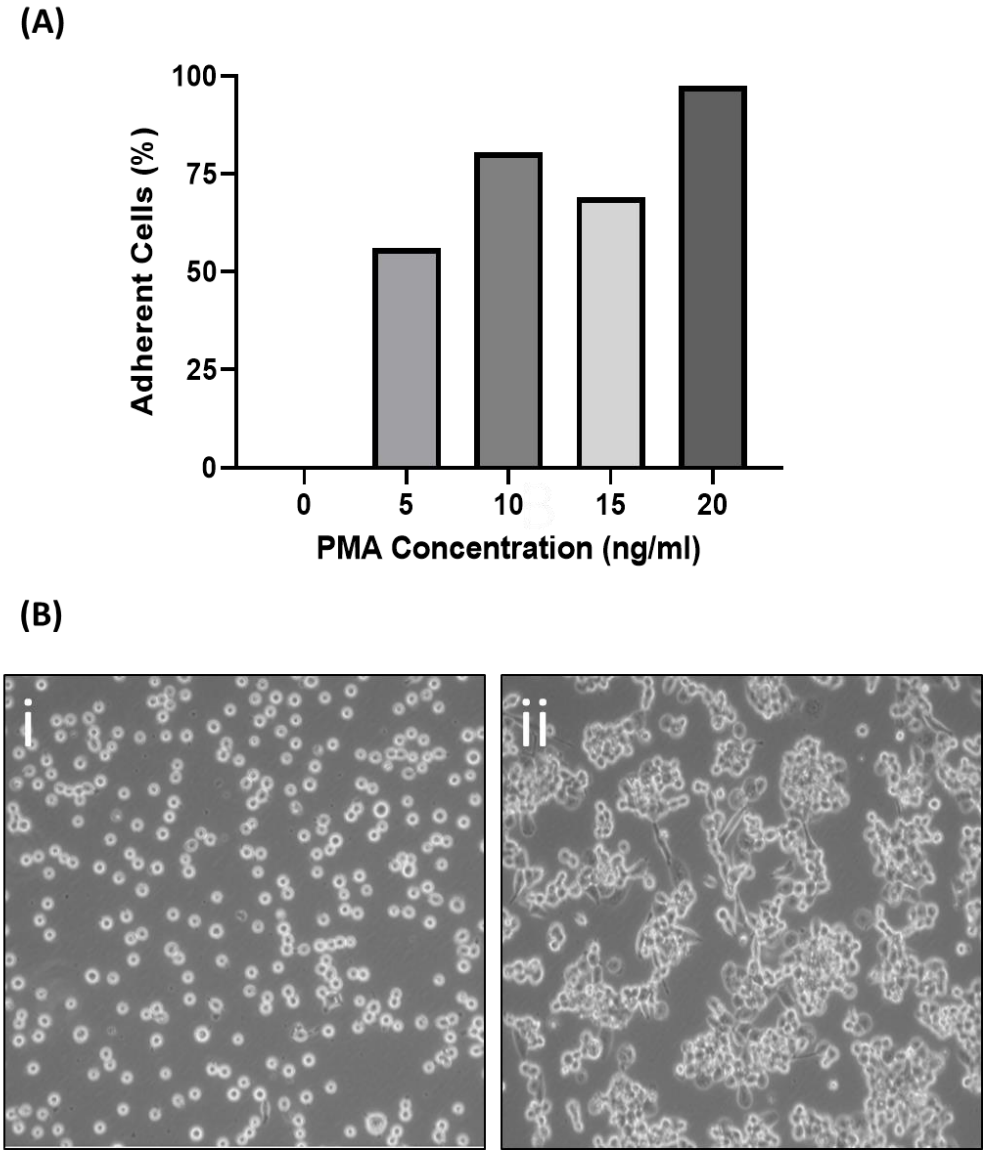

Figure 15 - PMA treatment induces THP-1 morphological changes and cellular adherence.

(A) – THP-1 cells were incubated with different concentrations of PMA (5-20ng/ml) for 48 hours, and then rested in fresh media for 24 hours. The number of non-adherent cells was subtracted from the seeding density to determine the % of adherence during each treatment. n=1.

(B) - THP-1 cells were treated with either, 5, 10, 15 or 20ng/ml of PMA for 48 hours and then rested in fresh media for 24 hours. Adherence was monitored through light microscopy. Images illustrate THP-1 cells before treatment and 48 hours with 20ng/ml PMA treatment. Images were captured at 100x magnification. Images shown are representative of n=3.

4.2.2. Characterisation of THP-1 derived macrophages

The morphological changes observed in THP-1 derived macrophages following PMA treatment required further validation using well-known macrophage surface markers to confirm if differentiation had occurred. Therefore, flow cytometric analysis was performed using common macrophage markers CD68, CD163 and CD80. Cells were also compared to M1 and M2-macrophage control cells to determine whether polarisation of cells occurs during PMA treatment. As shown in **Figure 16**, a clear difference in morphology was observed between PMA-treated cells **(Figure 16, panel iv)** and M1 **(Figure 16, panel v)** and M2 **(Figure 16, panel vi)** macrophages. M1 macrophages appear to show a more flattened morphology and M2 macrophages appear to exhibit more protrusions. As PMA-only treatment did not induce either of these morphological changes consistently, this indicates that PMA treatment did not polarise THP-1 cells towards either one of these particular subsets.

As shown in **Figure 17**, flow cytometric analysis revealed differences in marker expression between macrophage subsets. Undifferentiated THP-1 cells exhibited low expression for all markers examined. PMA-only treated cells exhibited a small increase in CD68 and CD80 expression compared to undifferentiated cells with an 18.33% and 20.79% increase in CD68 and CD80 expression, respectively, relative to the control. PMA-only treated cells exhibited a considerable increase in CD163 expression of 61.05% relative to untreated cells. PMA-only treated cells also exhibited a distinct difference in marker expression compared to the M1 and M2 macrophage controls, with PMA-only treated cells exhibiting low CD68 expression of 24.7% compared to 48.3% and 63.9% compared to the M1 and M2 macrophage controls respectively. PMA-only treated cells also did not exhibit similar CD80 expression to the M1 and M2 macrophages, with PMA-only treated cells showing a 26.2% expression of CD80 compared to the M1 and M2 macrophages that exhibited a 87.9% and 92.2% CD80 expression respectively, indicating that differentiation of THP-1 cells with PMA does not drive the cells into these particular subsets.

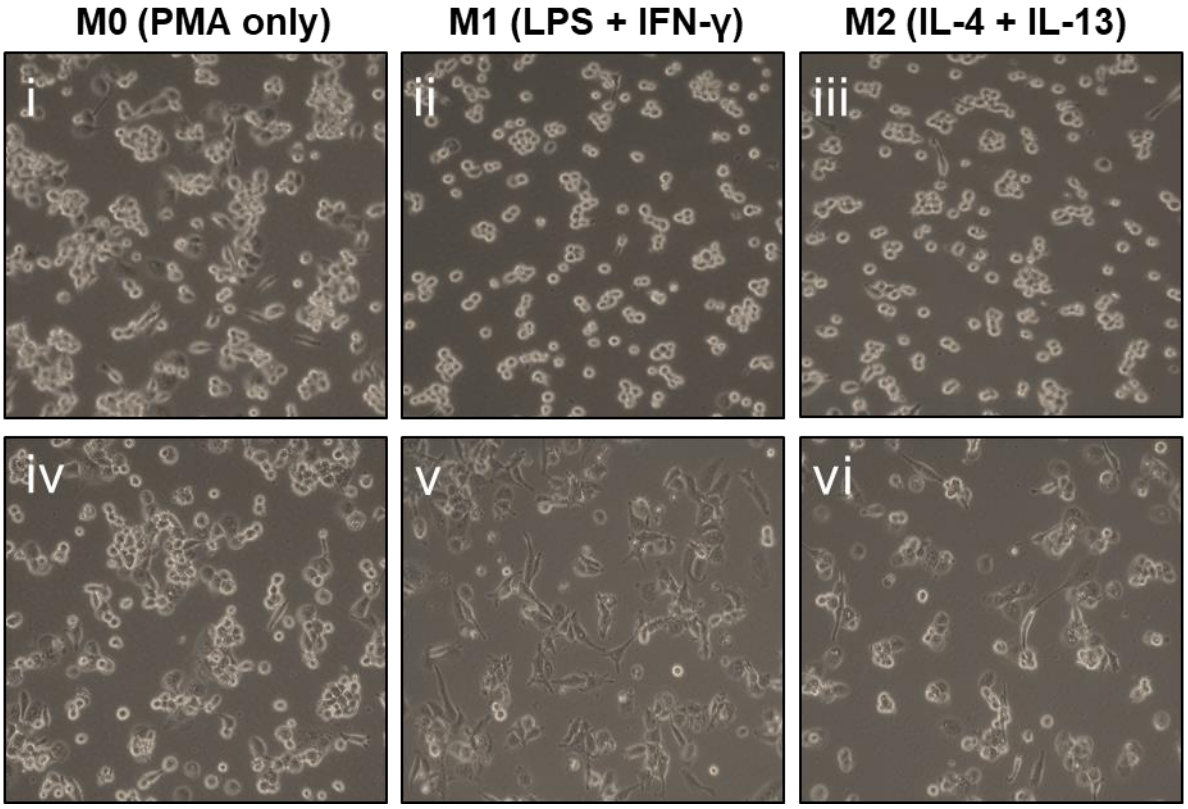

Figure 16 - Morphological changes during polarisation of THP-1 cells.

THP-1 cells were treated with PMA only (20ng/ml) for 48 hours (panels i + iv), treated with PMA for 24h and then supplemented with LPS (100ng/ml) and IFN-γ (20ng/ml) in PMA containing media for a further 24h (panels ii + v), or treated with PMA for 24h and subsequently treated with IL-4 (20ng/ml) and IL-13 (20ng/ml) in PMA containing media for a further 24h (panels iii + vi). Images were captured using Primovert light microscope at 100x magnification. Images shown are representative of n=1.

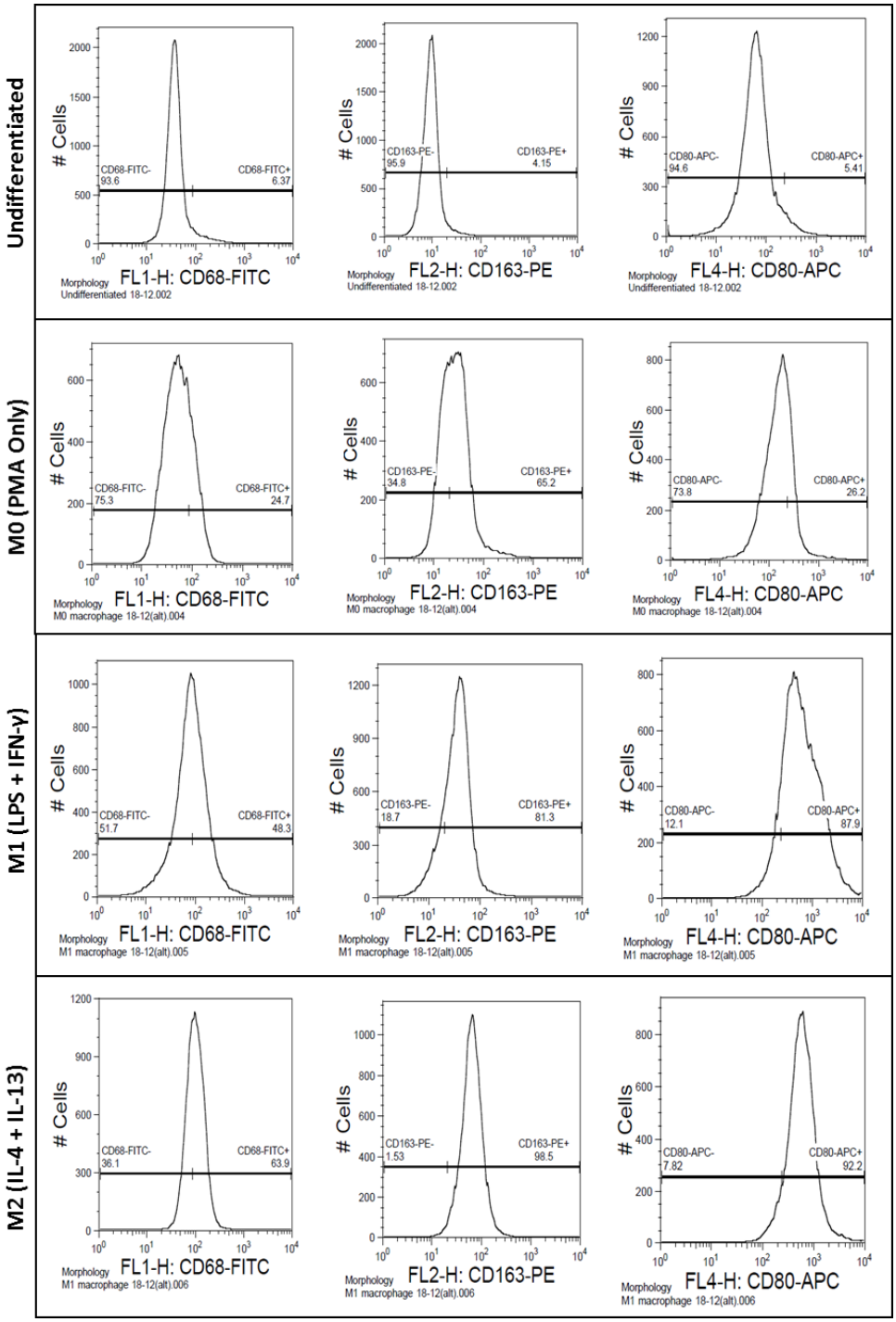

Figure 17 - Macrophage marker expression in polarised THP-1 cells.

THP-1 cells were seeded and either treated with PMA only (20ng/ml) for 48h, treated with PMA for 24h and subsequently treated with LPS (100ng/ml) and IFN-γ (20ng/ml) in PMA containing media for a further 24h (M1) or treated with PMA for 24h and subsequently treated with IL-4 (20ng/ml) and IL-13 (20ng/ml) in PMA containing media for a further 24h. Cells were then harvested and incubated with CD163-PE, CD68-FITC and CD80-APC antibody. Marker expression was analysed through flow cytometric analysis. n=1.

4.2.3. Time-Course of autophagy induction by thiopurines in THP-1 derived macrophages

A time course, utilising fixed cell imaging, was performed to assess any differences in autophagy activity mediated by thiopurines over a range of different time points, and to select an appropriate time point for subsequent experiments. Time points ranging between 2h to 8h were tested, as the 8h time point exhibited optimal autophagosome accumulation in thiopurine-treated HEK293 cells. As shown in **Figure 18 & 19A**, autophagosome accumulation was observed in response to thiopurine treatment in a time dependent manner. The 8h time point showed the highest accumulation of autophagosomes, with 6-MP treatment inducing the highest accumulation, with a 49% increase in cells exhibiting >6 LC3 puncta relative to the control. Similarly, AZA and 6-TG caused an increase in autophagosome accumulation, with a 31% increase in cells exhibiting >6 LC3 puncta and a 30% increase in cells exhibiting >6 LC3 puncta relative to control **(Figure 19B)**. This data demonstrates that the 8h time point is the optimum time point to observe autophagosome accumulation in response to thiopurines in THP-1 derived macrophages.

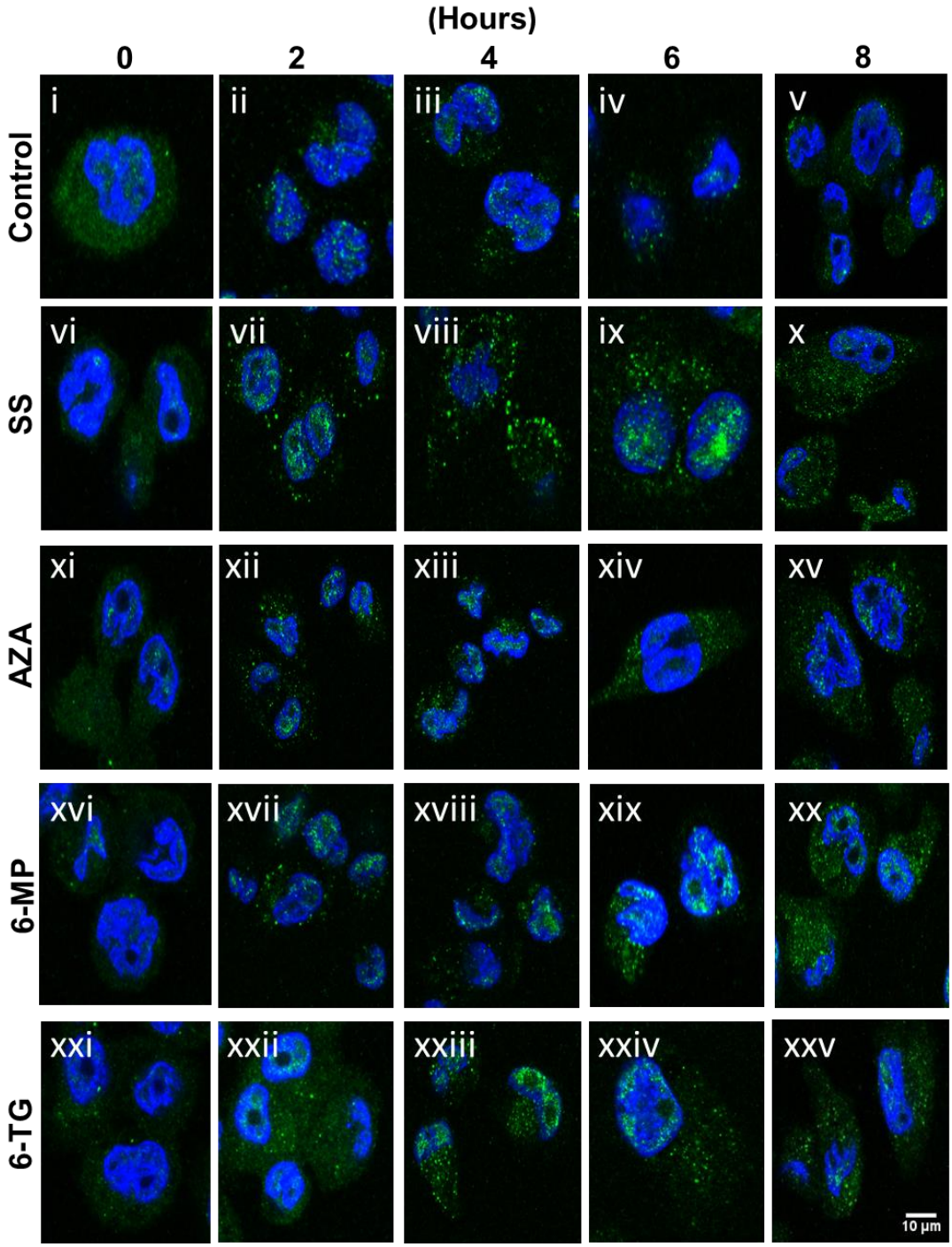

Figure 18 – Time course of autophagy induction in thiopurine treated THP-1 derived macrophages.

THP-1 derived macrophages were either treated with DMSO (Control), serum starved (SS), treated with 120µM AZA, 120µM of 6-MP, or 120µM of 6-TG. THP-1 derived macrophages were left to incubate for either 0, 2, 4, 6 or 8h with the pharmaceutical agent. Samples were fixed, immunostained using an anti-LC3 antibody and mounted using mounting media containing DAPI. Images were taken at 630x magnification using a Carl Zeiss LSM880 confocal microscope. n=1.

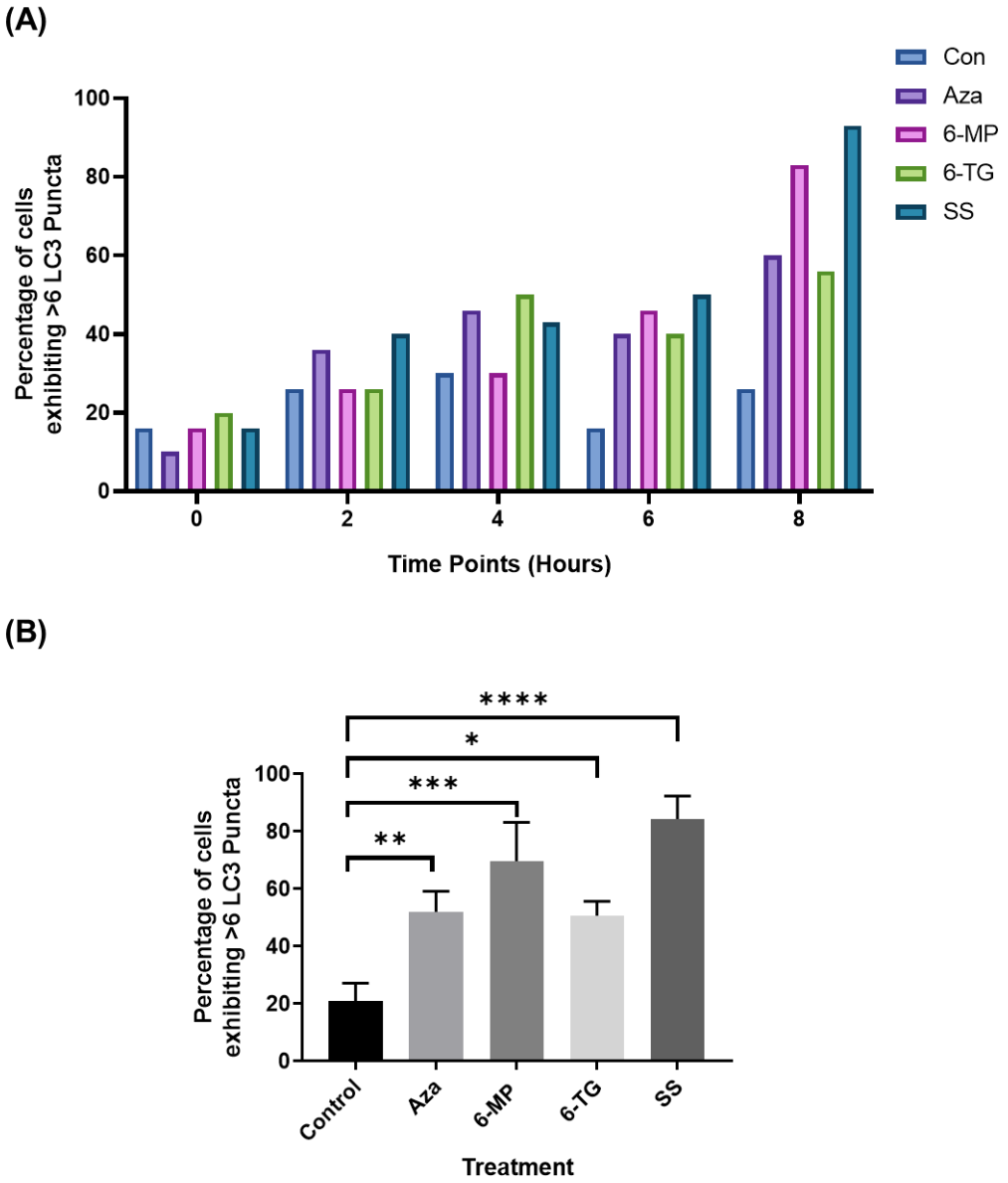

Figure 19 - Quantification of LC3 puncta in thiopurine treated THP-1 derived macrophages during a time course

(A) - Bar graph representing THP-1 derived macrophages with >6 LC3 puncta during thiopurine treatment. LC3 Puncta within 30 cells from each treatment group were quantified. n=1.

(B) - Bar graph representing THP-1 derived macrophages with >6 LC3 puncta during 8h of thiopurine treatment. LC3 Puncta within 30 cells from each treatment group were quantified. One-way anova with Tukey post-hoc multiple comparison was the statistical test performed (+/- SEM). n=3.

4.2.4. Autophagy activity of THP-1 derived macrophages treated with a range of thiopurine concentrations

As similar autophagy induction was observed with all three thiopurines at 120μM after 8h incubation, the effect of lower thiopurine concentrations was examined in an attempt to tease out any differences in autophagy induction. A concentration curve was performed from a range of 20-120μM of each thiopurine. As shown in **Figure 20 and 23A**, AZA treated cells exhibited a small increase of 11% in cells exhibiting >6 LC3 puncta relative to control during treatment at a concentration of 20μM, which increased up to 33% during treatment at a concentration of 120μM. 6-MP and 6-TG treated cells exhibited an increase in autophagosome puncta at lower concentrations tested, with 20μM exhibiting an increase of 20% and 22% in cells with >6 LC3 puncta respectively relative to the control, although this was not significant **(Figure 23B)**. Autophagosome accumulation increased by 57% when cells were treated with 6-MP at 120μM and 30%% when cells were treated with 6-TG at 120μM relative to the control **(Figure 21, 22 and 23A)**. This suggests that autophagosome accumulation is concentration dependent and the highest autophagosome accumulation can be observed when cells are treated with thiopurines at a concentration of 120μM with all concentrations tested.

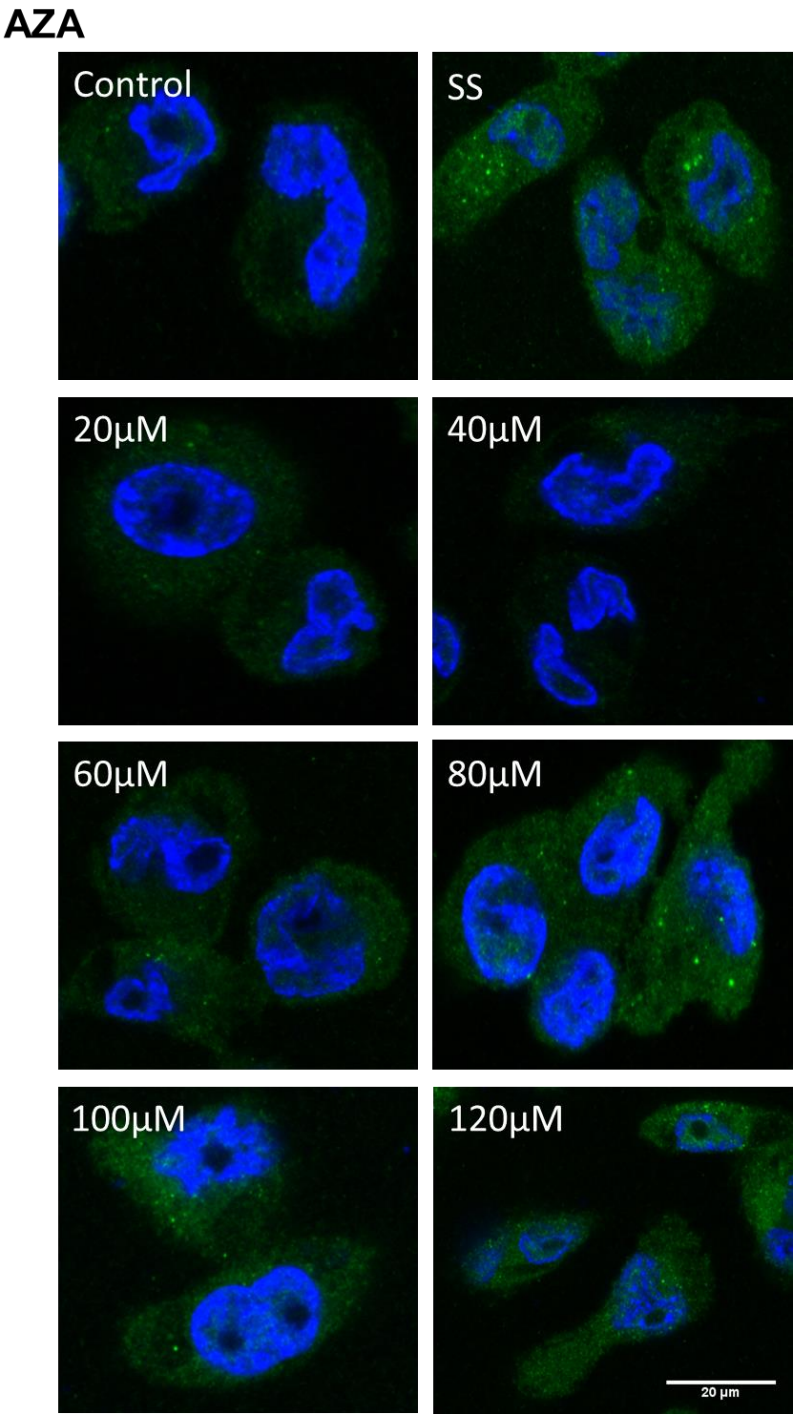

Figure 20 - Fixed cell imaging of immunostained LC3 in THP-1 derived macrophages treated with an AZA concentration curve.

THP-1 derived macrophages were either treated with DMSO (Control), serum starved (SS) or treated with 20-120µM AZA and incubated for 8h at 37°C / 5% CO_2. Samples were fixed, immunostained using LC3 antibody and mounted using DAPI mounting media. Images were taken at 630x magnification using a Carl Zeiss LSM880 confocal microscope. n=1.

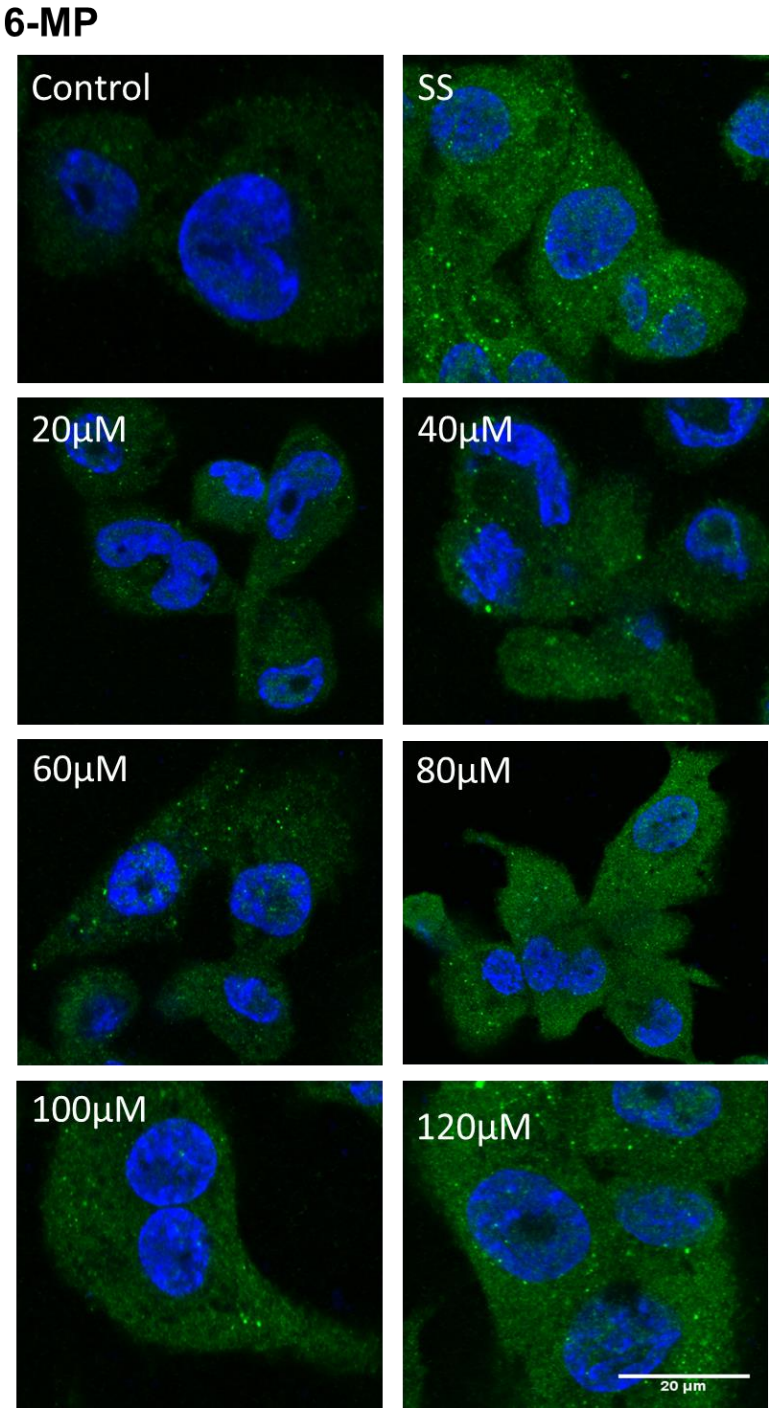

Figure 21 - Fixed cell imaging of immunostained LC3 in THP-1 derived macrophages treated with a 6-MP concentration curve.

THP-1 derived macrophages were either treated with DMSO (Control), serum starved (SS) or treated with 20-120µM 6-MP and incubated for 8h at 37°C / 5% CO_2. Samples were fixed, immunostained using LC3 antibody and mounted using DAPI mounting media. Images were taken at 630x magnification using a Carl Zeiss LSM880 confocal microscope. n=1.

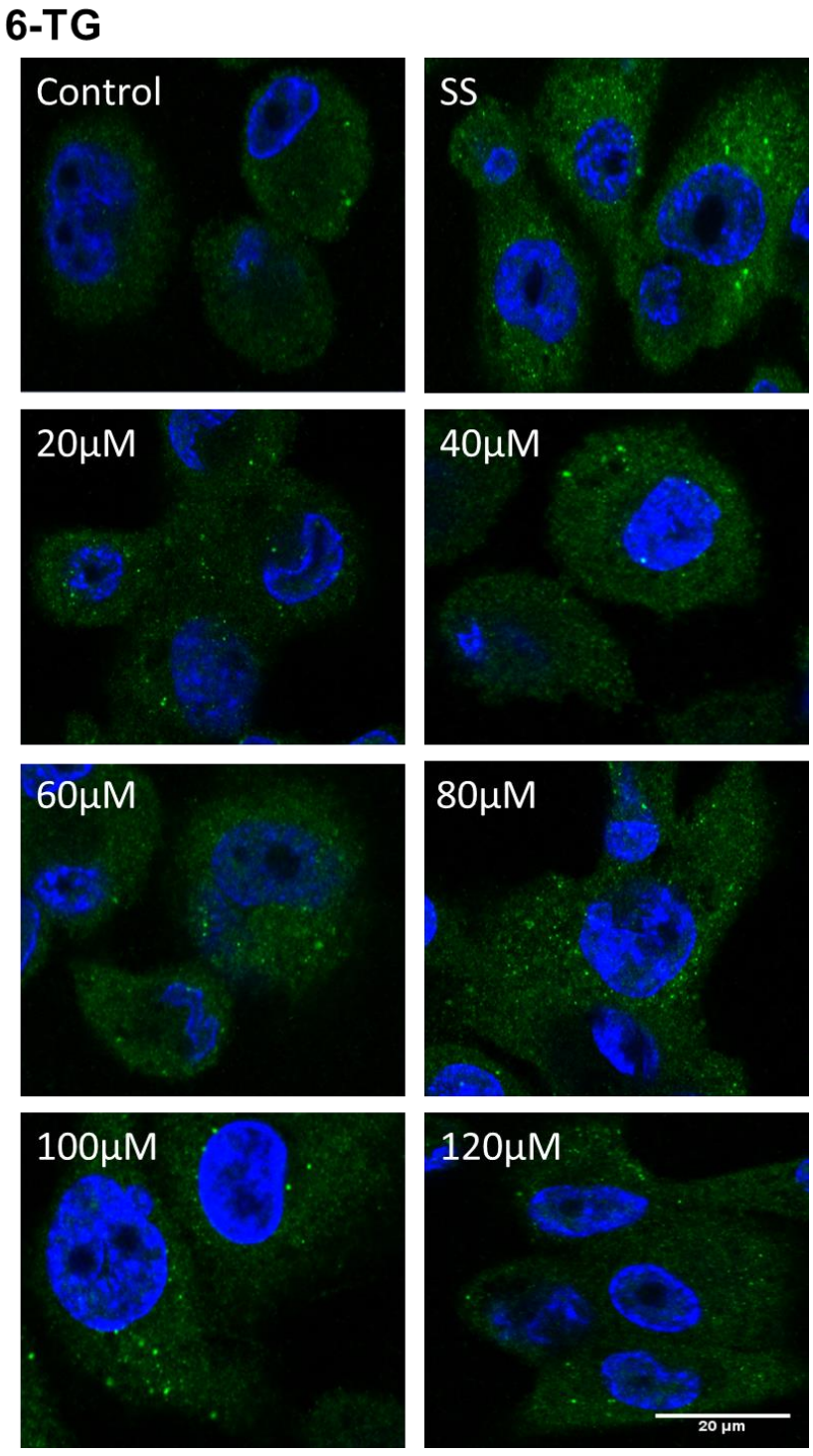

Figure 22 - Fixed cell imaging of immunostained LC3 in THP-1 derived macrophages treated with a 6-TG concentration curve.

THP-1 derived macrophages were either treated with DMSO (Control), serum starved (SS) or treated with 20-120µM 6-TG and incubated for 8h at 37°C / 5% CO_2. Samples were fixed, immunostained using LC3 antibody and mounted using DAPI mounting media. Images were taken at 630x magnification using a Carl Zeiss LSM880 confocal microscope. n=1.

(A)

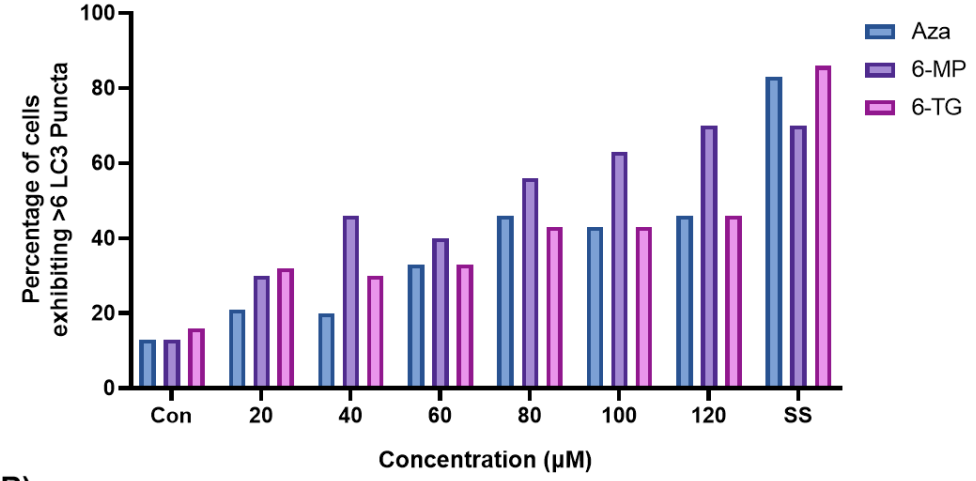

(B)

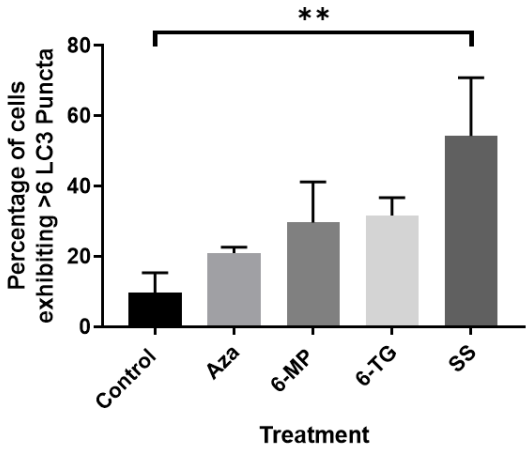

Figure 23 - Quantification of LC3 puncta in THP-1 derived macrophages treated with a thiopurine concentration curve.

(A) - Bar graph representing THP-1 derived macrophages with >6 LC3 puncta during 20-120μM treatment of thiopurines. LC3 Puncta within 30 cells from each treatment group were quantified. n=1.

(B) - Bar graph representing THP-1 derived macrophages with >6 LC3 puncta during 20μM treatment of thiopurines. LC3 Puncta within 30 cells from each treatment group were quantified. A one-way ANOVA with Tukey post-hoc multiple comparison was performed (+/- SEM). n=3.

4.2.5. Sustained autophagy induction in response thiopurine treatment.

Sustained autophagy induction was observed during a 24h incubation in HEK293 cells treated with thiopurines at 120μM. We therefore treated THP-1 derived macrophages with thiopurines for 24h to determine if a similar response was observed in the IBD relevant cell line. As shown on **Figure 24**, a sustained autophagy induction can be observed in all thiopurines tested. A significant increase in 31% of cells >6 LC3 puncta was observed during AZA and 6-TG treatment. The highest response was seen within 6-MP treated THP-1 derived macrophages, with a 35% significant increase in cells >6 LC3 puncta relative to the control **(Figure 25)**. These results confirm autophagy activity is sustained over a 24h period in THP-1 derived macrophages.

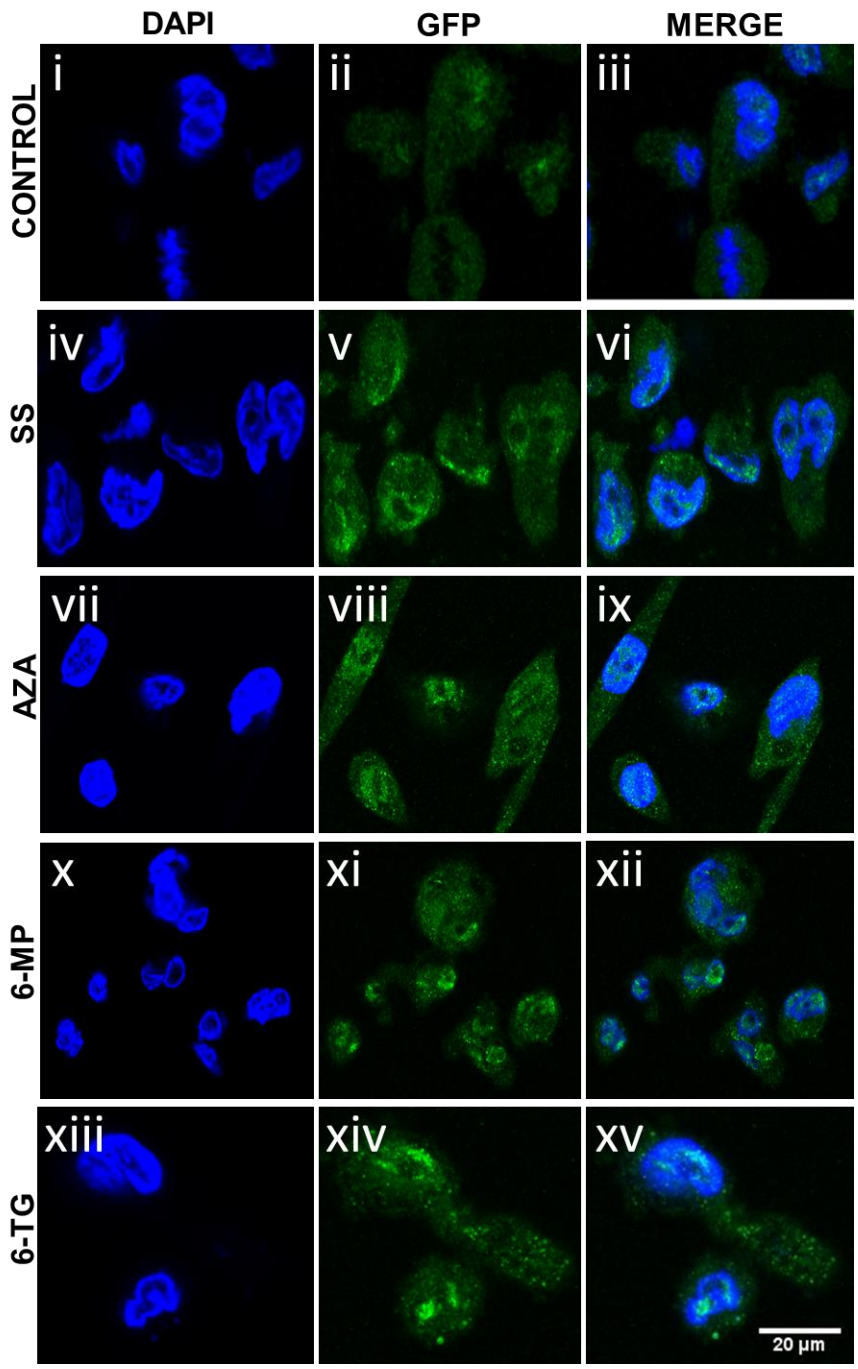

Figure 24 - Fixed cell imaging of Immunostained LC3 in THP-1 derived macrophages treated for 24h with thiopurines.

THP-1 derived macrophages were either treated with DMSO (Control), serum starved (SS), treated with 120µM AZA, 120µM of 6-MP, or 120µM of 6-TG. THP-1 derived macrophages were then incubated for 24h at 37ºC / 5% CO_2 with the pharmaceutical agent. Samples were fixed, immunostained using an anti-LC3 antibody and mounted using DAPI mounting media. Images were taken at 630x magnification using a Carl Zeiss LSM880 confocal microscope. Images shown are representative of n=3.

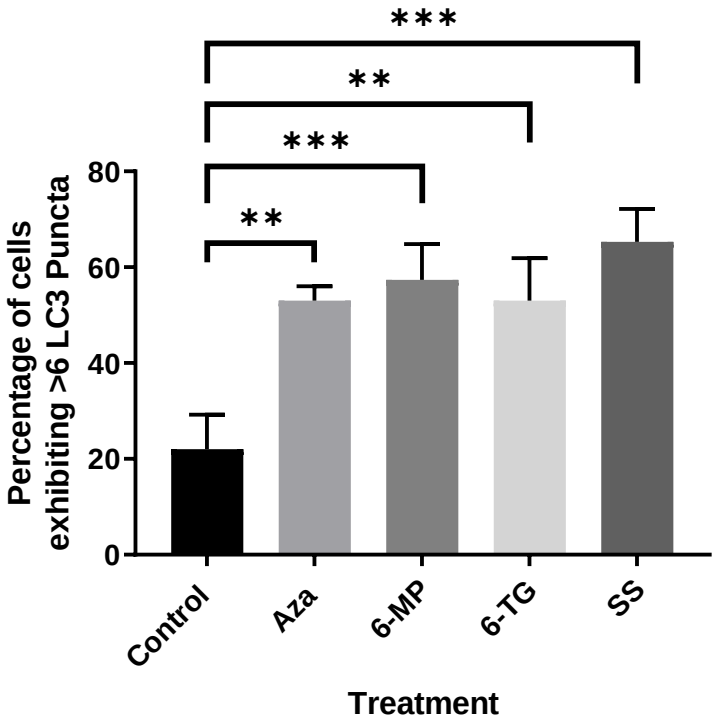

Figure 25 - Quantification of LC3 puncta in THP-1 derived macrophages treated for 24h with thiopurines.

Bar graph representing THP-1 derived macrophages with >6 LC3 puncta during thiopurine treatment. LC3 Puncta within 30 cells from each treatment group were quantified. A one-way ANOVA with Tukey post-hoc multiple comparison was performed (+/- SEM). n=3.

4.2.6. Activation of autophagy by thiopurines

An accumulation of autophagosomes does not necessarily signify the activation of autophagy, as an accumulation can also occur due the inhibition of the lysosome to autophagosomes (Mizushima *et al*., 2010). Therefore, a GFP-RFP-LC3 plasmid was utilised to verify the formation of autophagolysosomes, which would confirm the completion of autophagy. With this method, the GFP fluorophore is quenched during the formation of the autophagosolysosome, due to the acidic nature of lysosomes. Therefore, autophagolysosomes will fluoresce red within a transfected cell line, while cells within the intermediate stage of autophagosome formation will fluoresce both green and red. As indicated in **Figure 26**, thiopurine treatment increased the formation of autophagolysosomes within the cell, with AZA **(Figure 26, panel xvii)**, 6-MP **(Figure 26, panel xxii)** and 6-TG **(Figure 26, panel xxvi)** increasing the number of RFP puncta by 37%, 22% and 21% respectively compared to the DMSO carrier control **(Figure 27B)**. This demonstrates that all thiopurines can induce autophagy activity in THP-1 derived macrophages.

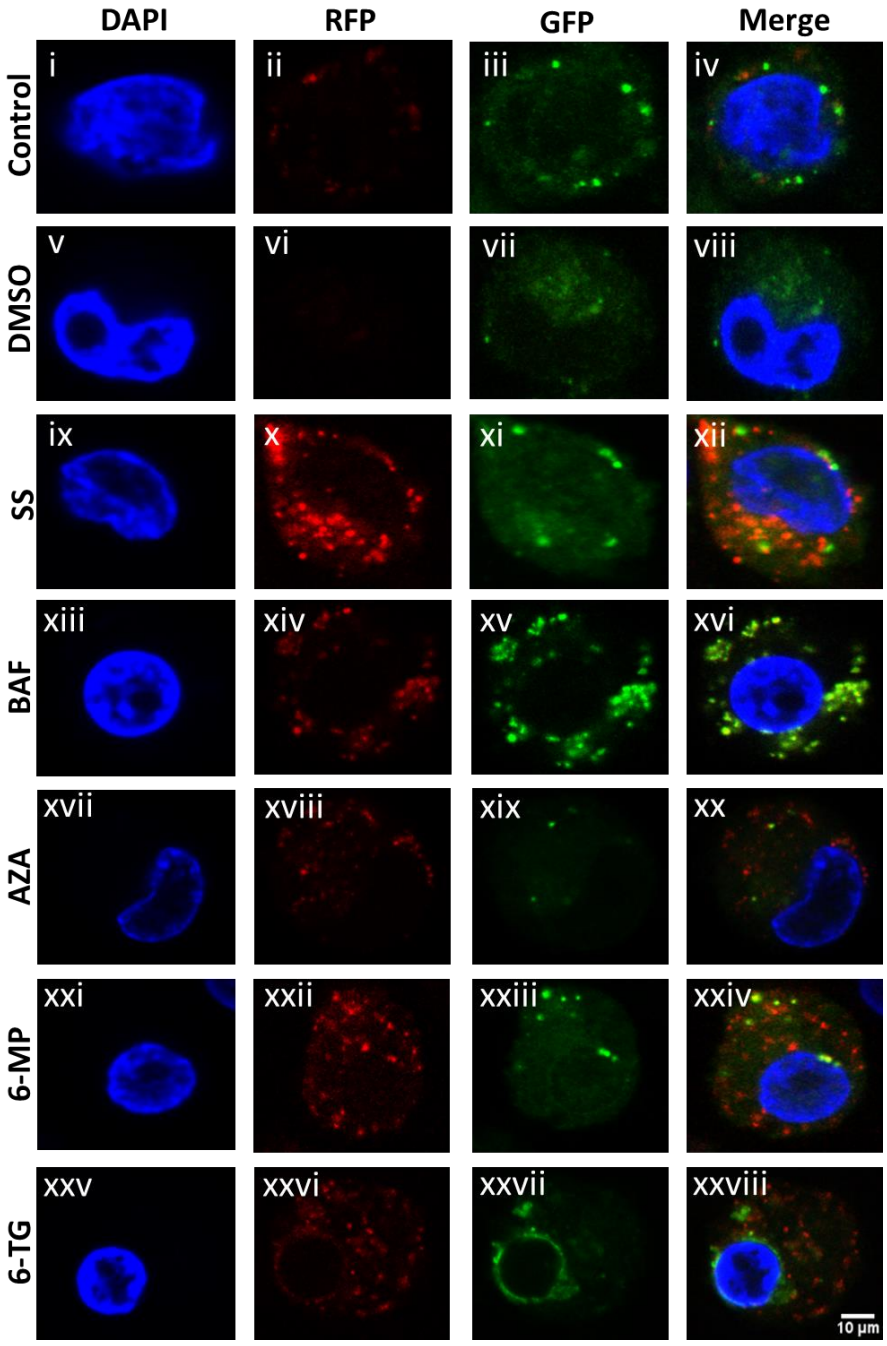

Figure 26 - THP-1 macrophages transiently transfected with GFP-RFP-LC3 plasmid to assess thiopurine-induced autophagy activation.

Representative images of thiopurine treated THP-1 macrophages transfected with a GFP-RFP-LC3 Plasmid. THP-1 cells were differentiated, transfected with a GFP-RFP-LC3 plasmid using nucleofection and were either left untreated (Control), serum starved (SS) or treated with 2µM of DMSO, 120µM of AZA, 120µM of 6-MP and 120µM of 6-TG for 8 hours. Cells were also treated with 160nm of bafilomycin, which would induce autophagosome accumulation by inhibiting autophagosome-lysosome fusion. Samples were fixed, immunostained using LC3 antibody and mounted using DAPI mounting media. Images were taken at 630x magnification using a Carl Zeiss LSM880 confocal microscope. Images shown are representative of n=2.

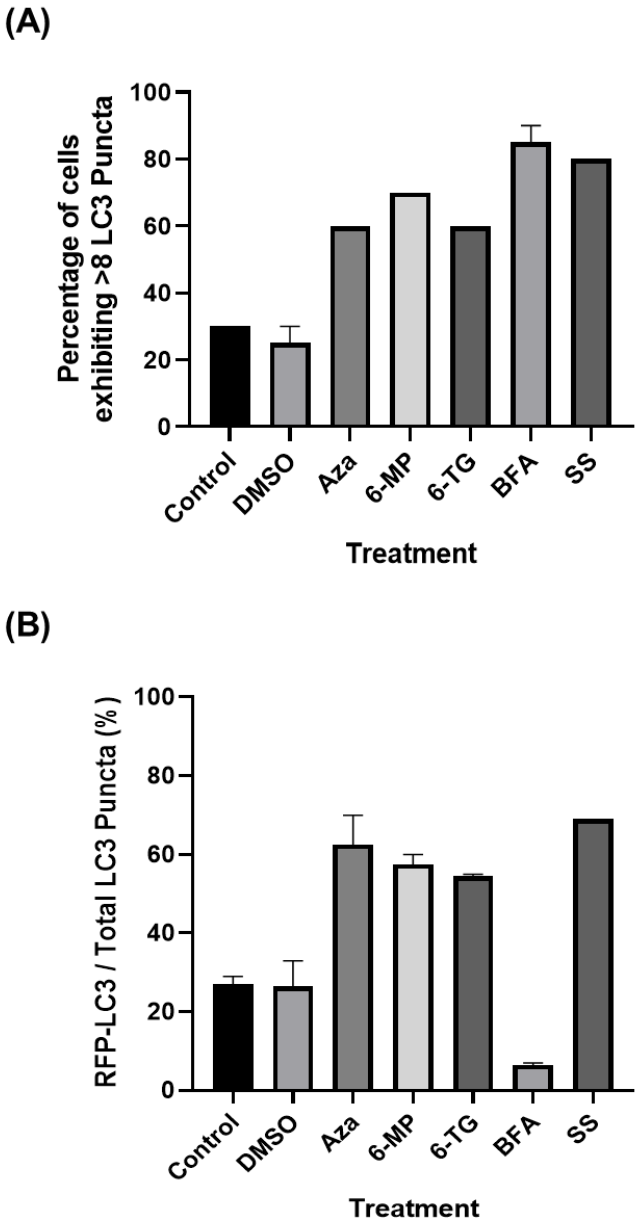

Figure 27 - Quantification of thiopurine-induced autophagy induction in GFP-RFP-LC3 transfected THP-1 derived macrophages.

(A) - Bar graph representing GFP-RFP-LC3 transfected THP-1 derived macrophages with >8 LC3 puncta during thiopurine treatment. LC3 Puncta within 10 cells from each treatment group were quantified. n=2.

(B) - Bar graph representing number of RFP-LC3 puncta within GFP-RFP-LC3 transfected thiopurine treated THP-1 macrophages. RFP-LC3 Puncta within 10 cells from each treatment group were quantified (+/- SEM). n=2.

4.2.7. The effects of thiopurines on apoptosis

Due to the relationship in signalling pathways between autophagy and apoptosis, we examined the effect of thiopurines on both the early and late stages of apoptosis. An Annexin-V/PI stain can differentiate between the early and late stages of apoptosis due to the availability of markers for apoptosis at the different stages of the pathway. Annexin V can bind to phosphatidylserine (PS) with high affinity, which becomes exposed on the outer leaflet of the plasma membrane during early stage apoptosis. Due to the permeabilisation or rupturing of the membrane that that can occur in cells during late apoptosis or necrosis, the DNA-binding molecule, (PI), can enter the cell and bind to DNA. Therefore, healthy cells (Annexin-V^-/PI^-), cells in early apoptosis (Annexin-V^+/PI^-) and those in the late stages of apoptosis or necrosis (Annexin-V^+/PI^+) can be differentiated. As shown on **Figure 28**, AZA and 6-TG treated cells exhibited a decrease in healthy cells, with AZA and 6-TG treated cells exhibiting a decrease of 15.4% and 10.6% respectively relative to the DMSO-treated control **(Figure 29)**. Treatment with 6-MP resulted in a similar percentage of healthy cells compared to the DMSO-treated control. An increase in early apoptosis was observed in both AZA and 6-TG treatment, with an increase of 11.2% and 7.5% in Annexin-V^+/PI^- cells relative to the DMSO-treated control **(Figure 29)**. A minor increase of 4.6% and 2.9% in Annexin-V^+/PI^+ cells was observed during AZA and 6-TG treatment relative to the DMSO-treated control **(Figure 29)**. These results would suggest that AZA and 6-TG induce early apoptotic signalling within THP-1 macrophages whereas 6-MP does not.

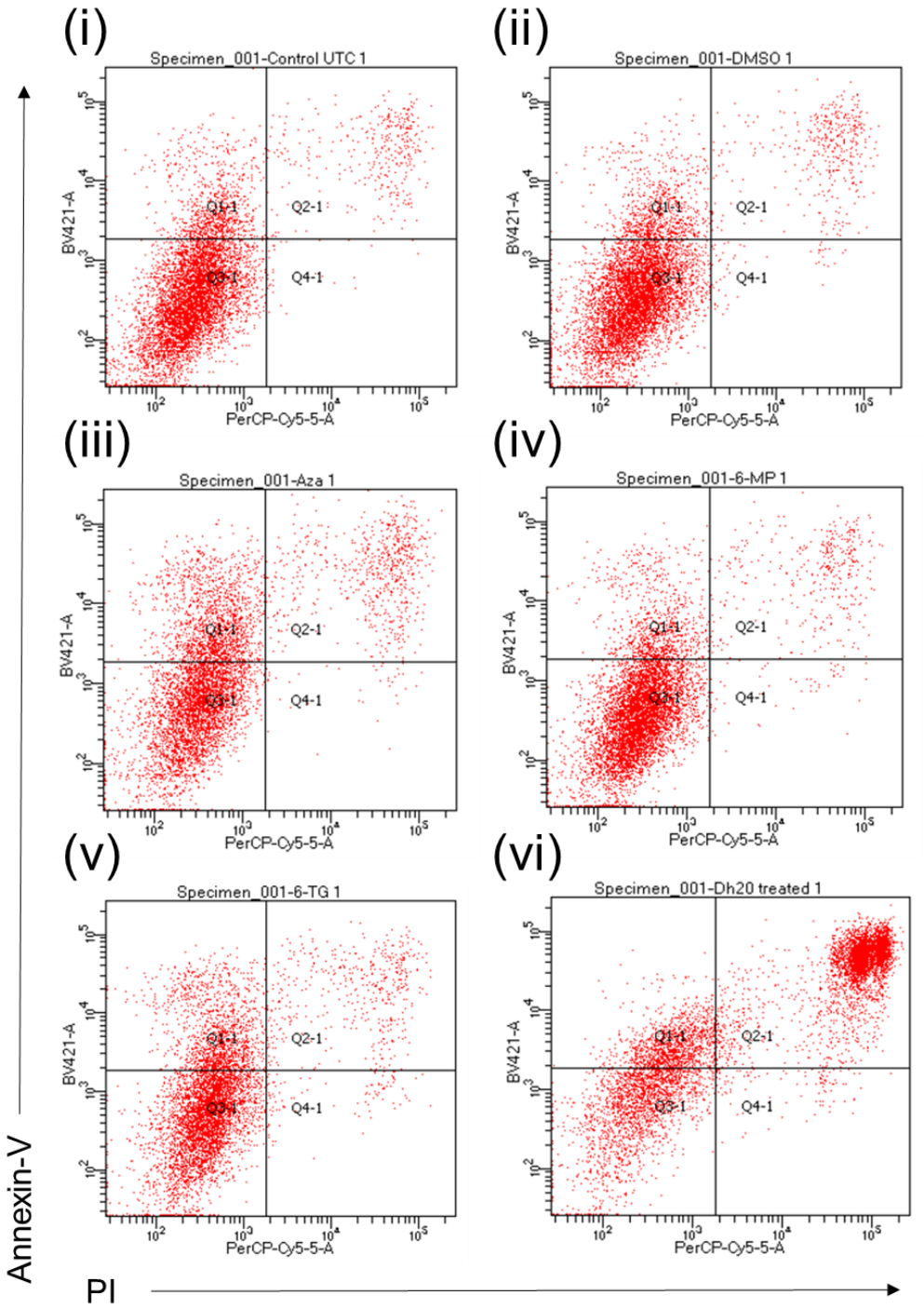

Figure 28 (i-vi) – Annexin V/PI staining utilising flow cytometry in thiopurine treated THP-1 macrophages.

THP-1 derived macrophages were either left untreated (i), treated with DMSO (ii), 120µM of AZA (iii), 120µM of 6-MP (iv), 120µM of 6-TG (v) or deionised H_20 (vi). Cells were stained using an Annexin-V kit and PI solution and were analysed by flow cytometry. Each treatment was performed in duplicate. n=1

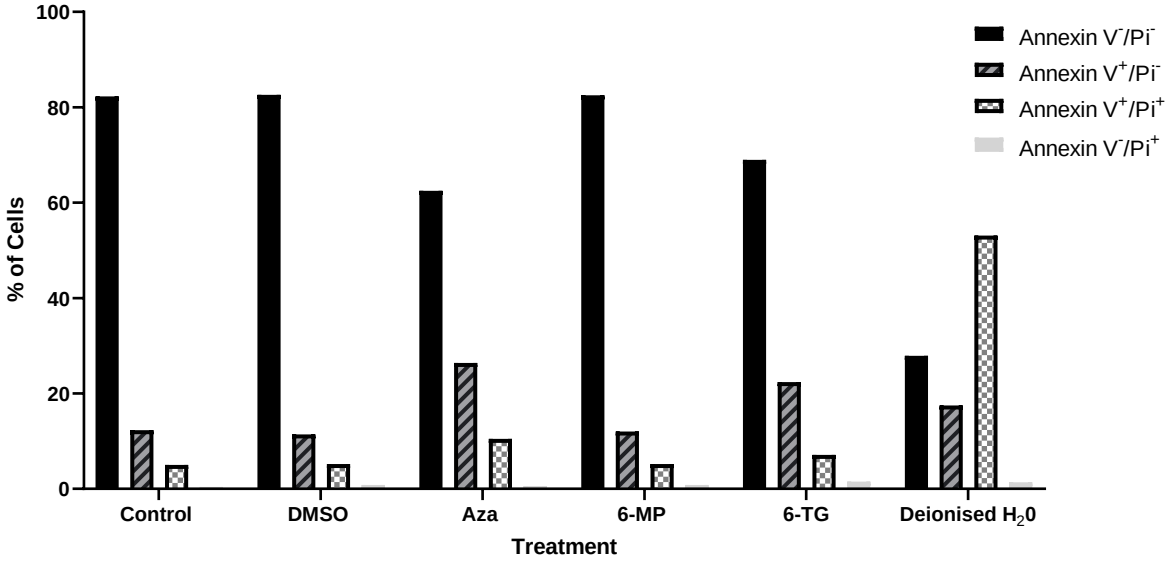

Figure 29 - Quantification of Annexin V/PI staining in thiopurine treated THP-1 macrophages.

THP-1 derived macrophages were either left untreated (i), treated with DMSO (ii), 120µM of AZA (iii), 120µM of 6-MP (iv), 120µM of 6-TG (v) or deionised H_20 (vi). Cells were stained using an Annexin-V kit and PI solution and were analysed by flow cytometry. Mean percentage population from each quadrant was quantified. Each treatment was performed in duplicate. n=1.

4.3. Summary

Initially, differentiation of THP-1 cells with PMA was assessed through the adherence of cells to the dish and it was concluded that 20ng/ml was the most effective concentration. Flow cytometric analysis of CD68, CD163 and CD80 surface marker expression indicated that differentiation with PMA using 20ng/ml did not polarise cells into an M1 or M2 state.

Utilising a thiopurine time-course, the highest autophagosome accumulation was observed at the 8h time point. Interestingly, 6-MP produced the highest autophagosome accumulation in comparison to all thiopurines tested. Furthermore, 6-MP and 6-TG induced a slight increase in autophagosome accumulation at low concentrations when compared to AZA and control cells, however this was non-significant. All thiopurines also induced autophagosome accumulation for up to 24h, indicating that autophagy induction is sustained during thiopurine treatment.

Utilising a GFP-RFP-LC3 plasmid, results demonstrate that activation of autophagy occurs in response to all thiopurines tested. Due to the interconnection of autophagy and apoptotic pathways, an Annexin V/PI Stain was performed to determine whether autophagy activation occurs independent of apoptosis. An increase in early apoptosis was observed in AZA and 6-TG treated cells, in contrast to 6-MP, which did not show an increase in cells undergoing early apoptotic signalling.

Taken altogether, these results suggest that all thiopurines induce autophagy activity in which 6-MP showed the highest autophagy induction compared to AZA and 6-TG. In addition, AZA and 6-TG also induced early apoptotic signalling whereas 6-MP did not. However, results cannot be conclusive as experiments were performed once. Therefore, future studies are required to confirm these findings. Further studies are also required to fully investigate apoptosis associated with autophagy activation.

Chapter 5. Characterisation of the ER-stress and unfolded protein response to thiopurines in macrophages

5.1. Introduction

Paneth cells are specialised intestinal epithelial cells which produce large amounts of host defence peptides to help maintain intestinal barrier integrity (Fritz *et al*., 2011). Increased demand for protein production in Paneth cells also increases susceptibility to the accumulation of misfolded proteins within the ER, termed as ER stress (Ma *et al*., 2017). Significantly, the ER stress marker protein BiP is increased in Paneth cells and in gut resident-inflammatory cells of patients with IBD, indicating increased ER stress (Bogaert *et al*., 2011).

Cells have evolved various mechanisms to adapt to unfolded and misfolded proteins in the ER; known collectively as the UPR (Ma *et al*., 2017). As shown in **Figure 30**, the UPR consists of three main signalling pathways which are the PERK-ATF4 pathway, IRE1α-XBP1 pathway and ATF6 pathway. The importance of the UPR in IBD-associated inflammation is highlighted in studies using transgenic mice. For example, *XBP1* -/- mice, when treated with DSS, develop more severe colitis compared to wild-type mice (Kaser *et al*., 2008b).

Importantly, studies have shown that the UPR and ER stress response functionally intersect with autophagy (Fritz *et al*., 2011). The UPR activates autophagy as a protective mechanism to reduce the burden of protein accumulation and maintain cell survival during ER stress (Ogata *et al*., 2006). Work from Hooper *et al*., (2019) has demonstrated that PERK gene expression is induced during AZA treatment, indicating activation of the UPR. Autophagy activity observed in response to AZA treatment was diminished in the presence of a pharmacological inhibitor of PERK , indicating that autophagy is activated in part through UPR-dependent mechanisms (Hooper *et al*., 2019). In addition, mTORC1, a critical pathway in metabolism and autophagy signalling, was found to be inhibited in the response to AZA treatment. However, mTORC1 signalling was not altered during the pharmacological inhibition of PERK, indicating mTORC1 signalling functions upstream or parallel to PERK signalling. In

this chapter, we aimed to further characterise the UPR and ER-stress response to thiopurine treatment in THP-1 derived macrophages. We also aim to identify if mTOR signalling is regulated in response to all thiopurines.

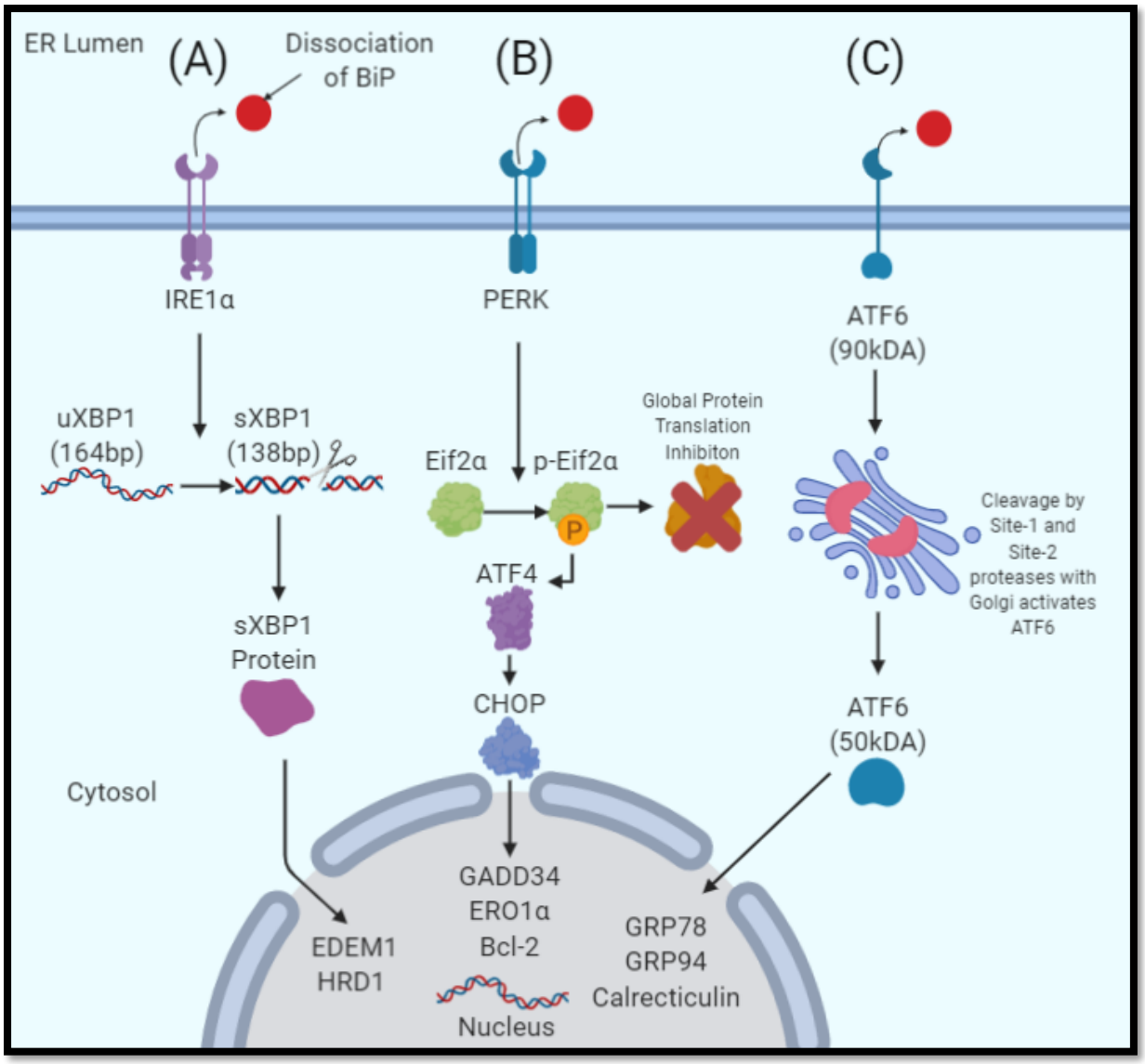

Figure 30 - The Unfolded Protein Response.

Author's illustration of the IRE1α, PERK and ATF6 signalling cascade. IRE1α, PERK and ATF6 are activated due to the dissociation of BiP that occurs in the presence of an accumulation of misfolded proteins in the ER lumen. **(A)** IRE1α induces the splicing of XBP1 mRNA which is a potent transcription factor that induces transcription of proteins such as EDEM1 and HRD1, proteins part of the ER-associated degradation pathway that function to remove misfolded proteins with the ER lumen. **(B)** PERK induces the phosphorylation of eif2α, which inhibits global protein translation within the cell. Eif2α phosphorylation subsequently induces ATF4 transcription which leads to CHOP transcription. CHOP induces the expression of, pro-apoptotic proteins GADD34, ERO1α and the down regulation of anti-apoptotic markers such as Bcl-2. **(C)** Activation of ATF6 leads to translocation to the Golgi apparatus where it is spliced through site-1 and site-2 proteases and can increase the expression of GRP78 (BiP), GRP94 and Calrecticulin. Illustration was created using Biorender Software.

Hypothesis: Induction of the UPR and autophagy by thiopurines occurs independent of ER stress.

Aim 1: Determine whether induction of the UPR response by thiopurines occurs independent of the ER stress response.

Aim 2: Characterise the expression of UPR genes in response to thiopurines.

Aim 3: Characterise the expression and activity of UPR proteins in response to thiopurines.

Aim 4: Assess mTORC1 activity in response to thiopurines.

5.2. Results

5.2.1. Evaluation of the ER stress response to thiopurines in macrophages

Induction of ER stress is a key event preceding UPR activation (Ma *et al*., 2017), therefore, we investigated whether thiopurines induce ER stress in THP-1 derived macrophages. Cells were treated with thiopurines for 8 hrs at 120μM and ER stress was assessed via endpoint PCR for *XBP1* splicing, an event that occurs during IRE1α activation and which is a well characterised marker for ER stress **(Figure 30, Part A).** Tunicamycin, a drug that inhibits N-linked glycosylation resulting in a build-up of misfolded protein in the ER, was used as a positive control for ER stress (Kishino *et al*., 2017). As shown in **Figure 31**, no *XBP1* splicing was observed in response to any of the thiopurines **(Lane 5,7,9),** in contrast tunicamycin resulted in clear splicing of *XBP1* **(Lane 3).** Two splice variants were observed during tunicamycin treatment **(Figure 31, Lane 11)**, which is caused by the formation of a hybrid product that is double stranded cDNA consisting of a single strand of *XBP1u* and a single strand of *XBP1s* (Chalmers *et al*., 2017). The formation of this hybrid product indicates the presence of mild ER stress in the cell and the activation of the IRE1α pathway (Shang and Lehrman, 2004). These results suggest that thiopurines do not induce ER stress in macrophages.

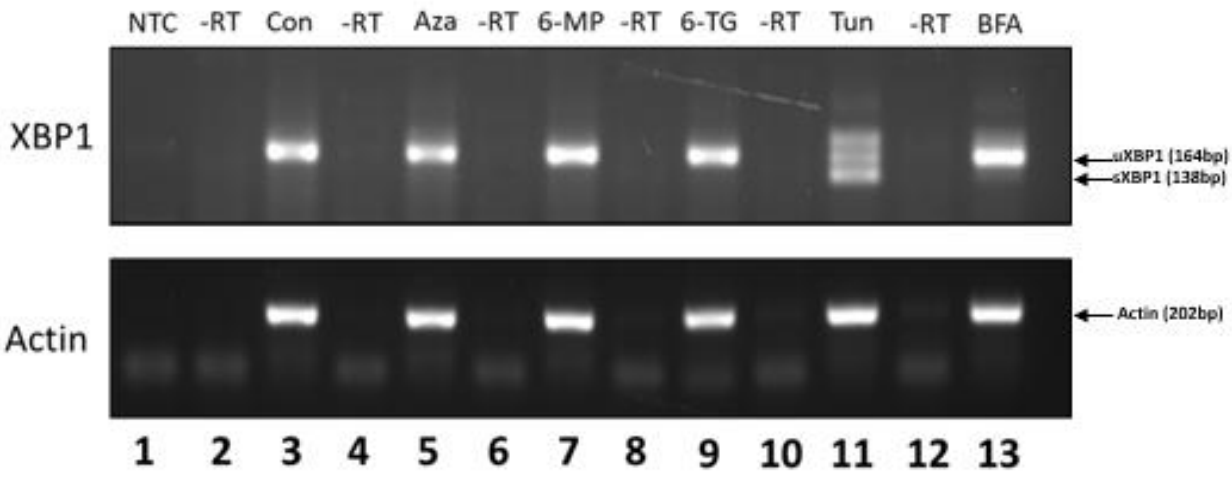

Figure 31 - End-point PCR analysis of XBP1 splicing in response to thiopurines.

THP-1-derived macrophages were either treated with DMSO (Control), 120µM AZA, 120µM 6-MP, 120µM 6-TG or 5µg/ml Tun for 8 hours. RNA was extracted and converted into cDNA. XBP1 PCR products were resolved on a 2% agarose gel containing safeview and analysed using Syngene software. Actin PCR products were resolved on a 1% agarose gel and analysed using syngene software. RT-ve samples were used to evaluate genomic DNA contamination. DEPC-treated deionised H_2O was substituted for template as a no template control (NTC). A representative image is shown (n=2).

5.2.2. Characterisation of UPR gene expression in response to thiopurine treatment

The expression of genes associated with the UPR response were investigated using real-time PCR. Surprisingly, expression of *PERK* was not affected by thiopurines (**Figure 32, iv),** however, the expression of genes downstream of PERK, namely *ATF4* and *CHOP* increased significantly in response to 6-TG **(Figure 32, i and iii)**. In contrast, expression of *ATF4* and *CHOP* were not affected by AZA or 6-MP **(Figure 32, i and iii)**. Furthermore, the expression of *EDEM1* and *BiP* were not affected by any of the thiopurines **(Figure 32, ii and v)**. Positive control, tunicamycin, significantly induced the expression of all UPR genes tested. Melt curves analysis showed a single, defined, peak in all amplicons tested, indicative of a single amplicon being generated as a final product **(Figure 33)**. Together, these results suggest that 6-TG activates UPR signalling downstream of PERK, whereas AZA and 6-MP do not.

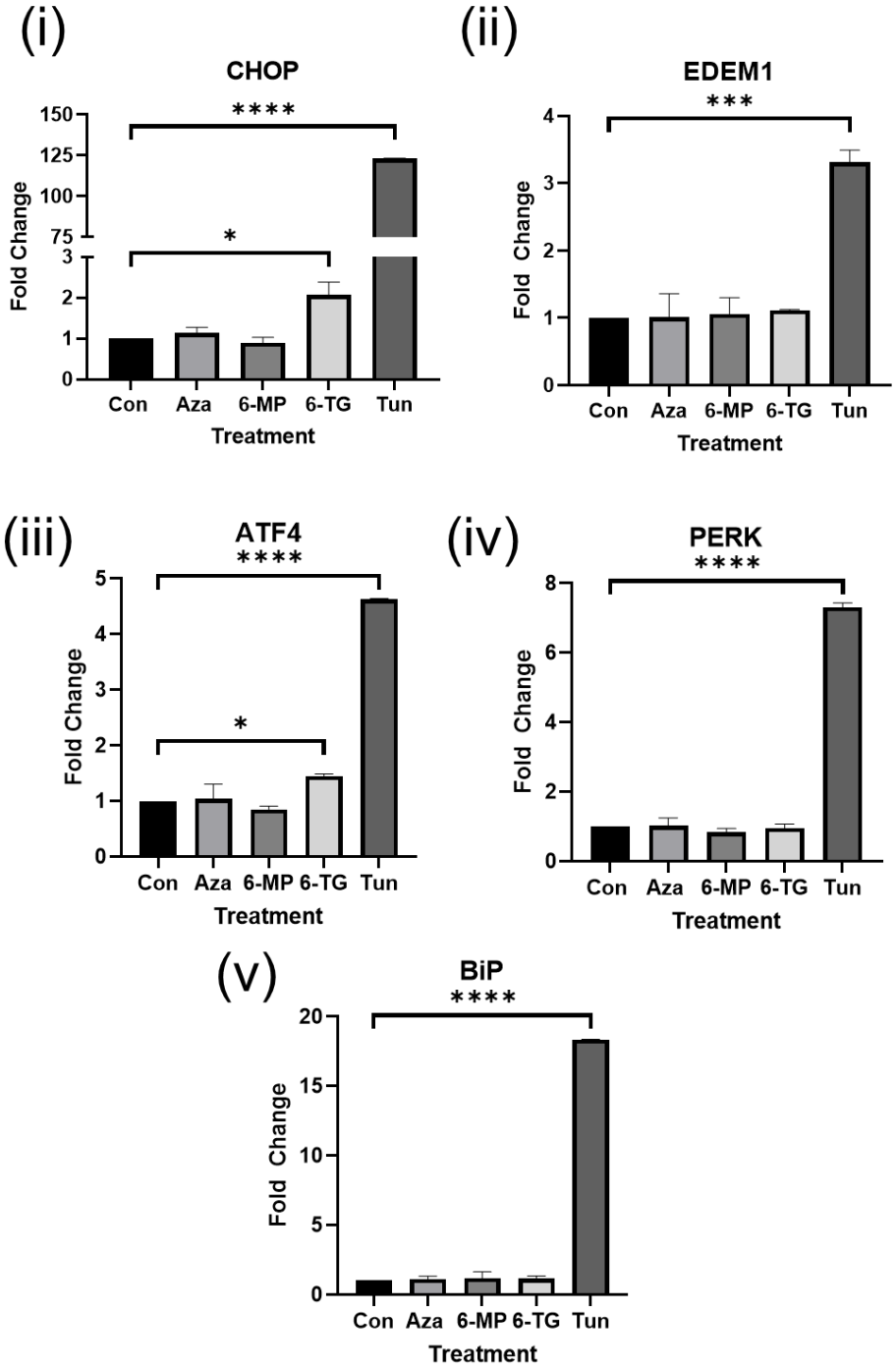

Figure 32 (i-v) – Real-time PCR analysis of UPR associated genes in response to thiopurines.

THP-1-derived macrophages were either treated with DMSO (Control), 120µM AZA, 120µM 6-MP, 120µM 6-TG or 5µg/ml Tun for 8 hours. RNA was extracted and converted into cDNA. cDNA was used as a template for qPCR analysis using primers specific for *CHOP*, *EDEM1*, *ATF4*, *PERK* and *BiP*. Values were normalised to the geometric mean of housekeeper genes *ATP5B* and *RPL13A* for corresponding treatments and time-points. Fold Change was calculated through the $2^{-\Delta\Delta Ct}$ method. One-way anova with Dunnett's multiple comparison was performed comparing ΔCt values for treatment and control groups (+/- SEM). n=3.

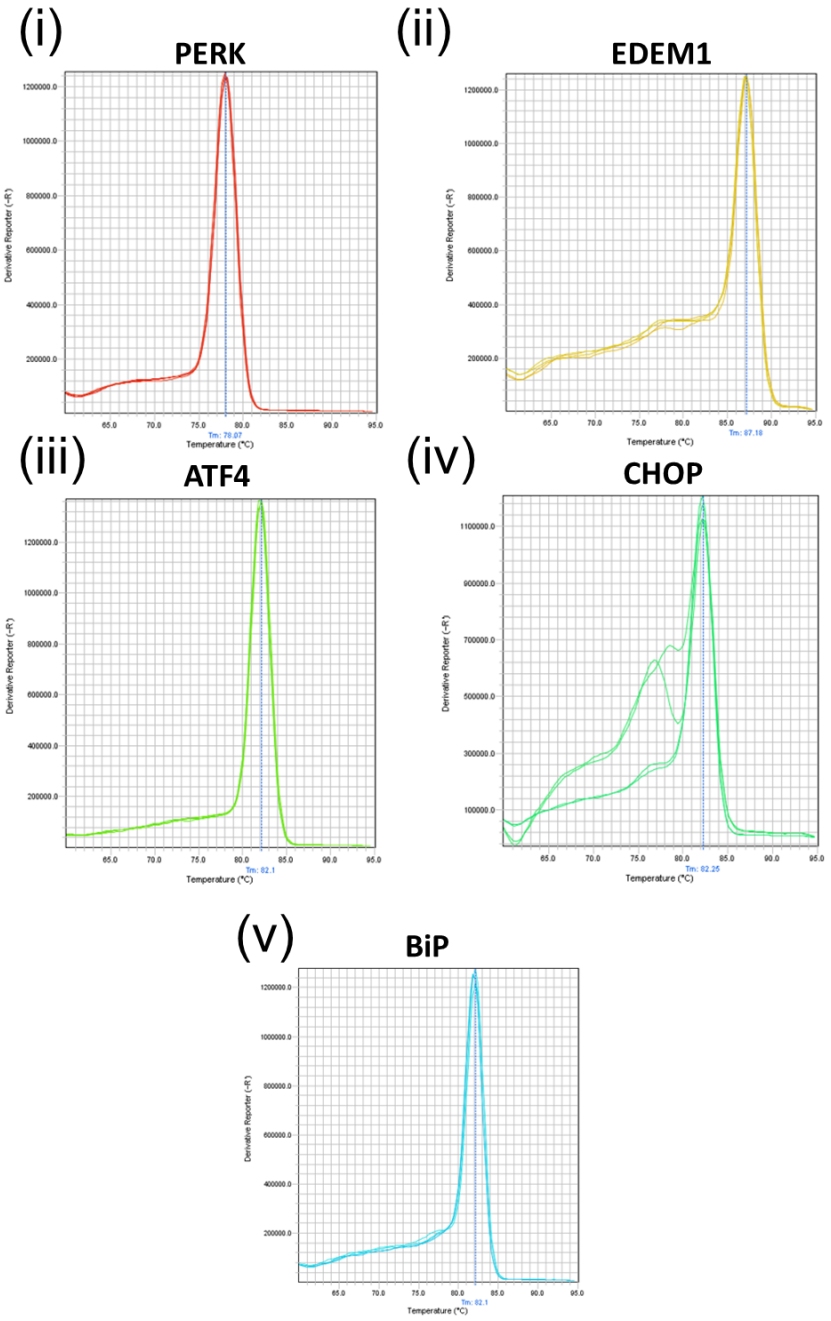

Figure 33 (i-v) – Melt curves of UPR associated genes in response to thiopurines.

THP-1-derived macrophages were either treated with DMSO (Control), 120µM AZA, 120µM 6-MP, 120µM 6-TG or 5µg/ml Tun for 8 hours. RNA was extracted and converted into cDNA. cDNA was used as a template for qPCR analysis using primers specific for *CHOP*, *EDEM1*, *ATF4*, *PERK* and *BiP*. Melt curves were generated using a StepOnePlus Real-time PCR system. n=3.

5.2.3. Assessment of Eif2α phosphorylation in response to thiopurine treatment

In the previous section we observed increased expression of UPR genes downstream of PERK in response to 6-TG. As a result of the activation of PERK, Eif2α is phosphorylated which causes global protein attenuation and the activation of ATF4 and CHOP. We therefore, examined the phosphorylation of eif2a (p-eif2a) at Ser51 in response to thiopurine treatment. Brefeldin A (BFA) can induce the UPR through the inhibition of intracellular vesicle formation and protein trafficking between the ER and Golgi apparatus (Colanzi *et al*., 2013). Therefore, BFA was used as a positive control for eif2α phosphorylation (Colanzi *et al*., 2013). As shown on **Figure 34**, increased phosphorylated of eif2a (S51) was observed in 6-TG treated cells **(Figure 34A, lane 4)** and the positive control, BFA **(Figure 34A, lane 5).** A small increase in eif2α phosphorylation was also observed in response to AZA relative to the control group **(Figure 34A, lane 1 and 2)**. No increase in eif2α phosphorylation was observed in response to 6-MP treatment. Total eif2α remained unchanged in all treatment groups tested relative to the control. Together, these results suggest that AZA and 6-TG activate the PERK pathway at the protein level.

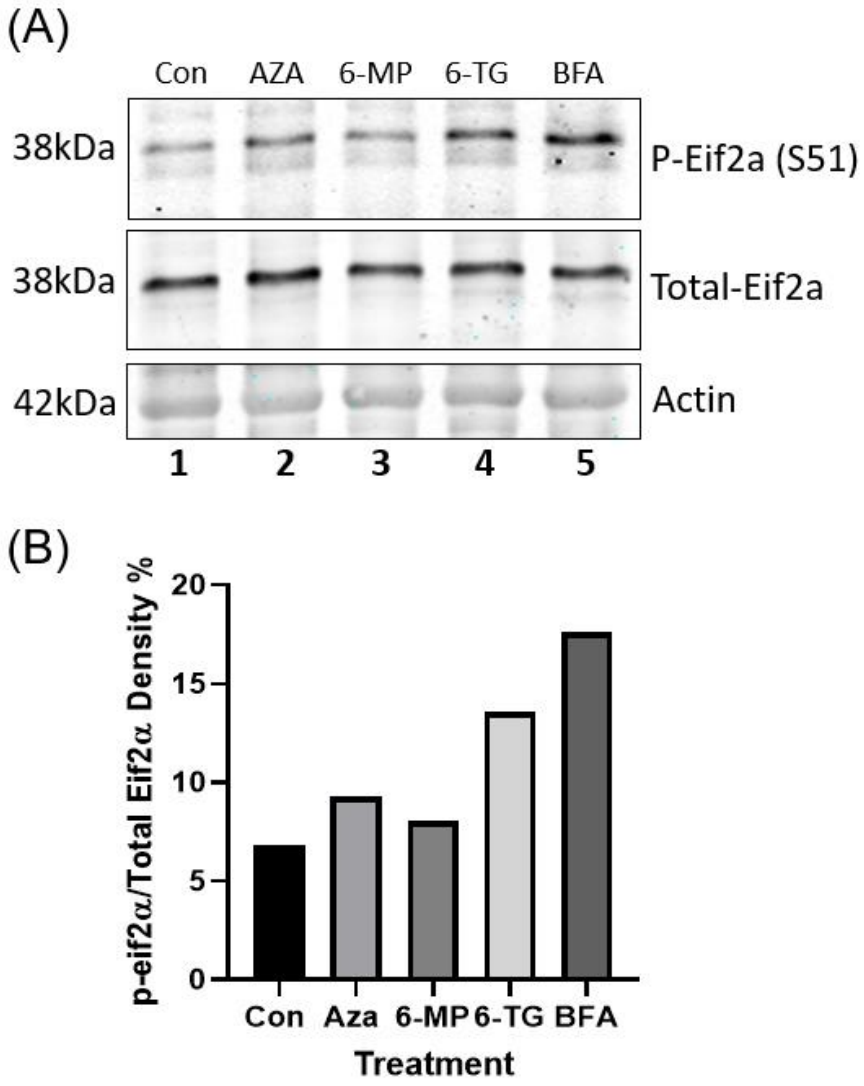

Figure 34 - Eif2α phosphorylation in response to thiopurine treatment.

(A) – THP-1-derived macrophages either treated with DMSO (Control), 120µM AZA, 120µM 6-MP, 120µM 6-TG or 1µg/ml BFA for 8 hours. Protein lysates were harvested and separated on an 8% SDS-page gel. Proteins were transferred onto nitrocellulose and immunoblotted using antibodies specific for p-eif2α (S51), eif2α and β-actin. Representative images are shown. n=3.

(B) – Densitometry was performed on immunoblots using licor software. P-eif2α (S51) mean intensity was normalised to total-eif2α mean intensity. n=3.

5.2.4. EDEM1 protein expression in response to thiopurine treatment

ER resident protein, EDEM1, is a mannose-binding protein involved in targeting of misfolded proteins for proteosomal degradation during ER stress (Zuber *et al*., 2007). As shown in **Figure 30, Part A**, EDEM1 is thought to be regulated through the IRE1α pathway. We therefore assessed changes in the abundance of EDEM1 in response to thiopurine treatment. As shown in **Figure 35**, no change in EDEM1 protein was observed in response to any thiopurine treatment, which is in agreement with the real-time PCR data **(Figure 35)**. Taken together, these results suggest that thiopurines do not act on the IRE1α pathway.

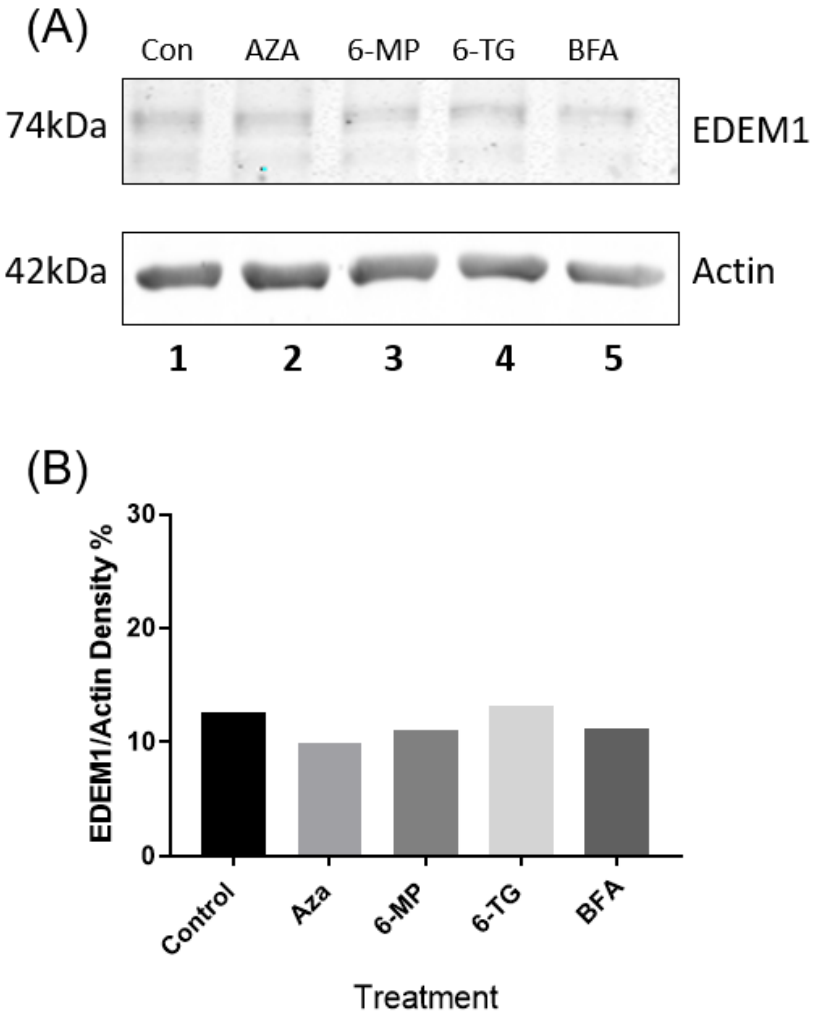

Figure 35 - EDEM1 protein expression in response to thiopurine treatment.

(A) - THP-1-derived macrophages either treated with DMSO (Control), 120µM AZA, 120µM 6-MP, 120µM 6-TG or 1ug/ml BFA for 8 hours. Protein lysates were harvested and separated on an 8% SDS-page gel. Proteins were transferred onto nitrocellulose and immunoblotted using antibodies specific for EDEM1 and β-actin. Density of EDEM1 was normalised to actin using Licor software. Representative images are shown. n=2.

(B) – Densitometry was performed on immunoblots using licor software. EDEM1 mean intensity was normalised to β-actin mean intensity. n=2.

5.2.5. Modulation of mTORC1 activity in response to thiopurines

mTORC1 is a key regulator of cell homeostasis and regulates numerous pathways including glucose metabolism, protein translation, and autophagy (Xie *et al*., 2018). mTORC1 inhibits autophagy activity during periods of amino acid sufficiency and induces autophagy activity during times of amino acid starvation, therefore mTORC1 activity is inversely correlated with autophagy activity (Rabanal-Ruiz *et al*., 2017). As shown in **Figure 36,** control of protein translation by mTORC1 is mediated by its ability to directly phosphorylate p70S6 kinase, which subsequently leads to the phosphorylation of ribosomal protein S6, a key protein within cap dependent translation and ribosomal biogenesis (p-rpS6) (Magnuson *et al*., 2012). Therefore, we measured p-rpS6 (S235/S236) as a surrogate marker of mTORC1 activity. As shown in **Figure 37B,** AZA decreased the levels of p-rpS6 by 43% relative to total rpS6 **(Figure 37A, Lane 1 and 2).** In contrast, 6-MP and 6-TG reduced phosphorylation by 6% compared to total rpS6 **(Figure 37A, Lanes 1, 3 and 4).** Unexpectedly, serum starvation induced only a moderate decrease of 24% in phospho-S6 ribosomal protein relative to total rpS6 **(Figure 37A, Lane 1 and 5).** Total rpS6 protein expression remained unchanged in all treatment groups tested relative to the control. Taken together, these results suggest that, AZA can strongly inhibit mTORC1 activity whereas the metabolites 6-MP and 6-TG have only a modest effect on mTORC1 activity.

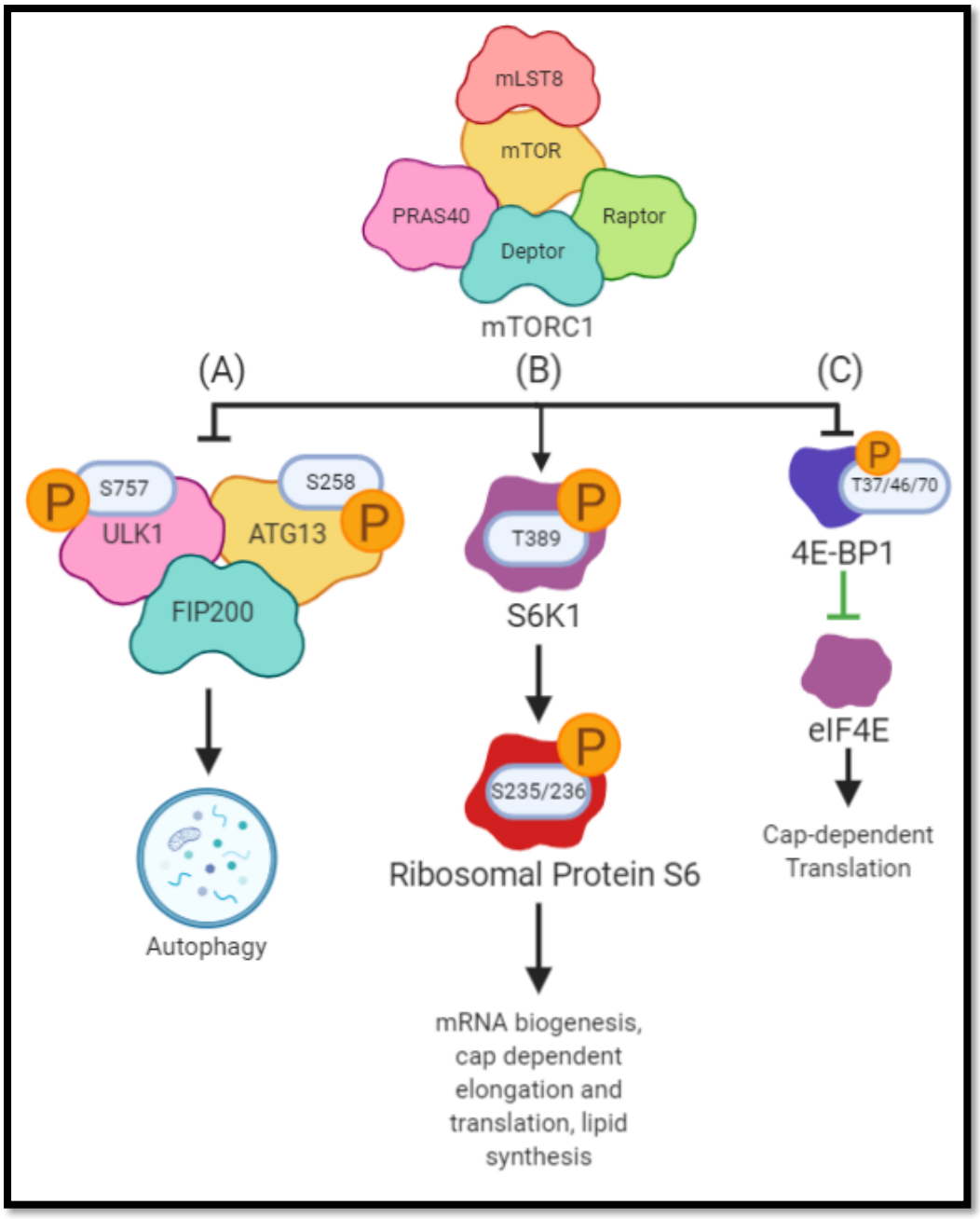

Figure 36 - mTORC1 signalling pathway.

Author's illustration of the signalling events associated with mTORC1 activation. **(A)** mTORC1 phosphorylates ULK1 and ATG13 at amino acids S757 and S258, respectively, which subsequently incorporates within the ULK-ATG13-FIP2000 complex, inhibiting autophagy. **(B)** mTORC1 induces the phosphorylation of S6K1 at amino acid T389, which subsequently phosphorylates S235/236 on ribosomal protein S6 and induces mRNA biogenesis, lipid synthesis and cap dependent elongation and translation. **(C)** mTORC1 phosphorylates amino acids T37/46, T70 and S5 on protein 4E-BP1, inhibiting its binding to eIF4E. This allows eiF4E to induce Cap-dependent translation. Illustration was created using Biorender Software.

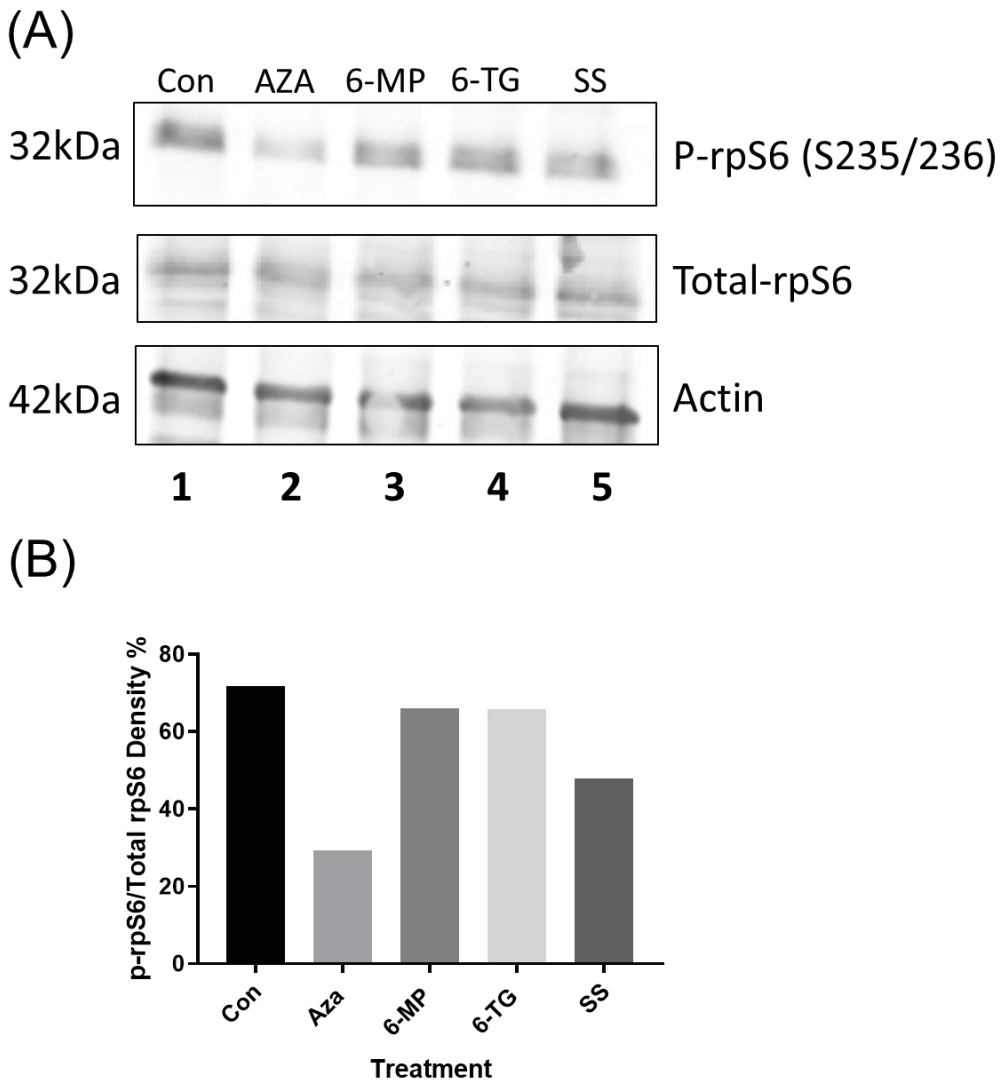

Figure 37 - Modulation of mTORC1 activity in response to thiopurine treatment.

(A) – THP-1-derived macrophages were either treated with DMSO (Control), 120µM AZA, 120µM 6-MP, 120µM 6-TG or serum starved for 8 hours. Protein lysates were harvested and separated on a 10% SDS-page gel. Protein was transferred onto nitrocellulose and immunoblotted using antibodies specific for p-rpS6 (S235/236), total-rpS6 and β-actin. Density of p-rpS6 (S235/236) was normalised to total-rpS6 using Licor software. western immunoblot is shown as a representative image. n=2.

(B) – Densitometry was performed on immunoblots using licor software. P-rpS6 (S235/236) mean intensity was normalised to total-rpS6 mean intensity. n=2.

5.3. Summary

Initially, splicing of ER stress marker *XBP1* was examined to determine whether thiopurines activate the ER stress response. XBP1 signalling was not increased in response to all thiopurines tested, indicating that thiopurines do not induce ER stress signalling.

At the 8h time-point, 6-TG significantly induced the expression of PERK downstream signalling genes, *ATF4* and *CHOP*. An increase in the phosphorylation of the downstream PERK substrate, eif2α, was also observed during 6-TG treatment, confirming the activation of PERK signalling by 6-TG. No increase was observed in all UPR genes tested in response to both AZA and 6-MP treatment. However, a slight increase in eif2α phosphorylation was observed in response to AZA treatment, but not 6-MP treatment. IRE1α signalling appears to be not regulated by thiopurine treatment as EDEM1 gene and protein expression was not altered in response to all thiopurines.

The activity of mTORC1 was analysed to determine whether thiopurines regulate autophagy through mTORC1 signalling. AZA markedly decreased rpS6 phosphorylation indicating a decrease in mTORC1 activity. In contrast, 6-MP and 6-TG exhibited no change in rpS6 phosphorylation.

Taken together these results suggest 6-TG induces PERK signalling at the time and dose assessed. AZA inhibits mTORC1 activity, which was not observed in 6-MP and 6-TG treatment. Further studies will be required to assess further time-points.

Chapter 6. Discussion

6.1. Overview

IBD treatment in the UK costs approximately £720 million per year, with 25% of this being associated with drug costs (NHS England). 1 in 5 UC patients have ineffective response rates and 60-75% of CD patients require surgery due to the ineffectiveness of treatment (nhs.uk, 2018). Therefore, it is important to identify the interaction of these drugs with pathways associated with IBD so that therapies can be more appropriately optimised. The immunosuppressive capabilities of thiopurines have been found to be beneficial for the treatment of IBD, for example in post-operative disease maintenance, prolonging disease remission and regulation of antibody production when used in conjunction with TNF-α therapy (Axelrad *et al*., 2016). However, thiopurines have been scrutinised due to their extensive side effects, including hepatotoxicity, pancreatitis and myelotoxicity, which limit their capabilities (Qiu *et al*., 2015). SNPs associated directly, and indirectly, with genes involved in the autophagy pathway have been linked to the pathogenesis of IBD (Massey *et al*., 2008). Interestingly, previous work by Hooper *et al*., (2019) found that thiopurines regulate autophagy activity. We therefore aimed to further characterise the regulation of autophagy activity by thiopurines.

6.2. HEK293 cells: A reporter cell line for autophagy modulation

Two types of methodologies can be utilised to investigate autophagy; experiments can either observe the presence and movement of autophagy-related proteins or can quantify proteins that are degraded through autophagy (Yoshii and Mizushima, 2017). LC3 was selected as a marker for autophagy activity due to its close association to autophagosomal membranes (Hansen and Johansen, 2011). This is due to the specific cleavage that occurs at the carboxyl terminal on LC3 proteins that forms LC3-I. This allows an exposed glycine group within the carboxyl terminal to conjugate to PE on autophagosomal membranes, forming LC3-II (Hansen and Johansen, 2011).

HEK293 cells are renowned for their robustness, rapid division rate and high DNA plasmid transfection efficiency (Ooi *et al*., 2016). In addition, the autophagy pathway is well characterised in HEK293 cells (Musiwaro *et al*., 2013). HEK293 cells engineered to stably express GFP-LC3 were available in our laboratory. This tool

allowed us to observe autophagy induction in response to thiopurines in real-time, which allowed for more accurate optimisation of drug concentrations and timepoints prior to moving our investigation into THP-1 macrophages. Therefore, initial experiments, such as assay optimisation, was performed in HEK293 cells and validated experimental findings were performed in THP-1 macrophages, due to the involvement of immune cells in IBD pathogenesis.

6.3. Induction of autophagy by thiopurines in HEK293 cells

Hooper *et al*., (2019) demonstrated that concentrations of AZA at 120μM induced autophagy and were not cytotoxic to HEK293 cells. However, 6-MP and 6-TG were not investigated. We therefore initially treated GFP-LC3 engineered HEK293 cells with AZA, 6-MP and 6-TG at a concentration of 120μM to determine effects on autophagy and cytotoxicity. We observed that all thiopurines induced autophagy modulation in HEK293 cells. Interestingly, AZA induced autophagosome accumulation more rapidly compared to 6-MP and 6-TG. This could suggest that secondary events resulting from the metabolism of AZA, including the depletion of GSH, increased ROS production, and release of the imidazole derivative may have an effect of autophagy induction.

ROS has been found to be critical in the induction of autophagy during AZA treatment, with ROS scavenging leading to a reduction in apoptosis and LC3-II (Chaabane and Appell, 2016). Excessive ROS production caused by AZA treatment results in mitochondrial damage and the depletion of ATP through the opening of mitochondrial permeability transition pores (Lee & Farrell, 2001). Additionally, Fernández-Ramos *et al*. (2017) found that 6-MP mediated ATP depletion regulated autophagy related signalling pathways such as the phosphorylation of AMPK and inhibition of mTORC1. Furthermore, moderate ROS concentrations inhibit protein tyrosine phosphatases, which can induce (PI3K) signalling, a major pathway involved in autophagy signalling (Zhao *et al*., 2017). This illustrates that ROS produced during the metabolism of thiopurines could regulate the primary pathways which directly regulate autophagy activity. ROS can be produced from several reactions that take place during the metabolism of thiopurines. For example, Al Maruf *et al*. (2014) found that the depletion of GSH was compulsory for ROS formation during AZA treatment. Depletion of GSH during AZA treatment is due to the conjugation of reduced GSH to AZA to form 6-MP, which is catalysed by glutathione S-transferase. (Al Maruf *et al*., 2014).

In the context of structural modifications to enhance biological activity of these therapeutics, the imidazole moiety was initially conjugated to 6-MP to extend the half-life of the substance as it protects its sulphur group from oxidation and hydrolysis. 6-MP with the addition of the imidazole moiety was then released as product called AZA, which initially showed more therapeutic effects than 6-MP during kidney transplants in humans (Murray *et al*., 1963). As much as 12% of AZA can be metabolised to hypoxanthine and imidazole (Fotoohi *et al*., 2010). Interestingly, imidazole conjugates have also illustrated PI3K inhibitory activity (Mohan *et al*., 2016). If the imidazole derivatives that are released during AZA metabolism also exhibited the same inhibitory effect towards PI3K, this may explain how AZA could induce autophagy activity more rapidly than 6-MP and 6-TG.

Live cell imaging is an effective method to observe autophagosome accumulation in real-time. However, due to stress that is caused by inducing cells to express fluorescent proteins, it is difficult to achieve this in sensitive cell lineages. In addition, due to GFP being a large protein (28kDa in size and 4.2nm in length), there is the possibility that the conjugation of GFP could affect the activity and localisation of LC3 (Hink *et al*., 2000). Fixed cell imaging is commonly employed to assess protein localisation as it is cost-effective, less time-consuming and easy to use. (Hobro and Smith, 2017). PFA is commonly utilised as a fixation agent during fixed cell imaging as it causes molecular cross-linking between amino groups of lysine resulting in methylene bridge formation, which preserves cellular architecture and bio-active molecules within their spatial relationship in the cell (Thavarajah *et al*., 2012). As both techniques utilise different methodologies, we aimed to assess if autophagosome accumulation was comparable between fixed cell imaging and live-cell imaging. We observed that 6-MP treatment in fixed cells was not in agreement with results from live cell imaging, as autophagosome accumulation was not observed in fixed cells during an 8h treatment course. Live cell imaging requires that intense light is used to excite the fluorophores of interest in the sample, which may result in phototoxicity in live samples (Icha *et al*., 2017). This may explain the induction of autophagy in the control group after the 12h timepoint during live cell imaging, which was not observed in fixed cell imaging. Therefore, despite live cell imaging being a powerful experimental tool, fixed cell imaging may produce more reliable results.

Using fixed cell imaging, we concluded that all thiopurines were shown to have sustained autophagosome accumulation at the 24h time point, indicating a prolonged response. Although 24h was the longest time point investigated, results from Fernández-Ramos *et al*. (2017) observed autophagy induction at both a 48h and 72h time point during 6-MP treatment in Jurkat T cells, indicating thiopurine induced autophagy activity is a more prolonged response than what was observed in our study. Thio-GTP has been found to be at concentration of 2.5mM in leukaemia cells after a 4-hour exposure to 6-TG at 25µM (Shi *et al*., 1998). The increased concentration of Thio-GTP inside the cell during 6-TG treatment found in the study by Shi *et al*., (1998) correlates with the rate at which 6-TG induced autophagy found in our study, indicating that the intercalation of thio-GTP into DNA may induce autophagy. The potential mechanism is supported by findings from Zeng *et al*., (2007) who observed that HCT116 cells which possess dysfunctional DNA mismatch repair (MMR) systems failed to induce autophagy after 3 days of 6-TG treatment, in contrast to MMR+ cells, which did induce autophagy. Therefore, a potential mechanism of autophagy induction could be due to the incorporation of drug metabolites into DNA and could be facilitated by metabolites released during the catabolism of thiopurines, which also could explain the differences in the rate of autophagy induction.

6.4. Effect of thiopurines on the metabolic activity of HEK293 cells

Our results illustrated that 6-TG has a more anti-proliferative effect than AZA and 6-MP, which in agreement with previous *in vitro* studies (Adamson *et al*., 1994). The increased anti-proliferative effect of 6-TG could be due to the direct conversion of 6-TG to its active substrate, 6-TGN, compared to 6-MP and AZA, which undergo a series of enzymatic steps that produce several inactive metabolites (Seinen *et al*., 2010). By avoiding many rate limiting enzymatic steps, particularly IMPDH, this allows 6-TG to be rapidly converted into 6-TGN. Significantly higher concentrations of 6-TGN have been found to be generated from 6-TG treatment compared to AZA and 6-MP due to increased bioavailability (Petit *et al*., 2008). Shi *et al*., (1998) demonstrated that 6-TG treated leukaemia cells, observed over a 24h period, had a higher accumulation of thio-GMP, GDP and GTP compared to 6-MP treated cells. This is reinforced by findings that the drug becomes undetectable in patient plasma 6 hours post-administration (Blaker *et al*., 2012). Therefore, it appears that 6-TG may have a more potent anti-proliferative effect compared to AZA and 6-MP due to producing a higher

concentration of metabolites that can intercalate into DNA. We observed a reduction in metabolic activity at the 2h timepoint and an increase in autophagy activity at the 4h timepoint in response to 6-TG treatment. Therefore, it could be speculated that the increase in autophagy activity is a survival mechanism responding to a decrease in metabolic activity. However, AZA and 6-MP also showed an increase in autophagy activity without observed changes to metabolic activity, indicating that the mechanisms may be independent.

6.5. THP-1 cells: An *in vitro* cell model of macrophage function

A dysregulation in the immune response is one of the key factors associated with IBD pathogenesis. The inability for gastrointestinal macrophage's to clear invading pathogens and an imbalance of pro-inflammatory to anti-inflammatory signalling has been found facilitate IBD development (Steinbach and Plevy, 2014). Therefore, we aimed to validate experimental findings in an *in vitro* macrophage model. The monocytic cell line, THP-1 cells, are the most commonly used cell line for *in vitro* studies investigating human macrophage function (Lund *et al*., 2016). They can be differentiated into a variety of macrophage subsets (Starr *et al*., 2018). PMA is a well-documented phorbol ester that can differentiate monocytes to macrophages through the activation of protein kinase C (Schwende *et al*., 1996). However, there is no gold-standard protocol for the differentiation of THP-1 cells into macrophages, and concentrations of PMA used range from 6 to 500nM throughout the published literature (Lund *et al*., 2016). Studies have found that higher concentrations of PMA can stimulate the expression of inflammatory genes, such as *IL-8, TNF-α* and *IL-1β* (Park *et al*., 2007). Given that exogenous TNF-α has been shown to induce autophagy (Yuan *et al*., 2018), lower concentrations of PMA were investigated for their ability to differentiate THP-1 monocytes to avoid autophagy induction from the differentiation process. Concentrations of PMA between 5-20ng/ml have been used in numerous studies due to their ability to stimulate differentiation of cells which retain common macrophage markers and response to stimuli (Lund *et al*., 2016; Starr *et al*., 2018). PMA at a concentration of 20ng/ml resulted in the highest level of adherence in THP-1 cells, and therefore this concentration of PMA was used to differentiate THP-1 cells for the entirety of this study.

Analysis of established macrophage markers was performed to determine whether PMA treatment successfully differentiated THP-1 cells into a macrophage-like cell phenotype. CD68 is a commonly used marker to identify a variety of different macrophage lineages (Chistiakov *et al*., 2017). An increase in CD68 expression was observed in THP-1 monocytes differentiated only with PMA relative to the control. This suggests that the PMA treatment used in our study is able to differentiate monocytes to macrophages. Although the increase was relatively limited, this could be explained by the nature of the protein, which is mainly found in the endosomal/lysosomal compartment of the cell (Chistiakov *et al*., 2017). Approximately 85-90% of murine CD68 is located within intracellular pools that can rapidly transfer to the cellular membrane (Kurushima *et al*., 2000). As the cells utilised in this study were not permeabilised prior to PMA treatment, this could explain the lack of considerable increase in CD68 expression.

Interestingly the M2 macrophage marker, CD163, was increased in THP-1 monocytes treated with PMA. Questions have been raised on the specificity of CD163 in terms of M2 macrophages, with prognostic studies in Hodgkin lymphoma exhibiting high numbers of CD163+ macrophages within a tumour microenvironment showing a Th1 signature (Barros *et al*., 2012). This could also explain the observation of high CD163+ marker expression in monocytes treated with LPS and IFN-γ, stimuli know to differentiate monocytes to M1 macrophages (Orecchioni *et al*., 2019). However, monocytes treated with PMA did not exhibit as high as an expression of CD163 compared to monocytes treated with IL-4 and IL-13, stimuli known to induce M2 macrophage differentiation. Therefore, the difference in marker expression between PMA-only treated THP-1 monocytes and THP-1 derived M1 and M2 macrophage used as positive controls would suggest that PMA does not drive THP-1 cells into a M1 or M2 subset.

6.6. Induction of autophagy by thiopurines in THP-1 derived macrophages

Using timepoints and concentrations optimised from findings in HEK293 cells, we investigated autophagy induction in response to thiopurines in THP-1 macrophages. Fixed THP-1 derived macrophages and HEK293 cells exhibited differences in the rate of autophagy induction following 6-MP treatment, with THP-1 derived macrophages

exhibiting an induction at the 8h timepoint compared to HEK293 cells, which did not. Interestingly, the rate at which thiopurines intercalate into DNA has been found to be cell type dependent. For example, after an 48h incubation with 1µM of 6-TG, 0.3% of guanine in nuclear DNA was substituted in HCT116, whereas this was two-fold higher in J774.a cells (Daehn *et al*., 2011). However, the induction of autophagy observed may not be solely due the incorporation of 6-TGN in DNA, as MMR deficient leukaemia cells are also sensitive to thiopurine drugs (Zhang *et al*., 2013).

Hepatoxic metabolites produced during the catabolism of thiopurines may induce autophagy. As discussed previously, autophagy is increased during thiopurine-induced hepatotoxicity to protect hepatocytes from the deleterious effects of thiopurines (Guijarro *et al*., 2012). Bradford and Shih, (2011) demonstrated that elevated concentrations of 6-MMP in erythrocytes is associated with hepatoxicity in patients; indicating 6-MMP may potentially regulate autophagy activity. TPMT is responsible for the conversion of thiopurines into inactive S-methyl derivatives, including 6-MMP (Cuffari, 2006). TPMT has also been directly associated with thiopurine efficacy, with findings in CCRF-CEM cells showing elevations of TPMT activity result in an increase in 6-MP sensitivity but a decrease in 6-TG sensitivity (Fotoohi *et al*., 2010). TPMT has been found to have trimodal distribution from patient to patient due to autosomal dominant inheritance of polymorphisms associated with the enzyme (González-Lama and Gisbert, 2016). This results in patients varying from low to high TPMT enzyme activity (González-Lama and Gisbert, 2016). Therefore, it would be of value to examine differences in TPMT activity in THP-1 macrophages and HEK293 cells to determine its association with thiopurine-induced autophagy activity. Increased autophagy activity seen during 6-MP treatment compared to AZA and 6-TG could be due to the catabolism of 6-MP to meTIMP. meTIMP is an inhibitor of phosphoribosylpyrophosphate amidotransferase, an enzyme critical for the initial stages of de novo purine biosynthesis (Karran, 2007). This can result in purine starvation in the cell, which may ultimately lead to metabolic stress and autophagy induction (Karran, 2007). This mechanism of action would only be applicable towards AZA and 6-MP, as 6-TG is not catabolised to form thioinosine monophosphate.

In addition, the metabolism of 6-MP to thiouric acid by xanthine oxidase is also a reaction known to produce ROS (Chaabane and Appell, 2016). Therefore, ROS produced during the metabolism of 6-MP to thiouric acid could result in an increase in

autophagosome accumulation observed. Interestingly, HEK293 cells do not express xanthine oxidase, which could explain the difference in autophagy induction observed between 6-MP-treated HEK293 cells and THP-1 derived macrophages (Haglund *et al*., 2017). However, studies have suggested ROS production is not a critical factor in the mechanism of action as AZA treatment in human hepatocytes had shown to only slightly increase ROS production (Petit *et al*., 2008). It was speculated that excessive ROS production by 6-TG and 6-MP may be restricted to tumour cell lines (Chaabane and Appell, 2016). In addition, Petit *et al*., (2008) observed an increase in ROS production in 6-TG-treated cells only after 96h. Therefore, next steps should attempt to identify if ROS production during thiopurines treatment is sufficient to induce autophagy in non-tumour cells. This could be assessed by inhibiting ROS production through the use of antioxidants, including N-acetylcysteine, and assessing autophagy induction during the use of these agents. ROS production could be examined through the use of 2', 7' dichlorofluorescein diacetate. Dichlorofluorescein is a substrate that is oxidised by intracellular ROS, which produces as fluorescent dichlorofluorescein and can be measured through spectrophotometry (Al Maruf *et al*., 2014).

We also observed a dose-dependent increase in autophagosome accumulation when concentrations of thiopurines between 20-120μM were tested. A slight increase in autophagosome accumulation was observed during treatment with 20μM of 6-MP and 6-TG compared to AZA, suggesting that catabolism of AZA is not the primary mechanism for autophagosome accumulation; however, these results were non-significant. These results may also suggest that the release of the imidazole derivative may inhibit AZA induced-autophagy activity. Imidazole has been shown to inhibit autophagy by impairing maturation of autophagosomes to lysosomes (Liu *et al*., 2015). It has been proposed that this is due to imidazole being a weak base, which can enter acidic organelles and cause dysfunction by elevated intra-lysosomal pH (Liu *et al*., 2015). Imidazole has also been shown to increase apoptosis inside HEC-1B cells, with an increase in pro-apoptotic markers Bim, caspase 3 and caspase 9 (Liu *et al*., 2015). This potentially could explain why three quarters of IBD patients intolerant to AZA treatment respond more effectively to 6-MP treatment (McGovern *et al*., 2002). One challenge when utilising *in vitro* tools is the translation of therapeutic concentrations of drugs to and from *in vivo* research. The concentrations used in this study were selected due to the use of these concentrations in previous studies and lack of

cytotoxicity observed from metabolic assays (Chaabane and Appell., 2016; Hooper *et al*., 2019). Lennard *et al*., (1997) suggested that drug concentrations are not likely to surpass 10µM within tissue when a dose of 2-3mg/kg is administered. However, we did not observe a sustained loss of metabolic activity or late apoptosis signalling in the highest dose used within this study, indicating that the concentration used were of physiological relevance.

6.7. Effect of thiopurines on autophagy activity in THP-1 derived macrophages

We analysed the accumulation of LC3-II as this protein accumulates on autophagosome membranes inside the cell. However, LC3-II abundance does not directly correlate with autophagy activity, as an increase in LC3-II can also result from the inhibition of autophagosome fusion and degradation by lysosomes (Yoshii *et al*., 2017). It was therefore critical that we distinguished if the increased autophagosome accumulation that we observed in response to thiopurines was due to activation or inhibition of the autophagy pathway. To elucidate if autophagy was activated during thiopurine treatment, we utilised a GFP-RFP-LC3 plasmid. We observed an increase in autophagic puncta (RFP+/GFP-) in response to thiopurines, indicating the complete progression of the autophagy pathway. As autophagy is found to be dysfunctional in IBD patients, the findings that autophagy is induced during thiopurine treatment could help partially explain its mechanism of action. The induction of autophagy has been shown be therapeutic in CD patients. Rapamycin, an mTOR inhibitor and inducer of autophagy, has been found to improve disease symptoms in CD patients (Massey *et al*., 2008). Moreover, rapamycin has been found to induce clinical remission and mucosal healing in refractory paediatric CD patients (Mutalib *et al*., 2014). These findings help support the theory that the induction of autophagy by thiopurines could be therapeutic in IBD patients.

As shown in **Figure 38,** the induction of autophagy activity by thiopurines could have a range of benefits in IBD patients. For example, Andrographolide, a known mitophagy inducer, has been shown to inhibit the NLRP3 inflammasome and reduce DSS-induced colitis (Larabi *et al*., 2020). In addition, autophagy has been found to regulate the secretion of the pro-inflammatory cytokine, IL-1β, through the degradation of pro-IL1β in a NLRP3 and TRIF-dependent manner **(Figure 38)** (Harris *et al*., 2011).

A common characteristic found in IBD is microbial dysbiosis, which leads to an increase in opportunistic pathogens; including AIEC (Vazeille *et al*., 2015). Autophagy is critical in regulating AIEC persistency and the pro-inflammatory cytokines released in response to AIEC infection (Small *et al*., 2013). AIEC has been shown to be persistent in human cell lines by suppressing autophagy, through the induction of microRNA *MIR106B* and *MIR93*, indicating the importance of functional autophagy in AIEC clearance (Lu *et al*., 2014). In addition, human primary macrophages that express the *ATG16L1*^{T300A} variant exhibit impaired mitophagy, an increase in ROS production and ineffective bacterial clearance during Salmonella Typhimurium infection (Zhang *et al*., 2017). Hooper *et al*., (2019) demonstrated that AZA-treated cells exhibited both an increase in autophagy activity and enhanced clearance of intracellular AIEC compared to a control group. AIEC-infected THP-1 macrophages also exhibited a decrease in TNF-α gene expression when treated with AZA, indicating a decrease in the inflammatory response associated with bacterial clearance (Hooper *et al*., 2019). It has also been hypothesised that the binding of ATG16L1 to NOD2 during bacterial invasion shifts the response towards autophagy signalling, and a suppression of functional ATG16L1 leads to a shift towards pro-inflammatory cytokine production (Plantinga *et al*., 2011). This hypothesis is supported by the isolation of macrophages and DC's from the mesenteric lymph nodes in *ATG16L1*-deficient mice, which exhibited an increase in pro-inflammatory cytokines IL-1β and TNF-α (Zhang *et al*., 2017). This could help explain the synergistic effect observed in AZA and anti-TNFα therapy in IBD patients. In addition, autophagy activation enhances the processing of antigens to be presented on MHC I and MHC II molecules and drives plasma cells differentiation, which induces the adaptive immune response against opportunistic pathogens **(Figure 39)** (Jiang *et al*., 2019). Autophagy has also been found to play a central role in CD4+ T cell stability, as ATG7-deficient Treg cells exhibit a reduction in Foxp3, Foxo and Bach2 which is accompanied by an increase in IFN-γ and IL-17 production (Jacquin and Apetoh, 2018). Therefore, thiopurines could induce autophagy activity that is otherwise impaired in immune cells harbouring the *ATG16L1* variant, which could promote bacterial clearance, cytokine and ROS regulation that is otherwise impaired in these cells.

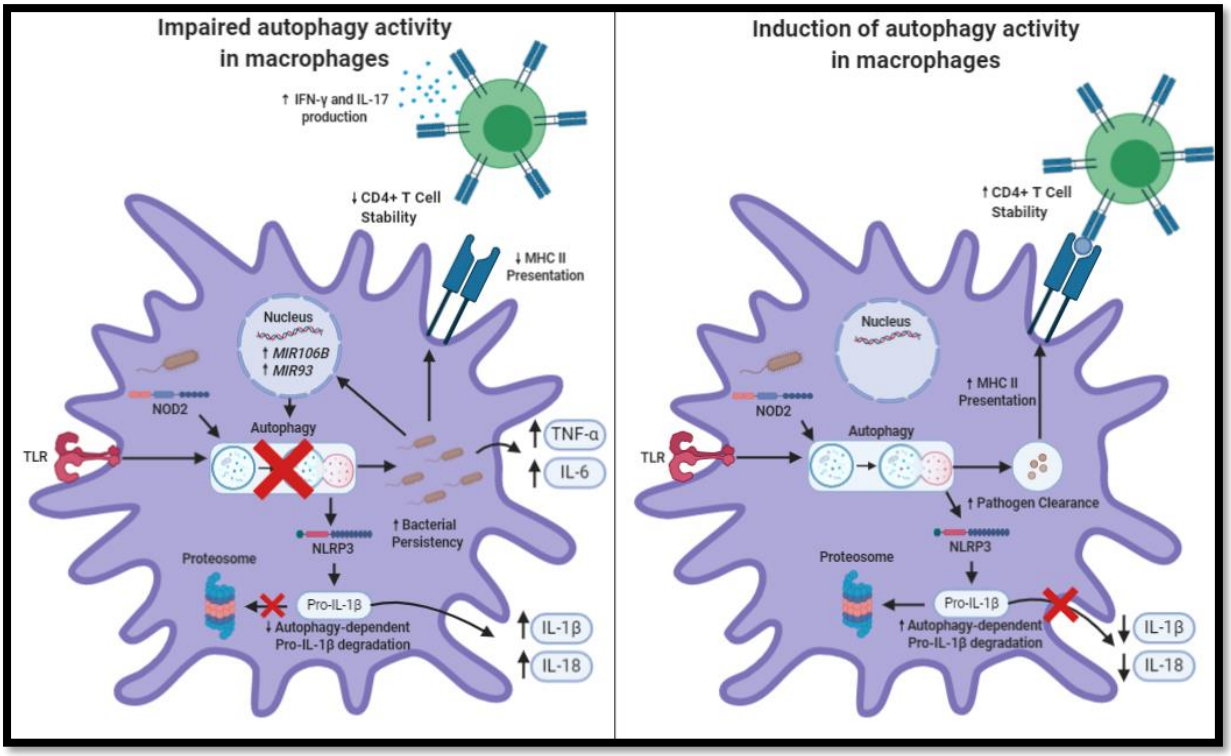

Figure 38 – Autophagy activation in Macrophages.

Illustration of the impact autophagy induction would have on macrophage's dysfunctional in autophagy signalling. Dysfunctional autophagy in macrophages (left) leads to bacterial persistence, reduced MHC presentation, reduced regulatory T cell stimulation and an increase in proinflammatory cytokines including IL-1β, TNF-α, IL-6 and IL-18. An induction of autophagy inside macrophages (right) leads to an increase in pathogen clearance, MHC presentation and regulatory T-cell stability. It would also increase the degradation of pro-IL-1β, leading to a reduction in the release of IL-1β. Image created on Biorender software.

6.8. Interplay between autophagy and apoptosis

Numerous studies have observed autophagy signalling accompanied with pro-apoptotic signalling during thiopurine treatment (Chaabane and Appell, 2016; Tiede *et al*., 2003; Zeng *et al*., 2007). Autophagy has been suggested to play a protective role during the induction of apoptosis in hepatocytes (Chaabane and Appell, 2016). We observed a slight increase in THP-1 macrophages undergoing early apoptotic signalling during AZA and 6-TG treatment. However, statistical significance was not established due to a lack of replicates. An increase in apoptotic signalling has previously been documented during thiopurine treatment. Tiede *et al*., (2003) also observed an increase in early apoptotic signalling during thiopurine treatment using

an Annexin V/PI stain. Although the authors observed apoptotic signalling during 6-MP treatment, the treatment method was significantly longer, with cells exposed to thiopurines for up to 5 days (Tiede *et al*., 2003). This could strengthen the hypothesis that thiopurine-induced autophagy may coincide with apoptotic signalling. Consistent with this hypothesis, suppression of autophagy by chloroquine during thiopurine treatment increased PARP cleavage (apoptotic marker) in a dose dependant manner (Chabbane and Appell, 2016). A colocalization of LC3-II fluorescence and the mitochondrial marker, tetramethylrhodamine methyl ester, was also observed, indicative of damaged mitochondria being degraded through mitophagy. Tiede *et al*., (2003) also provided evidence that thiopurine-induced apoptosis is dependent of mitochondrial injury, as mitochondrial membrane potential was reduced during 6-MP treatment and chemical inhibition of caspase 9 activity prevented 6-MP dependent apoptosis. Caspases are synthesised as precursors, which can be activated through the release of pro-apoptotic markers from the mitochondrial intermembrane space during mitochondrial permeabilization (Costantini *et al*., 2002; Tiede *et al*., 2003). An example of these markers includes cytochrome c, which initiates the formation of the apoptosome. One constituent of the apoptosome is pro-caspase 9, which is known to play a critical role in 6-MP dependent apoptosis (Costantini *et al*., 2002). These results indicate that the apoptotic signalling observed in our study could be due to mitochondrial injury, which could initiate autophagy as a survival mechanism. This could be investigated further following a similar approach to Tiede *et al*., (2003), in which markers of apoptosis that are release from injured mitochondria are measured. These markers, including pro-caspase 9, could then be regulated by chemical inhibition to examine their effect on autophagy signalling and localisation.

Early apoptotic signalling and autophagy induction observed in our study may also be a response to MMR processing caused by base pairing of 6-TGN in DNA, which resembles replication errors and drives apoptotic signalling by impairing the activity of enzymes involved with DNA replication and repair, such as Topoisomerase II and T4 DNA Ligase. (Misdaq *et al*., 2015). (Zeng and Kinsella, 2007) shown evidence of an induction of autophagy in a p53 dependent manner during 6-TG treatment, which was not observed in MMR-deficient human tumour cells. This mechanism of action would be possible in THP-1 macrophages and HEK293 cells as both cell lines are MMR proficient. Autophagy induction during DNA mismatch damage was also found to

inhibit apoptosis, supporting the hypothesis by Chaabane & Appell (2016) and strengthening the argument that autophagy and apoptosis are interlinked (Zeng and Kinsella, 2007). Although the distinct mechanisms are not elucidated, p53 is an important regulator in metabolic checkpoints and cell metabolism (Fernández-Ramos *et al*., 2017). Interestingly, during AZA treatment, energetic stress has been observed where AZA can alter glucose and glutamine metabolism. The adaptive changes during AZA treatment also corresponded with AMPK activation (Fernández-Ramos *et al*., 2017). Therefore, it could be speculated that the alteration in cell metabolism possibly caused by p53 could initiate AMPK as an adaptive response, which subsequently activates autophagy.

An increase in apoptotic signalling in immune cells has been found to be promote bacterial clearance and mediate pro-inflammatory signalling. Apoptosis prevents the initiation of an inflammatory response as it does not allow cytoplasmic content to be expelled into the extracellular environment (Lamkanfi and Dixit, 2010). In addition, apoptotic cells that are phagocytosed by macrophages do not induce inflammatory cytokines and does not induce the differentiation of DC's into a pro-inflammatory subset (Lamkanfi and Dixit, 2010). For example, the exposure of phosphatidylserine to the outer leaflet in apoptotic cells has been found to be essential for the engulfment of apoptotic cells by macrophages and fibroblasts (Fadok *et al*., 2001). Therefore, the induction of apoptotic signalling by thiopurines would allow macrophages burdened with bacterial infection to be cleared in the absence of a pro-inflammatory response, similar to what is seen during pyroptosis or necrosis (Lamkanfi and Dixit, 2010). In addition, deletion of proteins involved in the extrinsic apoptotic pathways, such as Fas, increased the susceptibility to sepsis associated death in mice during *Pseudomonas aeruginosa* infection, indicating its importance in bacterial clearance (Grassmé *et al*., 2000). Therefore, the induction of apoptotic signalling seen in our study may be beneficial to bacterial clearance in macrophages.

6.9. Effects of thiopurines on the ER-Stress response in THP-1 derived macrophages

XBP1 is a key regulatory protein in UPR signalling, which prevents chronic ER stress and the initiation of inflammatory response in multiple cell types (Cao, 2016). *XBP1* splicing is commonly used a marker for IRE1 activation and ER stress signalling (Cao,

2016; Kaser *et al*., 2008). Interestingly, deletion of *XBP1* in a murine model resulted in spontaneous enteritis, which was associated with increased ER stress signalling, indicating its importance in CD-associated inflammation (Kaser *et al*., 2008). In addition, SNPs located in intron 4 of *XBP1* have been significantly associated with IBD in a German cohort, indicating the importance of ER stress in IBD pathogenesis (Kaser *et al*., 2008). Thiopurine treatment induces stress in the cell, resulting in mitochondrial permeabilization, ROS production and the induction of MMR (Chabbane and Appell, 2016; Fernández-Ramos *et al*., 2017). We therefore investigated whether induction of the UPR reported in the study by Hooper *et al*., (2019) was direct or a secondary effect of induction of ER stress by thiopurines. In the presence of ER stress, a 26bp fragment from *XBP1* mRNA is excised, resulting in the production of a potent transcription factor for UPR associated genes, known as *sXBP1* (Calfon *et al*., 2002). Therefore, we investigated *XBP1* splicing as a marker for the presence of ER stress. Splicing of *XBP1* mRNA was not observed in all thiopurines tested, compared to the positive control Tunicamycin, which exhibited two splice variants.

Tunicamycin functions as a N-acetylglucosamine transferase, which blocks N-linked glycosylation and leads to the accumulation of misfolded proteins (Kishino *et al*., 2017). The largest splice variant observed during tunicamycin treatment has been observed from previous studies utilising this assay (Chalmers *et al*., 2017; Shang and Lehrman, 2004). Shang and Lehrman (2004) described the variant as a hybrid product that is double stranded cDNA consisting of a single strand of *XBP1u* and a single strand of *XBP1s*, which is formed during the final PCR step. Due to the larger size of the hybrid *XBP1* variant, it migrates slower down the gel, producing a distinct third band **(Figure 39)** (Chalmers *et al*., 2017). This third band is still a strong indication of the presence of ER stress as splicing of *XBP1* is occurring to produce this hybrid cDNA product. It was also described that *XBP1h* is most abundant during milder stresses, as both spliced and unspliced strands are present (Shang and Lehrman, 2004).

As we did not observe an increase in the ER stress response during thiopurine treatment, we suggest that thiopurines do not induce sufficient ER stress to initiate *XBP1* splicing. ER stress signalling has been observed within the colonic and ileal mucosa of IBD patients, with an increase in grp78 and XBP1 expression within both inflamed and non-inflamed CD patient biopsies (Kaser *et al*., 2008; Shkoda *et al*., 2007). Therefore, if thiopurines did cause ER stress in the cell, this could exacerbate the disease further. This indicates that thiopurines could assist in the removal of misfolded proteins in the cells by inducing the UPR independently of ER stress induction.

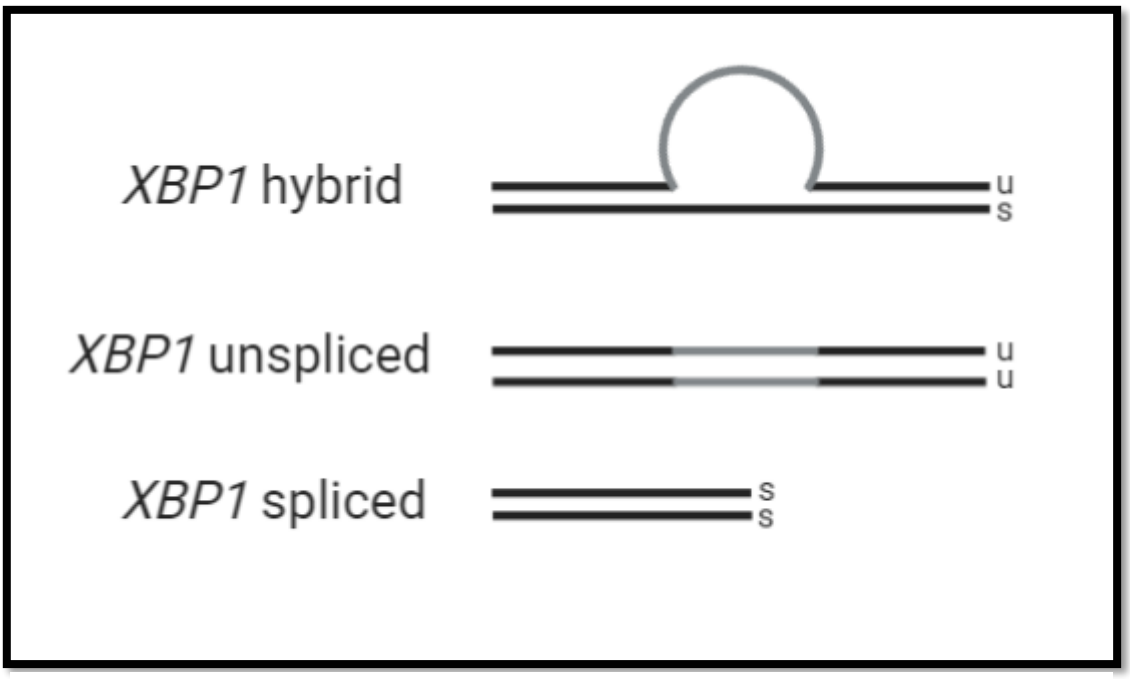

Figure 39 - XBP1 variants observed during End-point PCR.

Author's adaptation of an illustration by Chalmer *et al*., (2017). The *XBP1* hybrid variant is produced during the final step of the PCR process in which a single stand of spliced *XBP1* and a single strand of unspliced *XBP1* anneal together to form a larger cDNA structure that migrate slower through the gel. Illustration created using Biorender software.

6.10. Induction of the UPR by thiopurines

The highest level of autophagy activity in response to thiopurines was observed at the 8h timepoint, therefore, this timepoint was selected to investigate UPR activity in thiopurine treated THP-1 macrophages. Results demonstrated that, at the 8h time point, expression of genes downstream of PERK, such as *ATF4* and *CHOP*, were upregulated during 6-TG treatment. An increase in the phosphorylation of eif2α was also observed during 6-TG treatment, indicating the activation of the PERK pathway. However, PERK did not show an increase in gene expression at the 8h time point. Hooper *et al*., 2019 observed an increase in PERK gene expression at the 6h time point during AZA treatment, which began to decrease after 24h. Therefore, use of an 8h time point in our study may have resulted in an inability to quantify any increase in PERK gene expression, which appears to occur at an earlier time point (Hooper *et al*., 2019). Interestingly, studies in other cell types have identified the regulation of PERK has been closely associated with effects in proliferation. Liu *et al*., (2019) demonstrated that down-regulation of PERK through shRNA reduced the proliferation of Lgr5+ cells in mice, a marker for intestinal stem cells. PERK has also been found to regulate proliferation in β cells and T47D breast cancer cells (Bobrovnikova-Marjon *et al*., 2010; Zhang *et al*., 2006). Therefore, the induction of PERK observed during 6-TG treatment may be a response to the reduction in proliferation potentially caused by MMR processing.

6.11. Role of thiopurines and UPR in mitochondrial homeostasis

PERK may be induced during thiopurine treatment to protect the cells from oxidative stress; and consequently, induces autophagy as one of its protective mechanisms. During the presence of cellular stress, it is critical that mitochondrial proteostasis is maintained. PERK has been found to manipulate pathways involved in protein import, folding and proteolysis to protect the mitochondrial proteome (Rainbolt *et al*., 2014). Therefore, PERK could be induced to protect the mitochondria from ROS-associated oxidative damage during thiopurine treatment. PERK has been found to regulate ROS production. Amodio *et al*. (2019) illustrated in PARK20 fibroblasts that inhibition of the

PERK/eif2α/ATF4 pathway through GSK2606414 treatment, a PERK inhibitor, significantly induced ROS production. PERK has also been found to be a critical component within MAMs acting as functional tether between the mitochondria and ER (Verfaillie *et al*., 2012). It was discovered that PERK regulates ROS-induced cell death through MAMs and that it's structural function within MAMs was crucial in the induction of apoptosis, rather than its functional role in the UPR (Verfaillie *et al*., 2012). This hypothesis was formed as the loss of PERK resulted in severe structure changes within ER-mitochondria juxtapositions, and CHOP deficiency did not attenuate ROS associated apoptosis (Verfaillie *et al*., 2012). Therefore, the activation of PERK in response to mitochondrial injury and ROS accumulation could result in the activation of autophagy.

PERK can induce autophagy through a number of different mechanisms. We observed an increase in *ATF4* and *CHOP* expression during 6-TG treatment, as previously discussed, ATF4 and CHOP have been found to activate autophagy genes *p62, Atg16L1 and Map1lc3B* (B'Chir *et al*., 2013). The early apoptotic signalling observed through the staining of phosphatidylserine can also be initiated through this cascade, as CHOP is a well-defined inducer of pro-apoptotic genes, including the expression of two BH3-only pro-apoptotic Bcl-2 members, Bim and Puma (McQuiston and Diehl, 2017). Therefore, the induction of PERK/eif2α signalling may initiate apoptotic signalling through CHOP, which activates autophagy as a counter measure to maintain cell survival. The activation of MMR processing by thiopurines may also induce the UPR, as cellular energy is critical for correct protein folding and post-translation modifications of proteins in the ER (Bobrovnikova-Marjon *et al*., 2010). It has also been identified PERK can induce the AMPK/mTORC1 pathway during ECM detachment in which cells are exposed to ER stress conditions (Avivar-Valderas *et al*., 2011). Although this was only identified in endothelial cells, it illustrates a direct link between PERK and AMPK. Both PERK and AMPK have been found to be induced during AZA treatment, therefore it could be speculated that PERK modulates AMPK activity to induce autophagy. In addition, PERK has also been shown to upregulate the transcription of the E3 ligase, Parkin, in an ATG4 dependent manner to maintain mitochondrial turnover (Rainbolt *et al*., 2014). As increased expression of Parkin has been associated with the induction of mitophagy, it could suggest the induction of PERK during AZA treatment could facilitate the induction of mitophagy.

6.12. Regulation of mTORC1 signalling by thiopurines

mTORC1 signalling is a critical regulatory pathway in autophagy activity, which functions to inhibit autophagy in the presence of nutrient sufficiency. We observed a reduction in the phosphorylation of rpS6 during AZA treatment compared to 6-MP and 6-TG treatment, indicating that AZA inhibits mTORC1 signalling. This correlates with findings by Hooper *et al*., (2019) who also observed an inhibition of mTORC1 signalling in AZA treated THP-1 derived macrophages. However, Hooper *et al*., (2019) did not investigate mTORC1 activity during 6-MP and 6-TG treatment. Our results contradict findings by other studies which demonstrated that 6-MP strongly inhibits mTORC1 signalling (Fernández-Ramos *et al*., 2017; Huang *et al*., 2016). However, an explanation for this could be that earlier timepoints were investigated within our study compared to Fernandez Ramos *et al*., (2017), who observed a statistically significant difference at the 24-48h timepoint.

PERK has been found to regulate pro-survival and apoptotic signalling through mTORC1 signalling. ATF4 signalling regulates the expression of Sestrin2 and DNA damage and development 1 (REDD1), both of which have been found to inhibit mTORC1 signalling (McQuiston and Diehl, 2017). In addition, PERK mediates the production of phosphatidic acid due to its intrinsic lipid kinase activity, which subsequently can regulate mTORC1 formation and Akt phosphorylation (Bobrovnikova-Marjon *et al*., 2012; Toschi *et al*., 2009). AZA-induced autophagy activity was also suppressed by PERK inhibition, indicating that autophagy is in part induced by the PERK pathway (Hooper *et al*., 2019). However, Hooper *et al*., (2019) illustrated that PERK inhibition did not alter mTORC1 signalling during AZA treatment, suggesting that PERK signalling is either downstream or parallel to mTORC1 signalling. This mechanistic link has been characterised before in GI neuroendocrine cells lines, where it was observed that mTOR inhibitors induce PERK activation, which maintained cell viability (Freis *et al*., 2017).

mTORC1 activity is also positively correlated with mitochondrial activity, and has been found to decrease the anabolic state in the cell to reduce ROS production while enhancing autophagy (López *et al*., 2019). mTORC1 signalling has been found to be activated through RAC1, a known target of thiopurines. RAC1 inhibition by thiopurines

resulted in restored mobility in DC's that were autophagy deficient. mTORC1 activity, therefore, may function through the inhibition of RAC1 signalling (Wildenberg *et al*., 2017). The immunosuppressive effects of 6-TG were found to be associated with the interference of RAC1 protein function (Shin *et al*., 2016). However, our results suggest that 6-MP and 6-TG does not function through the mTORC1 pathway, as we did not observe a reduction in phosphorylated rpS6. Shin *et al*., (2016) observed the interference of RAC1 function after a 3-day treatment with 6-TG, suggesting that this response occurs at a later time-point. mTOR inhibitors could therefore be utilised to determine if PERK signalling is downstream of mTORC1 during AZA treatment. This would also aid in elucidating if 6-MP and 6-TG-induced autophagy is dependent on mTORC1 signalling or functions through independent mechanisms. AMPK signalling could also be investigated to determine if the regulation of mTORC1 signalling is due to the sensing of metabolic stress by AMPK.

The catabolism of AZA to 6-MP may also induce mTORC1 signalling due to the depletion of cysteine and GSH in the cell. Cysteine is oxidised to form cystine where it is shuttled to mammalian cells and is critical for the biosynthesis of GSH (Yu and Long, 2016). As discussed previously, biogenic thiols, GSH and cysteine, are critical in the metabolism of AZA due to the COO(-), SH and NH(3)(+) groups within GSH and cysteine reacting with the C(5i) atom present on the imidazole ring of AZA (Hoffmann *et al*., 2001). This reaction consumes intracellular GSH and has led to implications in hepatocytes such as a decreased metabolic activity, and necrosis (Menor *et al*., 2004). Interestingly, the decrease in cysteine and GSH pools have been found to suppress mTORC1 signalling, and induce the integrated stress response, including eif2α phosphorylation, similar to the response observed within our study (Yu and Long, 2016. However, GSH could not suppress mTORC1 signalling without also the deprivation of cystine, indicating that cystine pools regulate mTORC1 signalling (Yu and Long, 2016). This hypothesis is supported by the work of Menor *et al*., (2004), who found that treatment with N-acetyl-L-Cysteine played a protective role within the mitochondria of AZA treated-rat hepatocytes and completely abolished metabolic loss. This indicates that the inhibition of mTORC1 seen during AZA treatment could possibly be due to the initial reaction that occurs during the metabolism of AZA instead of via a direct mechanism of action.

6.13. Clinical Significance of Thiopurine-induced autophagy activity

6.13.1. Personalised therapies in IBD patients

Personalised medicine has become a target for healthcare professionals to reduce side effects found in patients and costs associated with failed treatment. Interestingly, the *ATG16L1 T300A* variant has been associated with an increased therapeutic effect of thiopurines (Wildenberg *et al*., 2017). Therefore, the enhanced therapeutic effect found in individuals harbouring the *T300A* variant may be due to thiopurines enhancing autophagy that is otherwise impaired. We observed that 6-TG was able to induce UPR signalling at the dose tested compared to AZA and 6-MP. As autophagy was also induced during 6-TG treatment, 6-TG may induce dysfunctional pathways more effectively that AZA and 6-MP, which could partially explain why 6-TG brings more therapeutic benefits than AZA clinically. It would be of use to compare the effectiveness of thiopurines, particularly 6-TG, in individuals harbouring variants associated with autophagy and the UPR pathway, and if their response the treatment is more effective than individuals that do not harbour these variants. This could help develop more appropriate treatment strategies that avoid unwanted side effects in patients.

Thiopurines play a key role in maintaining long-term remission in IBD patients (Lim and Chua, 2018). The recommendation by the European Crohn's and Colitis Organisation is that AZA and 6-MP should be administered at a daily dose of 2-3 mg/kg and 1-1.5 mg/kg respectively (Lim and Chua, 2018). However, the clinical use of 6-TG has been disputed. Daily dosage regimes when using 6-TG suggest not to exceed 20mg/day per patient irrespective of body weight (Goel *et al*., 2015). The findings that 6-TG is a more efficacious metabolite is supported by our findings that demonstrated 6-TG altered metabolic activity compared to AZA and 6-MP when all were used at the same concentrations. The increased activity of 6-TG has led to its use in IBD being restricted due to its hepatotoxic potential and its association with the onset of nodular regenerative hyperplasia (NRH) (Petit *et al*., 2008). However, these cases of NRH during 6-TG treatment were thought to be dose-dependent (Ward *et al*., 2017). For example, no cases of NRH have been found in patients treated with 6-TG at 20mg/day (Goel *et al*., 2015). Our results illustrated that 6-TG was able to induce the UPR and autophagy at the dose and time studied, compared to AZA and 6-MP which did not.

Therefore 6-TG appears to be a more efficacious metabolite than AZA and 6-MP. Currently used dosage regimes for AZA and 6-MP only see a therapeutic effect after 12-17 weeks of treatment (Lim and Chua, 2018). As 6-TG appears to be the most effective thiopurine at inducing signalling pathways that are impaired in IBD patients, 6-TG could induce a therapeutic effect more rapidly than AZA and 6-MP in IBD patients.

6.13.2. Use of combination therapy in IBD

Patients suffering from severe CD will initially be treated with therapies such as Infliximab, an anti-TNFα agent, which will induce remission in patients, and thiopurines will subsequently be giving to the patient (Lim and Chua, 2018). However, this drug regime has been placed under scrutiny in the past, as combination therapy has been proven to be more successful. For example, an open randomised trial found that a monotherapy approach only maintained steroid free remission in 35.9% of patients after 26 weeks compared to combination therapy, in which 60% of patients were maintained in steroid-free remission (D'Haens *et al*., 2008). Therefore, there is a need to find therapies that can be applied in combination without unwanted side effects. As we observed that thiopurines are able to activate autophagy activity, thiopurines could be used in combination with other known inducers of autophagy, including mTOR inhibitors such as Sirolimus (rapamycin), which has been found to be therapeutic in refractory CD (Massey *et al*., 2008). Thiopurines could also be used in conjunction with drugs known to alleviate ER stress. These include Tauroursodeoxycholic acid, which has been found to reduce ER stress and enhance protein folding in the liver of obese patients (Ma *et al*., 2017). These therapies in combination may induce dysfunctional pathway in patients that are genetically dispositioned and help maintain remission for longer.

6.13.3. Clinical impact of TPMT activity in autophagy activity

We observed that differences in cell types affect the rate at which autophagy is activated. Based upon previous findings, enzyme activity impacts the rate at which thiopurines are metabolised into its efficacious substrate (Chang and Cheon, 2019). TPMT is the most well documented enzyme associated with thiopurine metabolism and is largely considered the enzyme responsible for the variation in efficacy and toxicity in patients. The prevalence of genetic polymorphisms in TPMT is significant in

the population. 0.3% of the population are homozygous for absent TPMT activity, 10% are heterozygous for TPMT that produces intermediate activity and the polymorphisms that remain results in extensive TPMT activity in individuals (Kapur and Hanauer, 2019). Individuals expressing polymorphisms that result in no TPMT activity will have an inability to inactivate thiopurines, resulting in a preference for thiopurines to be converted to 6-TGN by HPRT. This can result in standardised dosing of AZA and 6-MP causing severe myelosuppression and, in some cases, can be life threatening (Chisick *et al*., 2013). In contrast, individuals with significantly higher TPMT enzyme activity will produce higher concentrations of inactive and hepatotoxic metabolites, such as 6-MMP, which can result in increased side effects. Both active and inactive metabolites produced by the enzymatic breakdown of thiopurines may have an impact on autophagy activation. Therefore, differences in TPMT enzyme activity found in patients may impact the rate at which autophagy is activated and therefore effect the efficacy of the drug. This reinforces the need for targeted therapeutic approaches when utilising thiopurines.

6.14. Future Research

6.14.1. ATF6 signalling in response to thiopurines

As PERK was not observed to be induced at the timepoint investigated in our study, it's beneficial to investigate further timepoints to characterise if the activation of PERK occurs at an earlier time point. ATF6 signalling was not characterised during our study due to the time constraints in investigating antibodies for ATF6. The ATF6 axis heavily contributes to the output found within the IRE1 axis, with ATF6 inducing the expression of *BiP*, *XBP1* and *EDEM1* (Hillary and Fitzgerald, 2018). Therefore, it would appear from the results found in our study that the ATF6 axis is not induced during thiopurine treatment. This could be confirmed with the use of an antibody that can detect the 90kDa type II transmembrane glycoprotein form of ATF6 and the 50kDa amino-terminal fragment of ATF6, which is cleaved as a result of the presence of ER stress (Hillary and FitzGerald, 2018).

6.14.2. mTORC1 signalling in response to thiopurines

We did not observe the regulation of mTORC1 signalling during 6-MP or 6-TG treatment at the 8h time point, however, 6-MP has been found to inhibit mTORC1

signalling during the 24-48h time point. Therefore, it would be of interest to explore the later timepoints from what was investigated in this study to conclude if the regulation of mTORC1 is solely seen in AZA treatment compared to 6-MP and 6-TG. mTORC1 inhibitors also should be utilised to determine if mTORC1 regulates induced autophagy activity in AZA, 6-MP and 6-TG. PERK signalling should also be characterised during mTORC1 inhibition to determine if mTORC1 signalling functions upstream of PERK.

6.14.3. Further assessment of autophagy signalling

We illustrated, using a GFP-RFP-LC3 plasmid, that autophagy is induced during thiopurine treatment. However, it is advised when assessing autophagy activity to utilise at least two separate methodologies. Therefore, further investigations should confirm autophagy induction we observed within this study, preferably using a time-course to compare the induction of autophagy between all thiopurines. Investigating p62 turnover through western blotting is an alternative method that can be utilised to monitor autophagy activity. p62 is involved in the shuttling of cargo proteins to the interior of autophagosomes, where it anchors to LC3 through LC3 interacting regions and is degraded and thus p62 is inversely correlated with autophagy activity (Yoshii and Mizushima, 2017). In addition, the activation of autophagy could be determined through the use of flow cytometry, in which the fluorescence of autophagosome associated LC3-II is quantified using the detergent saponin, which selects LC3-II through the removal of non-autophagosome specific LC3-I (Eng *et al*., 2010).

6.14.4. Therapeutic effect of imidazole derivatives

It was demonstrated that AZA induced autophagosome accumulation more rapidly than 6-MP or 6-TG. As this result was only performed once, it should be repeated to confirm the observation. Limited studies have investigated the therapeutic effect of the imidazole derivative which is produced during the catabolism of AZA. Studies indicate that the imidazole derivative may produce a potentially toxic effect as three quarters of patients who are intolerant to AZA treatment can tolerate 6-MP, with the only structural difference between the molecular structure between AZA and 6-MP being the imidazole derivative. However, this intolerance observed may be due to GSH depletion or excessive ROS production. In addition, in vitro studies have shown the imidazole derivative found on AZA can regulate immune activity (McGovern *et al*., 2002). Additional studies should be conducted to analyse the immunomodulatory

properties of the imidazole derivative released during thiopurine treatment. If It is found that the imidazole derivative produces a therapeutic effect by stimulating autophagy activity, imidazole could be used as an alternative therapy to AZA, avoiding the unwanted side effects.

6.14.5. Future use of *in vitro* and *ex vivo* models for IBD

Leukaemia-derived THP-1 derived macrophages were used in this study to investigate macrophage response in response to thiopurine treatment. Cancerous human cell lines are an essential *in vitro* tools utilised to investigate pathways, mechanisms and responses. They also possess a level of reliability due to their homogenous genetic nature, which reduces the level of variability that is found when acquiring PBMC-derived monocytes from blood donors. However, they also contain several drawbacks. For example, due to their malignant background and the culturing of these cell lines from outside their natural environment, these cell lines can become over-sensitised to various stimuli. This effect will portray mild responses to be much more significant. An example of this includes the excessive ROS production observed during 6-MP and 6-TG treatment that is mainly restricted to tumour cell lines (Chaabane and Appell, 2016). It is therefore suggested to perform an *ex vivo* study with a more clinically appropriate cell model, such as PBMC-derived macrophages. Selecting PBMC-derived macrophages from patients with known CD-associated SNP's could also be used to investigate the impact of these drugs on the induction of autophagy in these cells.

Many IBD-associated studies have identified intestinal epithelial barrier dysfunction as a major contributing factor to intestinal inflammation. Adolph *et al*., (2013), presented evidence illustrating that Paneth cell dysfunction was the origin of intestinal inflammation in CD. As we observed differences in autophagy activity by thiopurines in different cell lineages, it would be important in future research to investigate the effect of thiopurines in intestinal cell lines. However, Paneth cells have been shown to have high sensitivity to increased ER stress inside the cell, which is indicated by studies showing deletion of *XBP1* leads to defects in Paneth cells in the small intestine (Kaser *et al*., 2008). Therefore, it may be beneficial to utilise a mouse model similar to the methodology used by Adolf *et al*., (2013,), which involved generating a $XBP1^{-/-}$ mouse model through tamoxifen treatment or selective deletion of *ATG16L1* through

Cre-Lox recombination. Intestinal Crypts within the mice model could then be sectioned an analysed using immunofluorescent and histological techniques. This would allow us to analyse the effect of thiopurines on Paneth cell lineages in a mice model that resembles patients harbouring CD-associated SNPs. If, thiopurines can activate autophagy in IEC's and prevent integrity breakdown, it could help explain why thiopurines are effective in maintaining long-term remission in IBD patients.

6.14.6 Thiopurine induced mitochondrial dysfunction

As many studies have reported the loss of mitochondria function during thiopurine treatment, it would be beneficial to explore mitochondria function and its association with the UPR and autophagy activity. An example of this could be using lipophilic cationic fluorescent dyes which can be used to assess mitochondrial membrane potential. As PERK is closely associated with MAMs found on the mitochondria, this could help elucidate if mitochondrial events are the cause of PERK induction. ROS produced during mitochondrial permeabilization has also been found to regulate autophagy and apoptotic signalling. Chaabane and Appell, (2016) found that ROS scavenging, utilising NAC, reduced both autophagy marker, LC3-II, and apoptosis in the cell. It would be of interest to determine if ROS scavenging regulates PERK and mTORC1 signalling during thiopurine treatment or if these pathways act independently of ROS production. The regulation of ROS and autophagy by PERK could also be characterised through the inhibition of PERK and observing ROS toxicity and autophagy activity in the cell.

6.15. Conclusion

We have demonstrated that thiopurines, AZA, 6-MP and 6-TG are all inducers of autophagy in THP-1 derived macrophages. As autophagy dysfunction leads to bacterial persistency in macrophages during IBD pathogenesis, the induction of autophagy by thiopurines may partially explain the therapeutic nature of the drug. Our results indicated that 6-TG is a more potent pro-drug compared to AZA and 6-MP, and 6-TG induced downstream signalling of the UPR pathway, which could be therapeutic in CD patients that have been found to have elevated ER stress. We also observed an inhibition of mTORC1 signalling during AZA treatment, indicating the possibility of an independent mechanism of action for autophagy induction compared to 6-MP and 6-TG. Due to the multifactorial nature of the disease and the underlying risk factors

that are uniquely found within each patient, there is a need to develop personalised treatments for IBD patients. The findings shown in this study help elucidate a part of the mechanism of action of thiopurines and could lead to more appropriate dosage regimes with these drugs, which could help reduce unwanted side effects in patients.

7. References

Abegunde, A.T., Muhammad, B.H., Bhatti, O., Ali, T., 2016. Environmental risk factors for inflammatory bowel diseases: Evidence based literature review. World J. Gastroenterol. 22, 6296–6317. https://doi.org/10.3748/wjg.v22.i27.6296

Adams, C.J., Kopp, M.C., Larburu, N., Nowak, P.R., Ali, M.M.U., 2019. Structure and molecular mechanism of ER stress signaling by the unfolded protein response signal activator IRE1. Front. Mol. Biosci. 6, 1–12. https://doi.org/10.3389/fmolb.2019.00011

Adamson, P.C., Poplack, D.G., Balis, F.M., 1994. THE CYTOTOXICITY OF THIOGUANINE VS MERCAPTOPURINE IN ACUTE LYMPHOBLASTIC LEUKEMIA 2126, 805–810.

Adolph, T.E., Tomczak, M.F., Niederreiter, L., Ko, H.-J., Böck, J., Martinez-Naves, E., Glickman, J.N., Tschurtschenthaler, M., Hartwig, J., Hosomi, S., Flak, M.B., Cusick, J.L., Kohno, K., Iwawaki, T., Billmann-Born, S., Raine, T., Bharti, R., Lucius, R., Kweon, M.-N., Marciniak, S.J., Choi, A., Hagen, S.J., Schreiber, S., Rosenstiel, P., Kaser, A., Blumberg, R.S., 2013. Paneth cells as a site of origin for intestinal inflammation. Nature 503, 272–276. https://doi.org/10.1038/nature12599

Ahluwalia, B., Moraes, L., Magnusson, M.K., Öhman, L., 2018. Immunopathogenesis of inflammatory bowel disease and mechanisms of biological therapies. Scand. J. Gastroenterol. 53, 379–389. https://doi.org/10.1080/00365521.2018.1447597

Al Maruf, A., Wan, L., O'Brien, P.J., 2014. Evaluation of azathioprine-induced cytotoxicity in an in vitro rat hepatocyte system. Biomed Res. Int. 2014, 379748. https://doi.org/10.1155/2014/379748

Alatab, S., Sepanlou, S.G., Ikuta, K., Vahedi, H., Bisignano, C., Safiri, S., Sadeghi, A., Nixon, M.R., Abdoli, A., Abolhassani, H., Alipour, V., Almadi, M.A.H., Almasi-Hashiani, A., Anushiravani, A., Arabloo, J., Atique, S., Awasthi, A., Badawi, A., Baig, A.A.A., Bhala, N., Bijani, A., Biondi, A., Borzì, A.M., Burke, K.E., Carvalho, F., Daryani, A., Dubey, M., Eftekhari, A., Fernandes, E., Fernandes, J.C., Fischer, F., Haj-Mirzaian, Arvin, Haj-Mirzaian, Arya, Hasanzadeh, A., Hashemian, M., Hay, S.I., Hoang, C.L., Househ, M., Ilesanmi, O.S., Balalami, N.J., James, S.L., Kengne, A.P., Malekzadeh, M.M., Merat, S., Meretoja, T.J., Mestrovic, T., Mirrakhimov, E.M., Mirzaei, H., Mohammad, K.A., Mokdad, A.H., Monasta, L., Negoi, I., Nguyen, T.H., Nguyen, C.T., Pourshams, A., Poustchi, H., Rabiee, M., Rabiee, N., Ramezanzadeh, K., Rawaf, D.L., Rawaf, S., Rezaei, N., Robinson, S.R., Ronfani, L., Saxena, S., Sepehrimanesh, M., Shaikh, M.A., Sharafi, Z., Sharif, M., Siabani, S., Sima, A.R., Singh, J.A., Soheili, A., Sotoudehmanesh, R., Suleria, H.A.R., Tesfay, B.E., Tran, B., Tsoi, D., Vacante, M., Wondmieneh, A.B., Zarghi, A., Zhang, Z.J., Dirac, M., Malekzadeh, R., Naghavi, M., 2020. The global, regional, and national burden of inflammatory bowel disease in 195 countries and territories, 1990–2017: a systematic analysis for the Global Burden of Disease Study 2017. Lancet Gastroenterol. Hepatol. 5, 17–30. https://doi.org/10.1016/S2468-1253(19)30333-4

Amarante-Mendes, G.P., Adjemian, S., Branco, L.M., Zanetti, L.C., Weinlich, R., Bortoluci, K.R., 2018. Pattern recognition receptors and the host cell death molecular machinery. Front. Immunol. 9, 1–19. https://doi.org/10.3389/fimmu.2018.02379

Amodio, G., Moltedo, O., Fasano, D., Zerillo, L., Oliveti, M., Di Pietro, P., Faraonio, R., Barone, P., Pellecchia, M.T., De Rosa, A., De Michele, G., Polishchuk, E., Polishchuk, R., Bonifati, V., Nitsch, L., Pierantoni, G.M., Renna, M., Criscuolo, C., Paladino, S., Remondelli, P., 2019. PERK-mediated unfolded protein response activation and oxidative stress in PARK20 fibroblasts. Front. Neurosci. 13, 1–14. https://doi.org/10.3389/fnins.2019.00673

Ananthakrishnan, A.N., Bernstein, C.N., Iliopoulos, D., Macpherson, A., Neurath, M.F., Ali, R.A.R., Vavricka, S.R., Fiocchi, C., 2018. Environmental triggers in IBD: A review of progress and evidence. Nat. Rev. Gastroenterol. Hepatol. 15, 39–49. https://doi.org/10.1038/nrgastro.2017.136

Ananthakrishnan, A.N., Khalili, H., Konijeti, G.G., Higuchi, L.M., De Silva, P., Korzenik, J.R., Fuchs, C.S., Willett, W.C., Richter, J.M., Chan, A.T., 2013. A prospective study of long-term intake of dietary fiber and risk of Crohn's disease and ulcerative colitis. Gastroenterology 145, 970–977. https://doi.org/10.1053/j.gastro.2013.07.050

Andreu-Ballester, J.C., Pérez-Griera, J., Garcia-Ballesteros, C., Amigo, V., Catalán-Serra, I., Monforte-Albalat, A., Bixquert-Jiménez, M., Ballester, F., 2013. Deficit of interleukin-7 in serum of patients with Crohn's DISEASE. Inflamm. Bowel Dis. 19, 30–31. https://doi.org/10.1002/ibd.22914

Aniwan, S., Tremaine, W.J., Raffals, L.E., Kane, S. V., Loftus, E. V., 2018. Antibiotic use and new-onset inflammatory bowel disease in Olmsted county, Minnesota: A population-based case-control study. J. Crohn's Colitis 12, 137–144. https://doi.org/10.1093/ecco-jcc/jjx135

Antoni, L., Nuding, S., Wehkamp, J., Stange, E.F., 2014. Intestinal barrier in inflammatory bowel disease. World J. Gastroenterol. 20, 1165–1179. https://doi.org/10.3748/wjg.v20.i5.1165

Atreya, I., Neurath, M.F., 2008. Azathioprine in inflammatory bowel disease: Improved molecular insights and resulting clinical implications. Expert Rev. Gastroenterol. Hepatol. 2, 23–34. https://doi.org/10.1586/17474124.2.1.23

Avivar-Valderas, A., Salas, E., Bobrovnikova-Marjon, E., Diehl, J.A., Nagi, C., Debnath, J., Aguirre-Ghiso, J.A., 2011. PERK Integrates Autophagy and Oxidative Stress Responses To Promote Survival during Extracellular Matrix Detachment. Mol. Cell. Biol. 31, 3616–3629. https://doi.org/10.1128/MCB.05164-11

Axe, E.L., Walker, S.A., Manifava, M., Chandra, P., Roderick, H.L., Habermann, A., Griffiths, G., Ktistakis, N.T., 2008. Autophagosome formation from membrane compartments enriched in phosphatidylinositol 3-phosphate and dynamically connected to the endoplasmic reticulum. J. Cell Biol. 182, 685–701. https://doi.org/10.1083/jcb.200803137

Axelrad, J.E., Roy, A., Lawlor, G., Korelitz, B., Lichtiger, S., 2016. Thiopurines and inflammatory bowel disease: Current evidence and a historical perspective. World J. Gastroenterol. 22, 10103–10117. https://doi.org/10.3748/wjg.v22.i46.10103

B'Chir, W., Maurin, A.C., Carraro, V., Averous, J., Jousse, C., Muranishi, Y., Parry, L., Stepien, G., Fafournoux, P., Bruhat, A., 2013. The eIF2α/ATF4 pathway is essential for stress-induced autophagy gene expression. Nucleic Acids Res. 41, 7683–7699. https://doi.org/10.1093/nar/gkt563

Badadani, M., 2012. Autophagy Mechanism, Regulation, Functions, and Disorders. ISRN Cell Biol. 2012, 1–11. https://doi.org/10.5402/2012/927064

Bain, C.C., Scott, C.L., Uronen-Hansson, H., Gudjonsson, S., Jansson, O., Grip, O., Guilliams, M., Malissen, B., Agace, W.W., Mowat, A.M.I., 2013. Resident and pro-inflammatory macrophages in the colon represent alternative context-dependent fates of the same Ly6C hi monocyte precursors. Mucosal Immunol. 6, 498–510. https://doi.org/10.1038/mi.2012.89

Barros, M.H.M., Hassan, R., Niedobitek, G., 2012. Tumor-associated macrophages in pediatric classical Hodgkin lymphoma: Association with Epstein-Barr virus, lymphocyte subsets, and prognostic impact. Clin. Cancer Res. 18, 3762–3771. https://doi.org/10.1158/1078-0432.CCR-12-0129

Bastida, G., Beltrán, B., 2011. Ulcerative colitis in smokers, non-smokers and ex-smokers. World J. Gastroenterol. 17, 2740–2747. https://doi.org/10.3748/wjg.v17.i22.2740

Belarif, L., Vanhove, B., Poirier, N., Belarif, L., Danger, R., Kermarrec, L., Nerrière-daguin, V., Pengam, S., Durand, T., Mary, C., Kerdreux, E., Gauttier, V., Kucik, A., Thepenier, V., Martin, J.C., Chang, C., Rahman, A., Guen, N.S., Braudeau, C., Abidi, A., David, G., Malard, F., Macdonald, T.T., Desreumaux, P., Mai, H., Bas-bernardet, S. Le, Mosnier, J., Merad, M., Josien, R., Brouard, S., Soulillou, J., Blancho, G., Bourreille, A., 2019. IL-7 receptor influences anti-TNF responsiveness and T cell gut homing in inflammatory bowel disease Graphical abstract Find the latest version : IL-7 receptor influences anti-TNF responsiveness and T cell gut homing in inflammatory bowel disease. J. Clin. Invest. 129, 1910–1925.

Bernstein, C.N., Shanahan, F., 2008. Disorders of a modern lifestyle: Reconciling the epidemiology of inflammatory bowel diseases. Gut 57, 1185–1191. https://doi.org/10.1136/gut.2007.122143

Blaker, P.A., Arenas-Hernandez, M., Marinaki, A.M., Sanderson, J.D., 2012. The pharmacogenetic basis of individual variation in thiopurine metabolism. Per. Med. 9, 707–725. https://doi.org/10.2217/pme.12.85

Bobrovnikova-Marjon, E., Grigoriadou, C., Pytel, D., Zhang, F., Ye, J., Koumenis, C., Cavener, D., Diehl, J.A., 2010. PERK promotes cancer cell proliferation and tumor growth by limiting oxidative DNA damage. Oncogene 29, 3881–3895. https://doi.org/10.1038/onc.2010.153

Bobrovnikova-Marjon, E., Pytel, D., Riese, M.J., Vaites, L.P., Singh, N., Koretzky, G.A., Witze, E.S., Diehl, J.A., 2012. PERK Utilizes Intrinsic Lipid Kinase Activity

To Generate Phosphatidic Acid, Mediate Akt Activation, and Promote Adipocyte Differentiation. Mol. Cell. Biol. 32, 2268–2278. https://doi.org/10.1128/mcb.00063-12

Bogaert, S., de Vos, M., Olievier, K., Peeters, H., Elewaut, D., Lambrecht, B., Pouliot, P., Laukens, D., 2011. Involvement of endoplasmic reticulum stress in inflammatory bowel disease: A different implication for colonic and ileal disease? PLoS One 6. https://doi.org/10.1371/journal.pone.0025589

Bouman, L., Schlierf, A., Lutz, A.K., Shan, J., Deinlein, A., Kast, J., Galehdar, Z., Palmisano, V., Patenge, N., Berg, D., Gasser, T., Augustin, R., Trümbach, D., Irrcher, I., Park, D.S., Wurst, W., Kilberg, M.S., Tatzelt, J., Winklhofer, K.F., 2011. Parkin is transcriptionally regulated by ATF4: Evidence for an interconnection between mitochondrial stress and ER stress. Cell Death Differ. 18, 769–782. https://doi.org/10.1038/cdd.2010.142

Bradford, K., Shih, D.Q., 2011. Optimizing 6-mercaptopurine and azathioprine therapy in the management of inflammatory bowel disease. World J. Gastroenterol. 17, 4166–4173. https://doi.org/10.3748/wjg.v17.i37.4166

Bringer, M.A., Billard, E., Glasser, A.L., Colombel, J.F., Darfeuille-Michaud, A., 2012. Replication of Crohn's disease-associated AIEC within macrophages is dependent on TNF-α secretion. Lab. Investig. 92, 411–419. https://doi.org/10.1038/labinvest.2011.156

Calfon, M., Zeng, H., Urano, F., Till, J.H., Hubbard, S.R., Harding, H.P., Clark, S.G., Ron, D., 2002. IRE1 couples endoplasmic reticulum load to secretory capacity by processing the XBP-1 mRNA. Nature 415, 92–96. https://doi.org/10.1038/415092a

Cao, S.S., 2016. Epithelial ER stress in Crohn's disease and ulcerative colitis. Inflamm. Bowel Dis. 22, 984–993. https://doi.org/10.1097/MIB.0000000000000660

Cao, S.S., Kaufman, R.J., 2012. Unfolded protein response. Curr. Biol. 22, R622–R626. https://doi.org/10.1016/j.cub.2012.07.004

Carrara, M., Prischi, F., Ali, M.M.U., 2013. UPR signal activation by luminal sensor domains. Int. J. Mol. Sci. 14, 6454–6466. https://doi.org/10.3390/ijms14036454

Chaabane, W., Appell, M.L., 2016. Interconnections between apoptotic and autophagic pathways during thiopurine-induced toxicity in cancer cells: the role of reactive oxygen species. Oncotarget 7, 75616–75634. https://doi.org/10.18632/oncotarget.12313

Chakrabarti, A., Chen, A.W., Varner, J.D., 2011. A Review of the Mammalian Unfolded Protein Response. Biotechnol Bioeng 108, 2777–2793. https://doi.org/10.1038/jid.2014.371

Chalmers, F., Van Lith, M., Sweeney, B., Cain, K., Bulleid, N.J., 2017. Inhibition of IRE1α-mediated XBP1 mRNA cleavage by XBP1 reveals a novel regulatory process during the unfolded protein response. Wellcome Open Res. 2, 1–16. https://doi.org/10.12688/wellcomeopenres.11764.1

Chande, N., Patton, P.H., Tsoulis, D.J., Thomas, B.S., Macdonald, J.K., 2015. Azathioprine or 6-mercaptopurine for maintenance of remission in Crohn's disease. Cochrane Database Syst. Rev. 2017. https://doi.org/10.1002/14651858.CD000067.pub3

Chang, J.Y., Cheon, J.H., 2019. Thiopurine Therapy in Patients With Inflammatory Bowel Disease: A Focus on Metabolism and Pharmacogenetics. Dig. Dis. Sci. 64, 2395–2403. https://doi.org/10.1007/s10620-019-05720-5

Chen, Y., Brandizzi, F., 2013. IRE1: ER stress sensor and cell fate executor. Trends Cell Biol 23. https://doi.org/10.1038/jid.2014.371

Chisick, L., Oleschuk, C., Bernstein, C.N., 2013. The utility of thiopurine methyltransferase enzyme testing in inflammatory bowel disease. Can. J. Gastroenterol. 27, 39–43. https://doi.org/10.1155/2013/280860

Chistiakov, D.A., Killingsworth, M.C., Myasoedova, V.A., Orekhov, A.N., Bobryshev, Y. V., 2017. CD68/macrosialin: Not just a histochemical marker. Lab. Investig. 97, 4–13. https://doi.org/10.1038/labinvest.2016.116

Cho, J.H., Brant, S.R., 2011. Recent insights into the genetics of inflammatory bowel disease. Gastroenterology 140, 1704-1712.e2. https://doi.org/10.1053/j.gastro.2011.02.046

Colanzi, A., Grimaldi, G., Catara, G., Valente, C., Cericola, C., Liberali, P., Ronci, M., Lalioti, V.S., Bruno, A., Beccari, A.R., Urbani, A., De Florah, A., Nardini, M., Bolognesi, M., Luini, A., Corda, D., 2013. Molecular mechanism and functional role of brefeldin A-mediated ADP-ribosylation of CtBP1/BARS. Proc. Natl. Acad. Sci. U. S. A. 110, 9794–9799. https://doi.org/10.1073/pnas.1222413110

Colombel, J.F., Sandborn, W.J., Reinisch, W., Mantzaris, G.J., Kornbluth, A., Rachmilewitz, D., Lichtiger, S., D'Haens, G., Diamond, R.H., Broussard, D.L., Tang, K.L., Van Der Woude, C.J., Rutgeerts, P., 2010. Infliximab, azathioprine, or combination therapy for Crohn's disease. N. Engl. J. Med. 362, 1383–1395. https://doi.org/10.1056/NEJMoa0904492

Cooney, R., Baker, J., Brain, O., Danis, B., Pichulik, T., Allan, P., Ferguson, D.J.P., Campbell, B.J., Jewell, D., Simmons, A., 2010. NOD2 stimulation induces autophagy in dendritic cells influencing bacterial handling and antigen presentation. Nat. Med. 16, 90–97. https://doi.org/10.1038/nm.2069

Corazzari, M., Gagliardi, M., Fimia, G.M., Piacentini, M., 2017. Endoplasmic reticulum stress, unfolded protein response, and cancer cell fate. Front. Oncol. 7, 1–11. https://doi.org/10.3389/fonc.2017.00078

Corridoni, D., Chapman, T., Ambrose, T., Simmons, A., 2018. Emerging mechanisms of innate immunity and their translational potential in inflammatory bowel disease. Front. Med. 5, 1–22. https://doi.org/10.3389/fmed.2018.00032

Costantini, P., Bruey, J.M., Castedo, M., Métivier, D., Loeffler, M., Susin, S.A., Ravagnan, L., Zamzami, N., Garrido, C., Kroemer, G., 2002. Pre-processed caspase-9 contained in mitochondria participates in apoptosis. Cell Death Differ. 9, 82–88. https://doi.org/10.1038/sj.cdd.4400932

Courth, L.F., Ostaff, M.J., Mailänder-Sánchez, D., Malek, N.P., Stange, E.F., Wehkamp, J., 2015. Crohn's disease-derived monocytes fail to induce Paneth cell defensins. Proc. Natl. Acad. Sci. U. S. A. 112, 14000–14005. https://doi.org/10.1073/pnas.1510084112

Crawford, D.J.K., Maddocks, J.L., Jones, D.N., Szawlowski, P., 1996. Rational design of novel immunosuppressive drugs: Analogues of azathioprine lacking the 6-mercaptopurine substituent retain or have enhanced immunosuppressive effects. J. Med. Chem. 39, 2690–2695. https://doi.org/10.1021/jm960132w

Cuffari, C., 2006. A physician's guide to azathioprine metabolite testing. Gastroenterol. Hepatol. 2, 58–63.

Cummins, E.P., Crean, D., 2016. Hypoxia and inflammatory bowel disease. Microbes Infect. 19, 210–221. https://doi.org/10.1016/j.micinf.2016.09.004

D'Haens, 2008. Early combined immunosuppression or conventional management in patients with newly diagnosed Crohn's disease: an open randomised trial. Lancet 660–667.

D'Haens, G.R., Vermeire, S., Van Assche, G., Noman, M., Aerden, I., Van Olmen, G., Rutgeerts, P., 2008. Therapy of Metronidazole With Azathioprine to Prevent Postoperative Recurrence of Crohn's Disease: A Controlled Randomized Trial. Gastroenterology 135, 1123–1129. https://doi.org/10.1053/j.gastro.2008.07.010

Däbritz, J., 2015. GM-CSF and the role of myeloid regulatory cells in the pathogenesis and treatment of Crohn's disease. Mol. Cell. Pediatr. 2. https://doi.org/10.1186/s40348-015-0024-4

Daehn, I., Brem, R., Barkauskaite, E., Karran, P., 2011. 6-Thioguanine damages mitochondrial DNA and causes mitochondrial dysfunction in human cells. FEBS Lett. 585, 3941–3946. https://doi.org/10.1016/j.febslet.2011.10.040

Darfeuille-Michaud, A., Boudeau, J., Bulois, P., Neut, C., Glasser, A.L., Barnich, N., Bringer, M.A., Swidsinski, A., Beaugerie, L., Colombel, J.F., 2004. High prevalence of adherent-invasive Escherichia coli associated with ileal mucosa in Crohn's disease. Gastroenterology 127, 412–421. https://doi.org/10.1053/j.gastro.2004.04.061

De Filippo, C., Cavalieri, D., Di Paola, M., Ramazzotti, M., Poullet, J.B., Massart, S., Collini, S., Pieraccini, G., Lionetti, P., 2010. Impact of diet in shaping gut microbiota revealed by a comparative study in children from Europe and rural Africa. Proc. Natl. Acad. Sci. U. S. A. 107, 14691–14696. https://doi.org/10.1073/pnas.1005963107

De Lange, K.M., Moutsianas, L., Lee, J.C., Lamb, C.A., Luo, Y., Kennedy, N.A., Jostins, L., Rice, D.L., Gutierrez-Achury, J., Ji, S.G., Heap, G., Nimmo, E.R., Edwards, C., Henderson, P., Mowat, C., Sanderson, J., Satsangi, J., Simmons, A., Wilson, D.C., Tremelling, M., Hart, A., Mathew, C.G., Newman, W.G., Parkes, M., Lees, C.W., Uhlig, H., Hawkey, C., Prescott, N.J., Ahmad, T., Mansfield, J.C., Anderson, C.A., Barrett, J.C., 2017. Genome-wide association study implicates immune activation of multiple integrin genes in inflammatory bowel disease. Nat. Genet. 49, 256–261. https://doi.org/10.1038/ng.3760

De Schepper, S., Verheijden, S., Aguilera-Lizarraga, J., Viola, M.F., Boesmans, W., Stakenborg, N., Voytyuk, I., Smidt, I., Boeckx, B., Dierckx de Casterlé, I., Baekelandt, V., Gonzalez Dominguez, E., Mack, M., Depoortere, I., De Strooper, B., Sprangers, B., Himmelreich, U., Soenen, S., Guilliams, M., Vanden Berghe, P., Jones, E., Lambrechts, D., Boeckxstaens, G., 2018. Self-Maintaining Gut Macrophages Are Essential for Intestinal Homeostasis. Cell 175, 400-415.e13. https://doi.org/10.1016/j.cell.2018.07.048

Deffieu, M., Bhatia-Kiššová, I., Salin, B., Galinier, A., Manon, S., Camougrand, N., 2009. Glutathione participates in the regulation of mitophagy in yeast. J. Biol. Chem. 284, 14828–14837. https://doi.org/10.1074/jbc.M109.005181

Deuring, J.J., Fuhler, G.M., Konstantinov, S.R., Peppelenbosch, M.P., Kuipers, E.J., Haar, C. De, Van Der Woude, C.J., 2014. Genomic ATG16L1 risk allele-restricted Paneth cell ER stress in quiescent Crohn's disease. Gut 63, 1081–1091. https://doi.org/10.1136/gutjnl-2012-303527

Devereaux, K., Dall'Armi, C., Alcazar-Roman, A., Ogasawara, Y., Zhou, X., Wang, F., Yamamoto, A., de Camilli, P., Di Paolo, G., 2013. Regulation of Mammalian Autophagy by Class II and III PI 3-Kinases through PI3P Synthesis. PLoS One 8, 10–12. https://doi.org/10.1371/journal.pone.0076405

Eckmann, L., Karin, M., 2005. NOD2 and Crohn's disease: Loss or gain of function? Immunity. https://doi.org/10.1016/j.immuni.2005.06.004

Economou, M., Trikalinos, T.A., Loizou, K.T., Tsianos, E. V., Ioannidis, J.P.A., 2004. Differential effects of NOD2 variants on Crohn's disease risk and phenotype in diverse populations: A metaanalysis. Am. J. Gastroenterol. 99, 2393–2404. https://doi.org/10.1111/j.1572-0241.2004.40304.x

Eklund, B.I., Moberg, M., Bergquist, J., Mannervik, B., 2006. Divergent activities of human glutathione transferases in the bioactivation of azathioprine. Mol. Pharmacol. 70, 747–754. https://doi.org/10.1124/mol.106.025288

El-Khider, F., McDonald, C., 2016. Links of autophagy dysfunction to inflammatory bowel disease onset. Dig. Dis. 21, 129–139. https://doi.org/10.5588/ijtld.16.0716.Isoniazid

Eng, K.E., Panas, M.D., Karlsson Hedestam, G.B., McInerney, G.M., 2010. A novel quantitative flow cytometry-based assay for autophagy. Autophagy 6, 634–641. https://doi.org/10.4161/auto.6.5.12112

England, N., n.d. NHS Standard Contract For Colorectal: Complex Inflammatory Bowel Disease. Londan NHS Engl.

Fadok, V.A., De Cathelineau, A., Daleke, D.L., Henson, P.M., Bratton, D.L., 2001. Loss of phospholipid asymmetry and surface exposure of phosphatidylserine is required for phagocytosis of apoptotic cells by macrophages and fibroblasts. J. Biol. Chem. 276, 1071–1077. https://doi.org/10.1074/jbc.M003649200

Fang Zhao, Robert Edwardsb, Diana Dizona, Jennifer R. Mastroiannib, e, Mikhail Geyfmana, André J. Ouelletteb, c, e, Bogi Andersena, and Steven M Lipkina, D., 2010. Disruption of Paneth and goblet cell homeostasis and increased

endoplasmic reticulum stress in Agr2−/− mice. Dev Biol. 338, 1–7. https://doi.org/10.1038/jid.2014.371

Fernández-Ramos, A.A., Marchetti-Laurent, C., Poindessous, V., Antonio, S., Laurent-Puig, P., Bortoli, S., Loriot, M.-A., Pallet, N., 2017. 6-mercaptopurine promotes energetic failure in proliferating T cells. Oncotarget 8, 43048–43060. https://doi.org/10.18632/oncotarget.17889

Fotoohi, A.K., Coulthard, S.A., Albertioni, F., 2010. Thiopurines: Factors influencing toxicity and response. Biochem. Pharmacol. 79, 1211–1220. https://doi.org/10.1016/j.bcp.2010.01.006

Freis, P., Bollard, J., Lebeau, J., Massoma, P., Fauvre, J., Vercherat, C., Walter, T., Manié, S., Roche, C., Scoazec, J.Y., Ferraro-Peyret, C., 2017. mTOR inhibitors activate PERK signaling and favor viability of gastrointestinal neuroendocrine cell lines. Oncotarget 8, 20974–20987. https://doi.org/10.18632/oncotarget.15469

Fritz, T., Niederreiter, L., Adolph, T., Blumberg, R.S., Kaser, A., 2011. Crohn's disease : NOD2, autophagy and ER stress converge. Gut 60, 1580–1588. https://doi.org/10.1136/gut.2009.206466.Crohn

Fujita, N., Itoh, T., Omori, H., Fukuda, M., Noda, T., Yoshimori, T., 2008. The Atg16L Complex Specifies the Site of LC3 Lipidation for Membrane Biogenesis in Autophagy. Mol. Biol. Cell 19, 2091–2100. https://doi.org/10.1091/mbc.E07

G. Guijarro, L., D. Roman, I., Dolores Fernandez-Moreno, M., P. Gisbert, J., Hernandez- Breijo, B., 2012. Is the Autophagy Induced by Thiopurines Beneficial or Deleterious? Curr. Drug Metab. 13, 1267–1276. https://doi.org/10.2174/138920012803341366

Gandin, V., Masvidal, L., Cargnello, M., Gyenis, L., McLaughlan, S., Cai, Y., Tenkerian, C., Morita, M., Balanathan, P., Jean-Jean, O., Stambolic, V., Trost, M., Furic, L., Larose, L., Koromilas, A.E., Asano, K., Litchfield, D., Larsson, O., Topisirovic, I., 2016. MTORC1 and CK2 coordinate ternary and eIF4F complex assembly. Nat. Commun. 7, 1–15. https://doi.org/10.1038/ncomms11127

Gardner, B.M., Pincus, D., Gotthardt, K., Gallagher, C.M., Walter, P., 2013. Endoplasmic reticulum stress sensing in the unfolded protein response. Cold Spring Harb. Perspect. Biol. 5. https://doi.org/10.1101/cshperspect.a013169

Gasteiger, G., D'osualdo, A., Schubert, D.A., Weber, A., Bruscia, E.M., Hartl, D., 2017. Cellular Innate Immunity: An Old Game with New Players. J. Innate Immun. 9, 111–125. https://doi.org/10.1159/000453397

Gaudino, S.J., Kumar, P., 2019. Cross-talk between antigen presenting cells and T cells impacts intestinal homeostasis, bacterial infections, and tumorigenesis. Front. Immunol. 10, 1–14. https://doi.org/10.3389/fimmu.2019.00360

Gebauer, F., Hentze, M.W., 2004. Molecular mechanisms of translational control. Nat. Rev. Mol. Cell Biol. 5, 827–835. https://doi.org/10.1038/nrm1488

Ghosh, N., Premchand, P., 2015. A UK cost of care model for inflammatory bowel disease. Frontline Gastroenterol. 6, 169–174. https://doi.org/10.1136/flgastro-

2014-100514

Goel, R.M., Blaker, P., Mentzer, A., Fong, S.C. m., Sanderson, J.D., Marinaki, A.M., 2015. Optimizing the use of thiopurines in inflammatory bowel disease. Ther. Adv. Chronic Dis. 6, 138–146. https://doi.org/10.1177/2040622315579063

González-Lama, Y., Gisbert, J.P., 2016. Monitoring thiopurine metabolites in inflammatory bowel disease. Frontline Gastroenterol. 7, 301–307. https://doi.org/10.1136/flgastro-2015-100681

Grassmé, H., Kirschnek, S., Riethmueller, J., Riehle, A., Kürthy, G. Von, Lang, F., Weller, M., Gulbins, E., Grassme, H., Kirschnek, S., Riethmueller, J., Riehle, A., Kiirthy, G. Von, Lang, F., Weller, M., Gulbinsl, E., 2000. CD95 / CD95 Ligand Interactions on Epithelial Cells in Host Defense to Pseudomonas aeruginosa Published by : American Association for the Advancement of Science CD95 / CD95 Ligand Interactions on Epithelial Cells in Host Defense to Pseudomonas aeruginosa 290, 527–530.

Haglund, S., Almer, S., Peterson, C., Söderman, J., 2013. Gene Expression and Thiopurine Metabolite Profiling in Inflammatory Bowel Disease - Novel Clues to Drug Targets and Disease Mechanisms? PLoS One 8. https://doi.org/10.1371/journal.pone.0056989

Haglund, S., Vikingsson, S., Almer, S., Soderman, J., 2017. Combination treatment with 6-mercaptopurine and allopurinol in HepG2 and HEK293 cells-Effects on gene expression levels and thiopurine metabolism. PLoS One 12, 1–19. https://doi.org/10.1371/journal.pone.0173825

Hailey, D.W., Rambold, A.S., Satpute-Krishnan, P., Mitra, K., Sougrat, R., Kim, P.K., Lippincott-Schwartz, J., 2010. Mitochondria Supply Membranes for Autophagosome Biogenesis during Starvation. Cell 141, 656–667. https://doi.org/10.1016/j.cell.2010.04.009

Hamanaka, R.B., Bobrovnikova-Marjon, E., Ji, X., Liebhaber, S.A., Diehl, J.A., 2009. PERK-dependent regulation of IAP translation during ER stress. Oncogene 28, 910–920. https://doi.org/10.1038/onc.2008.428

Hamasaki, M., Furuta, N., Matsuda, A., Nezu, A., Yamamoto, A., Fujita, N., Oomori, H., Noda, T., Haraguchi, T., Hiraoka, Y., Amano, A., Yoshimori, T., 2013. Autophagosomes form at ER-mitochondria contact sites. Nature 495, 389–393. https://doi.org/10.1038/nature11910

Hampe, J., Franke, A., Rosenstiel, P., Till, A., Teuber, M., Huse, K., Albrecht, M., Mayr, G., De La Vega, F.M., Briggs, J., Günther, S., Prescott, N.J., Onnie, C.M., Häsler, R., Sipos, B., Fölsch, U.R., Lengauer, T., Platzer, M., Mathew, C.G., Krawczak, M., Schreiber, S., 2007. A genome-wide association scan of nonsynonymous SNPs identifies a susceptibility variant for Crohn disease in ATG16L1. Nat. Genet. 39, 207–211. https://doi.org/10.1038/ng1954

Hampton, R.Y., 2002. ER-associated degradation in protein quality control and cellular regulation. Curr. Opin. Cell Biol. 14, 476–482. https://doi.org/10.1016/S0955-0674(02)00358-7

Hansen, T.E., Johansen, T., 2011. Following autophagy step by step. BMC Biol. 9, 2–5. https://doi.org/10.1186/1741-7007-9-39

Harding, H.P., Novoa, I., Zhang, Y., Zeng, H., Wek, R., Schapira, M., Ron, D., 2000. Stress-Induced Gene Expression in Mammalian Cells. Mol. Cell 6, 1099–1108. https://doi.org/S1097-2765(00)00108-8 [pii]

Harris, J., Hartman, M., Roche, C., Zeng, S.G., O'Shea, A., Sharp, F.A., Lambe, E.M., Creagh, E.M., Golenbock, D.T., Tschopp, J., Kornfeld, H., 2011. Autophagy controls IL-1β secretion by targeting Pro-IL-1β for degradation. J. Biol. Chem. 286, 9587–9597. https://doi.org/10.1074/jbc.M110.202911

Heazlewood, C.K., Cook, M.C., Eri, R., Price, G.R., Tauro, S.B., Taupin, D., Thornton, D.J., Chin, W.P., Crockford, T.L., Cornall, R.J., Adams, R., Kato, M., Nelms, K.A., Hong, N.A., Florin, T.H.J., Goodnow, C.C., McGuckin, M.A., 2008. Aberrant mucin assembly in mice causes endoplasmic reticulum stress and spontaneous inflammation resembling ulcerative colitis. PLoS Med. 5, 0440–0460. https://doi.org/10.1371/journal.pmed.0050054

Heliö, T., Halme, L., Lappalainen, M., Fodstad, H., Paavola-Sakki, P., Turunen, U., Färkkilä, M., Krusius, T., Kontula, K., 2003. CARD15/NOD2 gene variants are associated with familially occurring and complicated forms of Crohn's disease. Gut 52, 558–562. https://doi.org/10.1136/gut.52.4.558

Hermiston, M.L., Gordon, J., 1995. Inflammatory Bowel Disease and Adenomas in Mice Expressing a Dominant Negative N- Cadherin 270, 1203–1207.

Hillary, R.F., Fitzgerald, U., 2018. A lifetime of stress: ATF6 in development and homeostasis. J. Biomed. Sci. https://doi.org/10.1186/s12929-018-0453-1

Hink, M.A., Griep, R.A., Borst, J.W., Van Hoek, A., Eppink, M.H.M., Schots, A., Visser, A.J.W.G., 2000. Structural dynamics of green fluorescent protein alone and fused with a single chain Fv protein. J. Biol. Chem. 275, 17556–17560. https://doi.org/10.1074/jbc.M001348200

Hobro, A.J., Smith, N.I., 2017. An evaluation of fixation methods: Spatial and compositional cellular changes observed by Raman imaging. Vib. Spectrosc. 91, 31–45. https://doi.org/10.1016/j.vibspec.2016.10.012

Hoffmann, M., Rychlewski, J., Chrzanowska, M., Hermann, T., 2001. Mechanism of activation of an immunosuppressive drug: Azathioprine. Quantum chemical study on the reaction of azathioprine with cysteine. J. Am. Chem. Soc. 123, 6404–6409. https://doi.org/10.1021/ja010378c

Hollien, J., Weissmann, J., 2006. Decay of Endoplasmic Reticulum-Localized mRNAs During the Unfolded Protein Response. Science (80-.). 104–107.

Holm H. Uhlig, Tobias Schwerd, Sibylle Koletzko, Neil Shah, Jochen Kammermeier, Abdul Elkadri, Jodie Ouahed, David C. Wilson, Simon P. Travis, Dan Turner, Christoph Klein, Scott B. Snapper, and A.M.M., 2014. The Diagnostic Approach to Monogenic Very Early Onset Inflammatory Bowel Disease. Gastroenterology 147, 4173–4183. https://doi.org/10.1021/acsnano.5b07425.Molecular

Holmes, E.A., Xiang, F., Lucas, R.M., 2015. Variation in incidence of pediatric Crohn's disease in relation to latitude and ambient ultraviolet radiation: A systematic review and analysis. Inflamm. Bowel Dis. 21, 809–817. https://doi.org/10.1097/MIB.0000000000000320

Hooper, K.M., Barlow, P.G., Henderson, P., Stevens, C., 2019a. Interactions between autophagy and the unfolded protein response: Implications for inflammatory bowel disease. Inflamm. Bowel Dis. 25, 661–671. https://doi.org/10.1093/ibd/izy380

Hooper, K.M., Casanova, V., Kemp, S., Staines, K.A., Satsangi, J., Barlow, P.G., Henderson, P., Stevens, C., 2019b. The Inflammatory Bowel Disease Drug Azathioprine Induces Autophagy via mTORC1 and the Unfolded Protein Response Sensor PERK. Inflamm. Bowel Dis. 25, 1481–1496. https://doi.org/10.1093/ibd/izz039

Houck, S.A., Ren, H.Y., Madden, V.J., Bonner, J.N., Michael, P., Janovick, J.A., Conn, P.M., Cyr, D.M., 2015. Quality control autophagy degrades soluble ERAD-resistant conformers of the misfolded membrane protein GnRHR 54, 166–179. https://doi.org/10.1016/j.molcel.2014.02.025.Quality

Huang, H.Y., Chang, H.F., Tsai, M.J., Chen, J.S., Wang, M.J., 2016. 6-Mercaptopurine attenuates tumor necrosis factor-α production in microglia through Nur77-mediated transrepression and PI3K/Akt/mTOR signaling-mediated translational regulation. J. Neuroinflammation 13, 1–20. https://doi.org/10.1186/s12974-016-0543-5

Icha, J., Weber, M., Waters, J.C., Norden, C., 2017. Phototoxicity in live fluorescence microscopy, and how to avoid it. BioEssays 39, 1–15. https://doi.org/10.1002/bies.201700003

Jacquin, E., Apetoh, L., 2018. Cell-Intrinsic roles for autophagy in modulating CD4 T cell functions. Front. Immunol. 9, 1–9. https://doi.org/10.3389/fimmu.2018.01023

Jiang, J., Natarajan, K., Margulies, D., 2019. MHC Molecules, T cell Receptors, Natural Killer Cell Receptors, and Viral Immunoevasins—Key Elements of Adaptive and Innate Immunity, in: Advances in Experimental Medicine and Biology. pp. 21–62.

Jiang, P., Mizushima, N., 2014. Autophagy and human diseases. Cell Res. 24, 69–79. https://doi.org/10.1038/cr.2013.161

Jiefei Geng, Usha Nair, Kyoko Yasumura-Yorimitsu, and D.J.K., 2010. Post-Golgi Sec Proteins Are Required for Autophagy in Saccharomyces cerevisiae. Mol. Biol. Cell 20, 4524–4530. https://doi.org/10.1091/mbc.E09

Kapur, S., Hanauer, S.B., 2019. The Evolving Role of Thiopurines in Inflammatory Bowel Disease. Curr. Treat. Options Gastroenterol. 17, 420–433. https://doi.org/10.1007/s11938-019-00244-3

Karanasios, E., Stapleton, E., Manifava, M., Kaizuka, T., Mizushima, N., Walker, S.A., Ktistakis, N.T., 2013. Dynamic association of the ULK1 complex with omegasomes during autophagy induction. J. Cell Sci. 126, 5224–5238.

https://doi.org/10.1242/jcs.132415

Karran, P., 2007. Thiopurines , DNA damage , DNA repair and therapy-related cancer 153–170. https://doi.org/10.1093/bmb/ldl020

Kaser, A., Lee, A., Franke, A., Glickman, J., 2008a. XBP1 links ER stress to intestinal inflammation and confers genetic risk for human inflammatory bowel disease. Cell 134, 743–756. https://doi.org/10.1016/j.cell.2008.07.021.XBP1

Kaser, A., Lee, A.H., Franke, A., Glickman, J.N., Zeissig, S., Tilg, H., Nieuwenhuis, E.E.S., Higgins, D.E., Schreiber, S., Glimcher, L.H., Blumberg, R.S., 2008b. XBP1 Links ER Stress to Intestinal Inflammation and Confers Genetic Risk for Human Inflammatory Bowel Disease. Cell 134, 743–756. https://doi.org/10.1016/j.cell.2008.07.021

Khor, B., Gardet, A., Xavier, R.J., 2011. Genetics and pathogenesis of IBD. Nature 474, 307–317. https://doi.org/10.1038/nature10209.Genetics

Kim, D.H., Cheon, J.H., 2017. Pathogenesis of inflammatory bowel disease and recent advances in biologic therapies. Immune Netw. 17, 25–40. https://doi.org/10.4110/in.2017.17.1.25

King, J.S., Veltman, D.M., Insall, R.H., 2011. The induction of autophagy by mechanical stress. Autophagy 7, 1490–1499. https://doi.org/10.4161/auto.7.12.17924

Kishino, A., Hayashi, K., Hidai, C., Masuda, T., Nomura, Y., Oshima, T., 2017. XBP1-FoxO1 interaction regulates ER stress-induced autophagy in auditory cells. Sci. Rep. 7, 1–15. https://doi.org/10.1038/s41598-017-02960-1

Klionsky, D.J., 2005. The molecular machinery of autophagy: unanswered questions. J. Cell Sci. 118, 7–18. https://doi.org/10.1242/jcs.01620

Kobayashi, K.S., Chamaillard, M., Ogura, Y., Henegariu, O., Inohara, N., Nuñez, G., Flavell, R.A., 2005. Nod2-dependent regulation of innate and adaptive immunity in the intestinal tract. Science (80-.). 307, 731–734. https://doi.org/10.1126/science.1104911

Kurushima, H., Ramprasad, M., Kondratenko, N., Foster, D.M., Quehenberger, O., Steinberg, D., 2000. Surface expression and rapid internalization of macrosialin (mouse CD68) on elicited mouse peritoneal macrophages. J. Leukoc. Biol. 67, 104–108. https://doi.org/10.1002/jlb.67.1.104

Ladoire, S., Chaba, K., Martins, I., Sukkurwala, A.Q., Adjemian, S., Michaud, M., Poirier-Colame, V., Andreiuolo, F., Galluzzi, L., White, E., Rosenfeldt, M., Ryan, K.M., Zitvogel, L., Kroemer, G., 2012. Immunohistochemical detection of cytoplasmic LC3 puncta in human cancer specimens. Autophagy 8, 1175–1184. https://doi.org/10.4161/auto.20353

Lamb, C.A., Yoshimori, T., Tooze, S.A., 2013. The autophagosome: Origins unknown, biogenesis complex. Nat. Rev. Mol. Cell Biol. 14, 759–774. https://doi.org/10.1038/nrm3696

Lamkanfi, M., Dixit, V.M., 2010. Manipulation of host cell death pathways during

microbial infections. Cell Host Microbe 8, 44–54. https://doi.org/10.1016/j.chom.2010.06.007

Lapaquette, P., Bringer, M.A., Darfeuille-Michaud, A., 2012. Defects in autophagy favour adherent-invasive Escherichia coli persistence within macrophages leading to increased pro-inflammatory response. Cell. Microbiol. 14, 791–807. https://doi.org/10.1111/j.1462-5822.2012.01768.x

Lapaquette, P., Guzzo, J., Bretillon, L., Bringer, M.A., 2015. Cellular and Molecular Connections between Autophagy and Inflammation. Mediators Inflamm. 2015. https://doi.org/10.1155/2015/398483

Larabi, A., Barnich, N., Nguyen, H.T.T., 2020. New insights into the interplay between autophagy, gut microbiota and inflammatory responses in IBD. Autophagy 16, 38–51. https://doi.org/10.1080/15548627.2019.1635384

Larsson, J.M.H., Karlsson, H., Crespo, J.G., Johansson, M.E.V., Eklund, L., Sjövall, H., Hansson, G.C., 2011. Altered O-glycosylation profile of MUC2 mucin occurs in active ulcerative colitis and is associated with increased inflammation. Inflamm. Bowel Dis. 17, 2299–2307. https://doi.org/10.1002/ibd.21625

Lebeau, J., Saunders, J.M., Moraes, V.W.R., Madhavan, A., Madrazo, N., Anthony, M.C., Wiseman, R.L., 2018. The PERK Arm of the Unfolded Protein Response Regulates Mitochondrial Morphology during Acute Endoplasmic Reticulum Stress. Cell Rep. 22, 2827–2836. https://doi.org/10.1016/j.celrep.2018.02.055

Lee, A.U., Farrell, G.C., 2001. Mechanism of azathioprine-induced injury to hepatocytes: Roles of glutathione depletion and mitochondrial injury. J. Hepatol. 35, 756–764. https://doi.org/10.1016/S0168-8278(01)00196-9

Lee, Y.K., Lee, J.A., 2016. Role of the mammalian ATG8/LC3 family in autophagy: Differential and compensatory roles in the spatiotemporal regulation of autophagy. BMB Rep. 49, 424–430. https://doi.org/10.5483/BMBRep.2016.49.8.081

Lennard, L., Welch, J.C., Lilleyman, J.S., 1997. Thiopurine drugs in the treatment of childhood leukaemia: the influence of inherited thiopurine methyltransferase activity on drug metabolism and cytotoxicity. Br. J. Clin. Pharmacol. 44, 455–461. https://doi.org/10.1046/j.1365-2125.1997.t01-1-00607.x

Lim, S.Z., Chua, E.W., 2018. Revisiting the Role of Thiopurines in Inflammatory Bowel Disease Through Pharmacogenomics and Use of Novel Methods for Therapeutic Drug Monitoring. Front. Pharmacol. 9, 1107. https://doi.org/10.3389/fphar.2018.01107

Liu, W.J., Ye, L., Huang, W.F., Guo, L.J., Xu, Z.G., Wu, H.L., Yang, C., Liu, H.F., 2016. P62 Links the Autophagy Pathway and the Ubiqutin-Proteasome System Upon Ubiquitinated Protein Degradation. Cell. Mol. Biol. Lett. 21, 1–14. https://doi.org/10.1186/s11658-016-0031-z

Liu, Z., Lee, J., Krummey, S., Lu, W., Cai, H., Lenardo, M.J., 2011. The kinase LRRK2 is a regulator of the transcription factor NFAT that modulates the severity of inflammatory bowel disease. Nat. Immunol. 12, 1063–1070.

https://doi.org/10.1038/ni.2113

Liu, Z., Liao, J., Wei, H., Yang, Z., Liu, J., Xu, J., Wu, X., Zhan, H., 2019. PERK is essential for proliferation of intestinal stem cells in mice. Exp. Cell Res. 375, 42–51. https://doi.org/10.1016/j.yexcr.2018.12.009

Liu, Z., Wang, Y., Zhao, S., Zhang, J., Wu, Y., Zeng, S., 2015. Imidazole inhibits autophagy flux by blocking autophagic degradation and triggers apoptosis via increasing FoxO3a-Bim expression. Int. J. Oncol. 46, 721–731. https://doi.org/10.3892/ijo.2014.2771

Loddo, I., Romano, C., 2015. Inflammatory bowel disease: Genetics, epigenetics, and pathogenesis. Front. Immunol. 6, 6–11. https://doi.org/10.3389/fimmu.2015.00551

Long, M.D., Kappelman, M.D., Martin, C.F., Chen, W., Anton, K., Sandler, R.S., 2017. of Inflammatory Bowel Disease 50, 152–156. https://doi.org/10.1097/MCG.0000000000000421.Role

López, K., Guzman, M., Sanchez, E., Carranca, A., 2019. mTORC1 as a Regulator of Mitochondrial Functions and a Therapeutic Target in Cancer. Front. Oncol. 9. https://doi.org/10.3389/fonc.2019.01373

Lotfi, N., Thome, R., Rezaei, N., Zhang, G.X., Rezaei, A., Rostami, A., Esmaeil, N., 2019. Roles of GM-CSF in the pathogenesis of autoimmune diseases: An update. Front. Immunol. 10, 1–14. https://doi.org/10.3389/fimmu.2019.01265

Lu, C., Chen, J., Xu, H.G., Zhou, X., He, Q., Li, Y.L., Jiang, G., Shan, Y., Xue, B., Zhao, R.X., Wang, Y., Werle, K.D., Cui, R., Liang, J., Xu, Z.X., 2014. MIR106B and MIR93 prevent removal of bacteria from epithelial cells by disrupting ATG16L1-mediated autophagy. Gastroenterology 146, 188–199. https://doi.org/10.1053/j.gastro.2013.09.006

Lund, M.E., To, J., O'Brien, B.A., Donnelly, S., 2016. The choice of phorbol 12-myristate 13-acetate differentiation protocol influences the response of THP-1 macrophages to a pro-inflammatory stimulus. J. Immunol. Methods 430, 64–70. https://doi.org/10.1016/j.jim.2016.01.012

M'Koma, A.E., 2013. Inflammatory bowel disease: An expanding global health problem. Clin. Med. Insights Gastroenterol. https://doi.org/10.4137/CGast.S12731

Ma, X., Dai, Z., Sun, K., Zhang, Y., Chen, J., Yang, Y., Tso, P., Wu, G., Wu, Z., 2017. Intestinal epithelial cell endoplasmic reticulum stress and inflammatory bowel disease pathogenesis: An update review. Front. Immunol. 8, 1–11. https://doi.org/10.3389/fimmu.2017.01271

Maeda, S., Hsu, L.-C., Liu, H., Bankston, L.A., Limura, M., Kagnoff, M.F., Eckmann, L., Karin, M., 2005. Nod2 Mutation in Crohn ' s Disease Potentiates NF- κ B Activity and IL-1ß Processing Nod2 Mutation in Crohn ' s Disease Potentiates NF-k B Activity and IL-1 b Processing 307, 734–738. https://doi.org/10.1126/science.1103685

Magnuson, B., Ekim, B., Fingar, D.C., 2012. Regulation and function of ribosomal protein S6 kinase (S6K) within mTOR signalling networks. Biochem. J. 441, 1–21. https://doi.org/10.1042/BJ20110892

Mahida, Y.R., 2000. The key role of macrophages in the immunopathogenesis of inflammatory bowel disease. Inflamm. Bowel Dis. 6, 21–33. https://doi.org/10.1097/00054725-200002000-00004

Margariti, A., Li, H., Chen, T., Martin, D., Vizcay-Barrena, G., Alam, S., Karamariti, E., Xiao, Q., Zampetaki, A., Zhang, Z., Wang, W., Jiang, Z., Gao, C., Ma, B., Chen, Y.G., Cockerill, G., Hu, Y., Xu, Q., Zeng, L., 2013. XBP1 mRNA splicing triggers an autophagic response in endothelial cells through BECLIN-1 transcriptional activation. J. Biol. Chem. 288, 859–872. https://doi.org/10.1074/jbc.M112.412783

Massey, D.C.O., Bredin, F., Parkes, M., 2008. Use of sirolimus (rapamycin) to treat refractory Crohn's disease. Gut 57, 1294–1296. https://doi.org/10.1136/gut.2008.157297

McCole, D.F., 2014. IBD candidate genes and intestinal barrier regulation. Inflamm. Bowel Dis. 20, 1829–1849. https://doi.org/10.1097/MIB.0000000000000090

McGovern, D.P.B., Travis, S.P.L., Duley, J., Shobowale-Bakre, E.M., Dalton, H.R., 2002. Azathioprine intolerance in patients with IBD may be imidazole-related and is independent of TPMT activity [2]. Gastroenterology 122, 838–839. https://doi.org/10.1053/gast.2002.32124

McNees, A.L., Markesich, D., Zayyani, N.R., Graham, D.Y., 2015. Mycobacterium paratuberculosis as a cause of crohn's disease. Expert Rev. Gastroenterol. Hepatol. 9, 1523–1534. https://doi.org/10.1586/17474124.2015.1093931

McQuiston, A., Diehl, A., 2017. Recent insights into PERK-dependent signaling from the stressed endoplasmic reticulum. F1000Research 6, 1–11. https://doi.org/10.12688/f1000research.12138.1

Menor, C., Fernandez-Moreno, M.D., Fueyo, J.A., Escribano, O., Olleros, T., Arriaza, E., Cara, C., Lorusso, M., Paola, M. Di, Roman, I.D., Guijarro, L.G., 2004. Azathioprine Acts upon Rat Hepatocyte Mitochondria and Stress-Activated Protein Kinases Leading to Necrosis: Protective Role of N-Acetyl-L-cysteine. J. Pharmacol. Exp. Ther. 311, 668–676. https://doi.org/10.1124/jpet.104.069286

Misdaq, M., Ziegler, S., Von Ahsen, N., Oellerich, M., Asif, A.R., 2015. Thiopurines induce oxidative stress in T-lymphocytes: A proteomic approach. Mediators Inflamm. 2015. https://doi.org/10.1155/2015/434825

Mizushima, N., Yoshimorim, T., Levine, B., 2010. Methods in Mammalian Autophagy Research. Cell 140, 313–326. https://doi.org/10.1016/j.cell.2010.01.028.Methods

Mohan, C.D., Srinivasa, V., Rangappa, S., Mervin, L., Mohan, S., Paricharak, S., Baday, S., Li, F., Shanmugam, M.K., Chinnathambi, A., Zayed, M.E., Alharbi, S.A., Bender, A., Sethi, G., Rangappa, K.S., 2016. Trisubstituted-Imidazoles Induce Apoptosis in Human Breast Cancer Cells by Targeting the Oncogenic PI3K / Akt / mTOR Signaling Pathway 1–15. https://doi.org/10.1371/journal.pone.0153155

Moulis, M., Vindis, C., 2017. Methods for Measuring Autophagy in Mice. Cells 6, 14. https://doi.org/10.3390/cells6020014

Murray, J., Merrill, J., Harrison, J., Wilson, R., Dammin, G., 1963. Prolonged Survival of Human-Kidney Homografts by Immunosuppressive Drug Therapy. N. Engl. J. Med. 13, 1315–1323. https://doi.org/10.1056/NEJM198603273141302

Musiwaro, P., Smith, M., Manifava, M., Walker, S.A., Ktistakis, N.T., 2013. Characteristics and requirements of basal autophagy in HEK 293 cells. Autophagy 9, 1407–1417. https://doi.org/10.4161/auto.25455

Mutalib, M., Borrelli, O., Blackstock, S., Kiparissi, F., Elawad, M., Shah, N., Lindley, K., 2014. The use of sirolimus (rapamycin) in the management of refractory inflammatory bowel disease in children. J. Crohn's Colitis 8, 1730–1734. https://doi.org/10.1016/j.crohns.2014.08.014

Na, Y.R., Stakenborg, M., Seok, S.H., Matteoli, G., 2019. Macrophages in intestinal inflammation and resolution: a potential therapeutic target in IBD. Nat. Rev. Gastroenterol. Hepatol. https://doi.org/10.1038/s41575-019-0172-4

Nakanishi, Y., Sato, T., Ohteki, T., 2015. Commensal Gram-positive bacteria initiates colitis by inducing monocyte/macrophage mobilization. Mucosal Immunol. 8, 152–160. https://doi.org/10.1038/mi.2014.53

Negroni, A., Pierdomenico, M., Cucchiara, S., Stronati, L., 2018. NOD2 and inflammation: Current insights. J. Inflamm. Res. https://doi.org/10.2147/JIR.S137606

Novak, E.A., Mollen, K.P., 2015. Mitochondrial dysfunction in inflammatory bowel disease. Front. Cell Dev. Biol. https://doi.org/10.3389/fcell.2015.00062

Oancea, I., Das, I., Cárcer, A. de, Movva, R., Schreiber, V., Yang, Y., Proctor, M., Wang, R., Sheng, Y., Lobb, M., Cuiv, P.Ó., Duley, J.A., Begun, J., Florin, T.H.J., 2016. Bacterial activation of thioguanine results in lymphocyte independent improvement in murine colitis. Gastroenterology 10, 117.

Ogata, M., Hino, S. -i., Saito, A., Morikawa, K., Kondo, S., Kanemoto, S., Murakami, T., Taniguchi, M., Tanii, I., Yoshinaga, K., Shiosaka, S., Hammarback, J.A., Urano, F., Imaizumi, K., 2006. Autophagy Is Activated for Cell Survival after Endoplasmic Reticulum Stress. Mol. Cell. Biol. 26, 9220–9231. https://doi.org/10.1128/MCB.01453-06

Ohsumi, Y., Mizushima, N., 2004. Two ubiquitin-like conjugation systems essential for autophagy. Semin. Cell Dev. Biol. 15, 231–236. https://doi.org/10.1016/j.semcdb.2003.12.004

Okamoto, R., Watanabe, M., 2016. Role of epithelial cells in the pathogenesis and treatment of inflammatory bowel disease. J. Gastroenterol. 51, 11–21. https://doi.org/10.1007/s00535-015-1098-4

Olga Biskou, Casanova, V., Hooper, K.M., Kemp, S., Wright, G.P., Satsangi, J., Barlow, P.G., Id, C.S., 2019. The type III intermediate filament vimentin regulates organelle distribution and modulates autophagy 1–20.

Ooi, A., Wong, A., Esau, L., Lemtiri-Chlieh, F., Gehring, C., 2016. A guide to transient expression of membrane proteins in HEK-293 cells for functional characterization. Front. Physiol. 7, 1–15. https://doi.org/10.3389/fphys.2016.00300

Orecchioni, M., Ghosheh, Y., Pramod, A.B., Ley, K., 2019. Macrophage polarization: Different gene signatures in M1(Lps+) vs. Classically and M2(LPS-) vs. Alternatively activated macrophages. Front. Immunol. 10, 1–14. https://doi.org/10.3389/fimmu.2019.01084

Oshima, S., Nakamura, T., Namiki, S., Okada, E., Tsuchiya, K., Okamoto, R., Yamazaki, M., Yokota, T., Aida, M., Yamaguchi, Y., Kanai, T., Handa, H., Watanabe, M., 2004. Interferon Regulatory Factor 1 (IRF-1) and IRF-2 Distinctively Up-Regulate Gene Expression and Production of Interleukin-7 in Human Intestinal Epithelial Cells. Mol. Cell. Biol. 24, 6298–6310. https://doi.org/10.1128/mcb.24.14.6298-6310.2004

Park, E.K., Jung, H.S., Yang, H.I., Yoo, M.C., Kim, C., Kim, K.S., 2007. Optimized THP-1 differentiation is required for the detection of responses to weak stimuli. Inflamm. Res. 56, 45–50. https://doi.org/10.1007/s00011-007-6115-5

Park, S.-W., Zhen, G., Verhaeghe, C., Nakagami, Y., Nguyenvu, L.T., Barczak, A.J., Killeen, N., Erle, D.J., 2009. The protein disulfide isomerase AGR2 is essential for production of intestinal mucus. Proc. Natl. Acad. Sci. U. S. A. 106, 6950–5. https://doi.org/10.1073/pnas.0808722106

Parkhouse, R., Monie, T.P., 2015. Dysfunctional Crohn's disease-associated NOD2 polymorphisms cannot be reliably predicted on the basis of RIPK2 binding or membrane association. Front. Immunol. 6, 1–9. https://doi.org/10.3389/fimmu.2015.00521

Patrick M. Smith, Michael R. Howitt, Nicolai Panikov, Monia Michaud, Carey Ann Gallini, Mohammad Bohlooly-Y, Jonathan N. Glickman, and W.S.G., 2013. The microbial metabolites, short chain fatty acids, regulate colonic Treg cell homeostasis. Natl. Instituite Heal. 341, 51–75. https://doi.org/10.1126/science.1241165.The

Petit, E., Langouet, S., Akhdar, H., Nicolas-Nicolaz, C., Guillouzo, A., Morel, F., 2008a. Differential toxic effects of azathioprine, 6-mercaptopurine and 6-thioguanine on human hepatocytes. Toxicol. Vitr. 22, 632–642. https://doi.org/10.1016/j.tiv.2007.12.004

Petit, E., Langouet, S., Akhdar, H., Nicolas-Nicolaz, C., Guillouzo, A., Morel, F., 2008b. Differential toxic effects of azathioprine, 6-mercaptopurine and 6-thioguanine on human hepatocytes. Toxicol. Vitr. 22, 632–642. https://doi.org/10.1016/j.tiv.2007.12.004

Pezze, P.D., Ruf, S., Sonntag, A.G., Langelaar-Makkinje, M., Hall, P., Heberle, A.M., Navas, P.R., Van Eunen, K., Tölle, R.C., Schwarz, J.J., Wiese, H., Warscheid, B., Deitersen, J., Stork, B., Fäßler, E., Schäuble, S., Hahn, U., Horvatovich, P., Shanley, D.P., Thedieck, K., 2016. A systems study reveals concurrent activation of AMPK and mTOR by amino acids. Nat. Commun. 7, 1–19. https://doi.org/10.1038/ncomms13254

Plantinga, T.S., Crisan, T.O., Oosting, M., Van De Veerdonk, F.L., De Jong, D.J., Philpott, D.J., Van Der Meer, J.W.M., Girardin, S.E., Joosten, L.A.B., Netea, M.G., 2011. Crohn's disease-associated ATG16L1 polymorphism modulates pro-inflammatory cytokine responses selectively upon activation of NOD2. Gut 60, 1229–1235. https://doi.org/10.1136/gut.2010.228908

Platt, A.M., Bain, C.C., Bordon, Y., Sester, D.P., Mowat, A.M., 2010. An Independent Subset of TLR Expressing CCR2-Dependent Macrophages Promotes Colonic Inflammation. J. Immunol. 184, 6843–6854. https://doi.org/10.4049/jimmunol.0903987

Qiu, Y., Mao, R., Zhang, S.H., Li, M.Y., Guo, J., Chen, B.L., He, Y., Zeng, Z.R., Chen, M.H., 2015. Safety profile of thiopurines in Crohn disease: Analysis of 893 patient-years follow-up in a southern China cohort. Med. (United States) 94, 1–8. https://doi.org/10.1097/MD.0000000000001513

Rabanal-Ruiz, Y., Otten, E.G., Korolchuk, V.I., 2017. MTORC1 as the main gateway to autophagy. Essays Biochem. 61, 565–584. https://doi.org/10.1042/EBC20170027

Rai, S., Manjithaya, R., 2015. Fluorescence microscopy: A tool to study autophagy. AIP Adv. 5. https://doi.org/10.1063/1.4928185

Rainbolt, T.K., Saunders, J.M., Wiseman, R.L., 2014. Stress-responsive regulation of mitochondria through the ER unfolded protein response. Trends Endocrinol. Metab. 25, 528–537. https://doi.org/10.1016/j.tem.2014.06.007

Ramos, G.P., Papadakis, K.A., 2019. Mechanisms of Disease: Inflammatory Bowel Diseases. Mayo Clin. Proc. 94, 155–165. https://doi.org/10.1016/j.mayocp.2018.09.013

Rashid, H.O., Yadav, R.K., Kim, H.R., Chae, H.J., 2015. ER stress: Autophagy induction, inhibition and selection. Autophagy 11, 1956–1977. https://doi.org/10.1080/15548627.2015.1091141

Ravikumar, B., Moreau, K., Jahreiss, L., Puri, C., David, C., 2011. Plasma membrane contributes to the formation of pre- autophagosomal structures 12, 747–757. https://doi.org/10.1038/ncb2078.Plasma

Roberts, C.L., Keita, Å. V., Duncan, S.H., O'Kennedy, N., Söderholm, J.D., Rhodes, J.M., Campbell, B.J., 2010. Translocation of Crohn's disease Escherichia coli across M-cells: Contrasting effects of soluble plant fibres and emulsifiers. Gut 59, 1331–1339. https://doi.org/10.1136/gut.2009.195370

Rolhion, N., Darfeuille-Michaud, A., 2007. Adherent-invasive Escherichia coli in inflammatory bowel disease. Inflamm. Bowel Dis. 13, 1277–1283. https://doi.org/10.1002/ibd.20176

Rubio, C.A., Schmidt, P.T., 2018. Severe defects in the macrophage barrier to gut microflora in inflammatory bowel disease and colon cancer. Anticancer Res. 38, 3811–3815. https://doi.org/10.21873/anticanres.12664

Runwal, G., Stamatakou, E., Siddiqi, F.H., Puri, C., Zhu, Y., Rubinsztein, D.C., 2019.

LC3-positive structures are prominent in autophagy-deficient cells. Sci. Rep. 9, 1–14. https://doi.org/10.1038/s41598-019-46657-z

Saci, A., Cantley, L.C., Carpenter, C.L., 2011. Rac1 Regulates the Activity of mTORC1 and mTORC2 and Controls Cellular Size. Mol. Cell 42, 50–61. https://doi.org/10.1016/j.molcel.2011.03.017.Rac1

Saitoh, T., Fujita, N., Jang, M.H., Uematsu, S., Yang, B.G., Satoh, T., Omori, H., Noda, T., Yamamoto, N., Komatsu, M., Tanaka, K., Kawai, T., Tsujimura, T., Takeuchi, O., Yoshimori, T., Akira, S., 2008. Loss of the autophagy protein Atg16L1 enhances endotoxin-induced IL-1β production. Nature 456, 264–268. https://doi.org/10.1038/nature07383

Salem, M., Ammitzboell, M., Nys, K., Seidelin, J.B., Nielsen, O.H., 2015. ATG16L1: A multifunctional susceptibility factor in crohn disease. Autophagy 11, 585–594. https://doi.org/10.1080/15548627.2015.1017187

Sanchez-Alvarez, M., Del Pozo, M.A., Bakal, C., 2017. AKT-mTOR signaling modulates the dynamics of IRE1 RNAse activity by regulating ER-mitochondria contacts. Sci. Rep. 7, 1–15. https://doi.org/10.1038/s41598-017-16662-1

Sano, R., Reed, J.C., 2013. ER stress-induced cell death mechanisms. Biochim. Biophys. Acta - Mol. Cell Res. 1833, 3460–3470. https://doi.org/10.1016/j.bbamcr.2013.06.028

Schauber, J., Svanholm, C., Termén, S., Iffland, K., Menzel, T., Scheppach, W., Melcher, R., Agerberth, B., Lührs, H., Gudmundsson, G.H., 2003. Expression of the cathelicidin LL-37 is modulated by short chain fatty acids in colonocytes: Relevance of signalling pathways. Gut 52, 735–741. https://doi.org/10.1136/gut.52.5.735

Schröder, M., Kaufman, R.J., 2005. ER stress and the unfolded protein response. Mutat. Res. - Fundam. Mol. Mech. Mutagen. 569, 29–63. https://doi.org/10.1016/j.mrfmmm.2004.06.056

Schwende, H., Fitzke, E., Ambs, P., Dieter, P., 1996. Differences in the state of differentiation of THP-1 cells induced by phorbol ester and 1,25-dihydroxyvitamin D3. J. Leukoc. Biol. 59, 555–561. https://doi.org/10.1002/jlb.59.4.555

Seinen, M.L., van Asseldonk, D.P., Mulder, C.J.J., de Boer, N.K.H., 2010. Dosing 6-thioguanine in inflammatory bowel disease: Expert-based guidelines for daily practice. J. Gastrointest. Liver Dis. 19, 291–294.

Seinen, M.L., van Nieuw Amerongen, G.P., de Boer, N.K.H., van Bodegraven, A.A., 2016. Rac Attack: Modulation of the Small GTPase Rac in Inflammatory Bowel Disease and Thiopurine Therapy. Mol. Diagnosis Ther. 20, 551–557. https://doi.org/10.1007/s40291-016-0232-1

Shang, J., Lehrman, M.A., 2004. Discordance of UPR signaling by ATF6 and Ire1p-XBP1 with levels of target transcripts. Biochem. Biophys. Res. Commun. 317, 390–396. https://doi.org/10.1016/j.bbrc.2004.03.058

Shaw, K.A., Cutler, D.J., Okou, D., Dodd, A., Aronow, B.J., Haberman, Y., Stevens,

C., Walters, T.D., Griffiths, A., Baldassano, R.N., Noe, J.D., Hyams, J.S., Crandall, W. V., Kirschner, B.S., Heyman, M.B., Snapper, S., Guthery, S., Dubinsky, M.C., Shapiro, J.M., Otley, A.R., Daly, M., Denson, L.A., Kugathasan, S., Zwick, M.E., 2019. Genetic variants and pathways implicated in a pediatric inflammatory bowel disease cohort. Genes Immun. 20, 131–142. https://doi.org/10.1038/s41435-018-0015-2

Shaw, T.N., Houston, S.A., Wemyss, K., Bridgeman, H.M., Barbera, T.A., Zangerle-Murray, T., Strangward, P., Ridley, A.J.L., Wang, P., Tamoutounour, S., Allen, J.E., Konkel, J.E., Grainger, J.R., 2018. Tissue-resident macrophages in the intestine are long lived and defined by Tim-4 and CD4 expression. J. Exp. Med. 215, 1507–1518. https://doi.org/10.1084/jem.20180019

Shen, J., Prywes, R., 2004. Dependence of site-2 protease cleavage of ATF6 on prior site-1 protease digestion is determined by the size of the luminal domain of ATF6. J. Biol. Chem. 279, 43046–43051. https://doi.org/10.1074/jbc.M408466200

Shi, R.Z., Lyons, S.D., Christopherson, R.I., 1998. Metabolic effects of thiopurine derivatives against human CCRF-CEM leukaemia cells. Int. J. Biochem. Cell Biol. 30, 885–895. https://doi.org/10.1016/S1357-2725(98)00053-3

Shin, J.Y., Wey, M., Umutesi, H.G., Sun, X., Simecka, J., Heo, J., 2016. Thiopurine prodrugs mediate immunosuppressive effects by interfering with Rac1 protein function. J. Biol. Chem. 291, 13699–13714. https://doi.org/10.1074/jbc.M115.694422

Shkoda, A., Ruiz, P.A., Daniel, H., Kim, S.C., Rogler, G., Sartor, R.B., Haller, D., 2007. Interleukin-10 Blocked Endoplasmic Reticulum Stress in Intestinal Epithelial Cells: Impact on Chronic Inflammation. Gastroenterology 132, 190–207. https://doi.org/10.1053/j.gastro.2006.10.030

Sidiq, T., Yoshihama, S., Downs, I., Kobayashi, K.S., 2016. Nod2: A critical regulator of ileal microbiota and Crohn's disease. Front. Immunol. 7, 18–20. https://doi.org/10.3389/fimmu.2016.00367

Sidrauski, C., Walter, P., 1997. The transmembrane kinase Ire1p is a site-specific endonuclease that initiates mRNA splicing in the unfolded protein response. Cell 90, 1031–1039. https://doi.org/10.1016/S0092-8674(00)80369-4

Slack Emma, Siegfried Hapfelmeier, Bärbel Stecher, Yuliya Velykoredko, Maaike Stoel, Melissa Lawson, Markus B Geuking, Bruce Beutler, Thomas F Tedder, Wolf- Dietrich Hardt, Premysl Bercik, Elena F Verdu, Kathy D McCoy, and A.J.M., 2009. A flexible continuum between adaptive and innate immunity in maintaining host-microbiota mutualism. Am. J. Int. Law 325, 617–620. https://doi.org/10.1126/science.1172747

Small, C.L.N., Reid-Yu, S.A., McPhee, J.B., Coombes, B.K., 2013. Persistent infection with Crohn's disease-associated adherent-invasive Escherichia coli leads to chronic inflammation and intestinal fibrosis. Nat. Commun. 4. https://doi.org/10.1038/ncomms2957

Smythies, Jan M. Orenstein, P.D.S., 2005. Human intestinal macrophages display profound inflammatory anergy despite avid phagocytic and bacteriocidal activity.

J. Clin. Invest. 115, 787–796. https://doi.org/10.1172/JCI200519229.66

Starr, T., Bauler, T.J., Malik-Kale, P., Steele-Mortimer, O., 2018. The phorbol 12-myristate-13-acetate differentiation protocol is critical to the interaction of THP-1 macrophages with Salmonella Typhimurium. PLoS One 13, 1–13. https://doi.org/10.1371/journal.pone.0193601

Steinbach, E., Plevy, S., 2014. The role of macrophages and dendritic cells in the initiation of inflammation in IBD. Inflamm. Bowel Dis. 20, 1–7. https://doi.org/10.1038/jid.2014.371

Stocco, G., Cuzzoni, E., De Iudicibus, S., Franca, R., Favretto, D., Malusà, N., Londero, M., Cont, G., Bartoli, F., Martelossi, S., Ventura, A., Decorti, G., 2014a. Deletion of glutathione-S-transferase M1 reduces azathioprine metabolite concentrations in young patients with inflammatory bowel disease. J. Clin. Gastroenterol. 48, 43–51. https://doi.org/10.1097/MCG.0b013e31828b2866

Stocco, G., Pelin, M., Franca, R., De Iudicibus, S., Cuzzoni, E., Favretto, D., Martelossi, S., Ventura, A., Decorti, G., 2014b. Pharmacogenetics of azathioprine in inflammatory bowel disease: A role for glutathione-S-transferase? World J. Gastroenterol. 20, 3534–3541. https://doi.org/10.3748/wjg.v20.i13.3534

Takeshige, K., Baba, M., Tsuboi, S., Noda, T., Ohsumi, Y., 1992. Autophagy in Yeast Demonstrated with Proteinase-deficient Mutants and Conditions for its Induction. J. Cell Biol. 119, 3–8. https://doi.org/10.1083/jcb.119.2.301

Tan, G., Zeng, B., Zhi, F.C., Parkhouse, R., Monie, T.P., Economou, M., Trikalinos, T.A., Loizou, K.T., Tsianos, E. V., Ioannidis, J.P.A., 2015. Regulation of human enteric α-defensins by NOD2 in the Paneth cell lineage. Eur. J. Cell Biol. 99, 1–9. https://doi.org/10.1111/j.1572-0241.2004.40304.x

Tanida, I., Ueno, T., Kominami, E., 2004. Human light chain 3/MAP1LC3B Is cleaved at its carboxyl-terminal Met 121 to expose Gly120 for lipidation and targeting to autophagosomal membranes. J. Biol. Chem. 279, 47704–47710. https://doi.org/10.1074/jbc.M407016200

Thavarajah, R., Kazhiyur, V., Ranganathan, K., 2012. Chemical and physical basics of routine formaldehyde fixation. J. Oran Maxillofavcial Pathol. 16, 400–405.

Thursby, E., Juge, N., 2017. Introduction to the human gut microbiota. Biochem. J. 474, 1823–1836. https://doi.org/10.1042/BCJ20160510

Tiede, I., Fritz, G., Strand, S., Poppe, D., Dvorsky, R., Strand, D., Lehr, H.A., Wirtz, S., Becker, C., Atreya, R., Mudter, J., Hildner, K., Bartsch, B., Holtmann, M., Blumberg, R., Walczak, H., Iven, H., Galle, P.R., Ahmadian, M.R., Neurath, M.F., 2003. CD28-dependent Rac1 activation is the molecular target of azathioprine in primary human CD4+ T lymphocytes. J. Clin. Invest. 111, 1133–45. https://doi.org/10.1172/JCI200316432.Introduction

Toschi, A., Lee, E., Xu, L., Garcia, A., Gadir, N., Foster, D.A., 2009. Regulation of mTORC1 and mTORC2 Complex Assembly by Phosphatidic Acid: Competition with Rapamycin. Mol. Cell. Biol. 29, 1411–1420. https://doi.org/10.1128/mcb.00782-08

Travassos, L.H., Carneiro, L.A.M., Ramjeet, M., Hussey, S., Kim, Y.G., Magalhes, J.G., Yuan, L., Soares, F., Chea, E., Le Bourhis, L., Boneca, I.G., Allaoui, A., Jones, N.L., Nũez, G., Girardin, S.E., Philpott, D.J., 2010. Nod1 and Nod2 direct autophagy by recruiting ATG16L1 to the plasma membrane at the site of bacterial entry. Nat. Immunol. 11, 55–62. https://doi.org/10.1038/ni.1823

Tschurtschenthaler, M., Adolph, T.E., Ashcroft, J.W., Niederreiter, L., Bharti, R., Saveljeva, S., Bhattacharyya, J., Flak, M.B., Shih, D.Q., Fuhler, G.M., Parkes, M., Kohno, K., Iwawaki, T., van der Woude, C.J., Harding, H.P., Smith, A.M., Peppelenbosch, M.P., Targan, S.R., Ron, D., Rosenstiel, P., Blumberg, R.S., Kaser, A., 2017. Defective ATG16L1-mediated removal of IRE1α drives Crohn's disease-like ileitis. J. Exp. Med. 214, 401–422. https://doi.org/10.1084/jem.20160791

Tsuboyama, K., Koyama-honda, I., Sakamaki, Y., Koike, M., Morishita, H., 2016. The ATG conjugation systems are important for degradation of the inner autophagosomal membrane. Science (80-.). 6136, 1–10.

Upton, J., Wang, L., Han, D., Wang, E.S., Huskey, N.E., Lim, L., Truitt, M., Mcmanus, M.T., Ruggero, D., Goga, A., Papa, F.R., Oakes, S.A., 2013. IRE1α Cleaves Select microRNAs During ER Stress to Derepress Translation of Proapoptotic Caspase-2 338, 818–822. https://doi.org/10.1126/science.1226191.IRE1

Van der Sluis, M., De Koning, B.A.E., De Bruijn, A.C.J.M., Velcich, A., Meijerink, J.P.P., Van Goudoever, J.B., Büller, H.A., Dekker, J., Van Seuningen, I., Renes, I.B., Einerhand, A.W.C., 2006. Muc2-Deficient Mice Spontaneously Develop Colitis, Indicating That MUC2 Is Critical for Colonic Protection. Gastroenterology 131, 117–129. https://doi.org/10.1053/j.gastro.2006.04.020

Vandussen, K.L., Liu, T., Li, D., Towfic, F., Modiano, N., Haritunians, T., Taylor, K.D., Dhall, D., Targan, S.R., Ramnik, J., Mcgovern, D.P.B., Stappenbeck, T.S., 2014. Genetic Variants Synthesize to Produce Paneth Cell Phenotypes that Define Subtypes of Crohn's Disease 146, 200–209. https://doi.org/10.1053/j.gastro.2013.09.048.Genetic

Vazeille, E., Buisson, A., Bringer, M.A., Goutte, M., Ouchchane, L., Hugot, J.P., de Vallée, A., Barnich, N., Bommelaer, G., Darfeuille-Michaud, A., 2015. Monocyte-derived macrophages from Crohn's disease patients are impaired in the ability to control intracellular adherent-invasive Escherichia coli and exhibit disordered cytokine secretion profile. J. Crohns. Colitis 9, 410–420. https://doi.org/10.1093/ecco-jcc/jjv053

Venegas, D.P., De La Fuente, M.K., Landskron, G., González, M.J., Quera, R., Dijkstra, G., Harmsen, H.J.M., Faber, K.N., Hermoso, M.A., 2019. Short chain fatty acids (SCFAs)mediated gut epithelial and immune regulation and its relevance for inflammatory bowel diseases. Front. Immunol. 10. https://doi.org/10.3389/fimmu.2019.00277

Verfaillie, T., Rubio, N., Garg, A.D., Bultynck, G., Rizzuto, R., Decuypere, J.P., Piette, J., Linehan, C., Gupta, S., Samali, A., Agostinis, P., 2012. PERK is required at the ER-mitochondrial contact sites to convey apoptosis after ROS-based ER stress. Cell Death Differ. 19, 1880–1891. https://doi.org/10.1038/cdd.2012.74

Verway, M., 2010. Vitamin D , NOD2 , autophagy and Crohn ' s disease 505–508.

Vinolo, M.A.R., Rodrigues, H.G., Nachbar, R.T., Curi, R., 2011. Regulation of inflammation by short chain fatty acids. Nutrients 3, 858–876. https://doi.org/10.3390/nu3100858

Walczak, A., Gradzik, K., Kabzinski, J., Przybylowska-Sygut, K., Majsterek, I., 2019. The role of the ER-induced UPR pathway and the efficacy of its inhibitors and inducers in the inhibition of tumor progression. Oxid. Med. Cell. Longev. 2019. https://doi.org/10.1155/2019/5729710

Wang, Y., Shen, J., Arenzana, N., Tirasophon, W., Kaufman, R.J., Prywes, R., 2000. Activation of ATF6 and an ATF6 DNA binding site by the endoplasmic reticulum stress response. J. Biol. Chem. 275, 27013–27020. https://doi.org/10.1074/jbc.M003322200

Ward, M.G., Patel, K. V., Kariyawasam, V.C., Goel, R., Warner, B., Elliott, T.R., Blaker, P.A., Irving, P.M., Marinaki, A.M., Sanderson, J.D., 2017. Thioguanine in inflammatory bowel disease: Long-term efficacy and safety. United Eur. Gastroenterol. J. 5, 563–570. https://doi.org/10.1177/2050640616663438

Warner, B., Johnston, E., Arenas-HernandeZ, M., Marinaki, A., Irving, P., Sanderson, J., 2016. A practical guide to thiopurine prescribing and monitoring in IBD. Frontline Gastroenterol. 9, 10–15. https://doi.org/10.1136/flgastro-2016-100738

Watanabe, M., Ueno, Y., Yajima, T., Okamoto, S., Hayashi, T., Yamazaki, M., Iwao, Y., Ishii, H., Habu, S., Uehira, M., Nishimoto, H., Ishikawa, H., Hata, J.I., Hibi, T., 1998. Interleukin 7 transgenic mice develop chronic colitis with decreased interleukin 7 protein accumulation in the colonic mucosa. J. Exp. Med. 187, 389–402. https://doi.org/10.1084/jem.187.3.389

Wei, Y., Sinha, S., Levine, B., 2008. Dual Role of JNK1-Mediated Phosphorylation of Bcl-2 in Autophagy and Apoptosis Regulation. Autophagy 4, 949–951. https://doi.org/10.1097/MCA.0000000000000178.Endothelial

Wildenberg, M.E., Koelink, P.J., Diederen, K., Te Velde, A.A., Wolfkamp, S.C.S., Nuij, V.J., Peppelenbosch, M.P., Nobis, M., Sansom, O.J., Anderson, K.I., Van Der Woude, C.J., D'Haens, G.R.A.M., Van Den Brink, G.R., 2017. The ATG16L1 risk allele associated with Crohn's disease results in a Rac1-dependent defect in dendritic cell migration that is corrected by thiopurines. Mucosal Immunol. 10, 352–360. https://doi.org/10.1038/mi.2016.65

Wilson, C.L., Ouellette, A.J., Satchell, D.P., Ayabe, T., López-Boado, Y.S., Stratman, J.L., Hultgren, S.J., Matrisian, L.M., Parks, W.C., 1999. Regulation of intestinal α-defensin activation by the metalloproteinase matrilysin in innate host defense. Science (80-.). 286, 113–117. https://doi.org/10.1126/science.286.5437.113

Wong, A.S.L., Cheung, Z.H., Ip, N.Y., 2011. Molecular machinery of macroautophagy and its deregulation in diseases. Biochim. Biophys. Acta - Mol. Basis Dis. 1812, 1490–1497. https://doi.org/10.1016/j.bbadis.2011.07.005

Wu, R., Zhang, Q.H., Lu, Y.J., Ren, K., Yi, G.H., 2015. Involvement of the IRE1α-XBP1 pathway and XBP1s-dependent transcriptional reprogramming in metabolic

diseases. DNA Cell Biol. 34, 6–18. https://doi.org/10.1089/dna.2014.2552

Xie, Xiaoduo, Hu, H., Tong, X., Li, L., Liu, X., Chen, M., Xie, Xia, Li, Q., Zhang, Y., Ouyang, H., Wei, M., Liu, P., Gan, W., Liu, Y., Xie, A., Kuai, X., Chirn, W., Zhou, H., Zeng, R., Hu, R., Qin, J., Meng, F., Wei, W., Ji, H., Gao, D., Biology, C., Biology, C., Biology, C., Road, Y., 2018. The mTOR-S6K Pathway Links Growth Signaling to DNA Damage Response by Targeting RNF168 20, 320–331. https://doi.org/10.1038/s41556-017-0033-8.The

Yona, S., Viukov, S., Guilliams, M., Misharin, A., 2013. Tissue Macrophages Under Homeostasis. Immunity 38, 79–91. https://doi.org/10.1016/j.immuni.2012.12.001.Fate

Yorimitsu, T., Klionsky, D., 2005. Autophagy: molecular machinery for self-eating. Cell Death Differ. 12, 1542–1552. https://doi.org/10.1002/ana.22528.Toll-like

Yoshida, H., Matsui, T., Yamamoto, A., Okada, T., Mori, K., 2001. XBP1 mRNA Is Induced by ATF6 and Spliced by IRE1 in Response to ER Stress to Produce a Highly Active Transcription Factor phorylation, the activated Ire1p specifically cleaves HAC1 precursor mRNA to remove an intron of 252 nucle-otides. The cleaved 5 and . Cell 107, 881–891.

Yoshida, H., Uemura, A., Mori, K., 2009. pXBP1(U), a negative regulator of the unfolded protein response activator pXBP1(S), targets ATF6 but not ATF4 in proteasome-mediated degradation. Cell Struct. Funct. 34, 1–10. https://doi.org/10.1247/csf.06028

Yoshii, S.R., Mizushima, N., 2017. Monitoring and measuring autophagy. Int. J. Mol. Sci. 18, 1–13. https://doi.org/10.3390/ijms18091865

Yu, X., Long, Y.C., 2016. Crosstalk between cystine and glutathione is critical for the regulation of amino acid signaling pathways and ferroptosis. Sci. Rep. 6, 1–11. https://doi.org/10.1038/srep30033

Yuan, Y., Ding, D., Zhang, N., Xia, Z., Wang, J., Yang, H., Guo, F., Li, B., 2018. TNF-α induces autophagy through ERK1/2 pathway to regulate apoptosis in neonatal necrotizing enterocolitis model cells IEC-6. Cell Cycle 17, 1390–1402. https://doi.org/10.1080/15384101.2018.1482150

Zeng, X., Kinsella, T.J., 2007. A novel role for DNA mismatch repair and the autophagic processing of chemotherapy drugs in human tumor cells. Autophagy 3, 368–370. https://doi.org/10.4161/auto.4205

Zeng, X., Yan, T., Schupp, J.E., Seo, Y., Kinsella, T.J., 2007. DNA mismatch repair initiates 6-thioguanine-induced autophagy through p53 activation in human tumor cells. Clin. Cancer Res. 13, 1315–1321. https://doi.org/10.1158/1078-0432.CCR-06-1517

Zhang, F., Fu, L., Wang, Y., 2013. 6-Thioguanine induces mitochondrial dysfunction and oxidative dna damage in acute lymphoblastic leukemia cells. Mol. Cell. Proteomics 12, 3803–3811. https://doi.org/10.1074/mcp.M113.029595

Zhang, H., Zheng, L., McGovern, D.P.B., Hamill, A.M., Ichikawa, R., Kanazawa, Y.,

Luu, J., Kumagai, K., Cilluffo, M., Fukata, M., Targan, S.R., Underhill, D.M., Zhang, X., Shih, D.Q., 2017. Myeloid ATG16L1 Facilitates Host–Bacteria Interactions in Maintaining Intestinal Homeostasis. J. Immunol. 198, 2133–2146. https://doi.org/10.4049/jimmunol.1601293

Zhang, W., Feng, D., Li, Y., Iida, K., McGrath, B., Cavener, D.R., 2006. PERK EIF2AK3 control of pancreatic β cell differentiation and proliferation is required for postnatal glucose homeostasis. Cell Metab. 4, 491–497. https://doi.org/10.1016/j.cmet.2006.11.002

Zhang, Y.-Z., Li, Y.-Y., 2014. Inflammatory bowel disease: Pathogenesis. World J. Gastroenterol. 20, 91–99. https://doi.org/10.3748/wjg.v20.i1.91

Zhao, Y., Hu, X., Liu, Y., Dong, S., Wen, Z., He, W., Zhang, S., Huang, Q., Shi, M., 2017. ROS signaling under metabolic stress: Cross-talk between AMPK and AKT pathway. Mol. Cancer 16, 1–12. https://doi.org/10.1186/s12943-017-0648-1

Zheng, W., Rosenstiel, P., Huse, K., Sina, C., Valentonyte, R., Mah, N., Zeitlmann, L., Grosse, J., Ruf, N., Nürnberg, P., Costello, C.M., Onnie, C., Mathew, C., Platzer, M., Schreiber, S., Hampe, J., 2006. Evaluation of AGR2 and AGR3 as candidate genes for inflammatory bowel disease. Genes Immun. 7, 11–18. https://doi.org/10.1038/sj.gene.6364263

Zuber, C., Cormier, J.H., Guhl, B., Santimaria, R., Hebert, D.N., Roth, J., 2007. EDEM1 reveals a quality control vesicular transport pathway out of the endoplasmic reticulum not involving the COPII exit sites. Proc. Natl. Acad. Sci. U. S. A. 104, 4407–4412. https://doi.org/10.1073/pnas.0700154104

Zuo, T., Ng, S.C., 2018. The Gut Microbiota in the Pathogenesis and Therapeutics of Inflammatory bowel disease. Front. Microbiol. 9, 1–13. https://doi.org/10.3389/fmicb.2018.02247